Fluorinated Biphenyl Phosphine Ligands for Accelerated [Au(I)]-Catalysis

Riccardo Pedrazzani,[a] Sofia Kiriakidi,[b] Magda Monari,*[a,c] Irene Lazzarini,[a] Giulio Bertuzzi,[a,b] Carlos Silva López,*[b] Marco Bandini*[a,c]

[a] Dipartimento di Chimica "Giacomo Ciamician", Alma Mater Studiorum – Università di Bologna, via Selmi 2, 40126, Bologna – Italy. [b] Departamento de Química Orgánica, Universidade de Vigo, AS Lagoas (Marcosende) s/n, 36310 Vigo, Spain. [c] Center for Chemical Catalysis - C3, via Selmi 2, 40126, Bologna – Italy.

Email: MM: magda.monari@unibo.it; CSL: csilval@uvigo.gal; MB: marco.bandini@unibo.it

Table of contents

General methods

^{1}H NMR spectra were recorded on Varian 400 (400 MHz) or Bruker 600 (600 MHz) spectrometers. Chemical shifts are reported in ppm from TMS with the solvent resonance as the internal standard (deuterochloroform: 7.26 ppm). Data are reported as follows: chemical shift, multiplicity (s = singlet, d = doublet, t = triplet, q = quartet, sext = sextet, sept = septet, p = pseudo, b = broad, m = multiplet), coupling constants (Hz). ^{13}C NMR spectra were recorded on a Varian 400 (100 MHz) or Bruker 600 (150 MHz) spectrometers with complete proton decoupling. Chemical shifts are reported in ppm from TMS with the solvent as the internal standard (deuterochloroform: 77.0 ppm). ^{19}F NMR spectra were recorded on a Varian 400 (377 MHz) or Bruker 600 (565 MHz). Chemical shifts are reported in ppm from $CFCl_3$. ^{31}P NMR spectra were recorded on a Varian 400 (162 MHz) or Bruker 600 (243 MHz). Chemical shifts are reported in ppm from PPh_3 (-4.71ppm) as external standard.

GC-MS spectra were taken by EI ionization at 70 eV on a Hewlett-Packard 5971 with GC injection. They are reported as: m/z (rel. intense).

LC-electrospray ionization mass spectra were obtained with Agilent Technologies 1260 Infinity II single-quadrupole mass spectrometer.

Elemental analyses were carried out by using a EACE 1110 CHNOS analyser.

Melting points were determined with Büchi Melting Point B-540 with a scan of 5°C/min and are not corrected.

Chromatographic purification was done with 240-400 mesh silica gel.

The SCF convergence was conducted using an ultrafine grid. The nature of the stationary points as minima or TSs was characterized by analysis of the normal modes via diagonalization of the Hessian matrix. In challenging cases, IRC calculations were performed to connect the minima that are associated with a TS without ambiguity. The geometry optimizations were carried out at the gas phase, due to high computational cost of the involved structures, while the final energies that are reported are electronic energies acquired by performing single point calculations with a dichloromethane (DCM) solvent environment on the gas phase optimized geometry. The solvation effects were considered using the PCM implicit solvation model.

Anhydrous solvents were supplied by Sigma Aldrich in Sureseal® bottles and used without any further purification. Commercially available chemicals were purchased from Sigma Aldrich, Fluorochem, Strem Chemicals and TCI and used without any further purification.

Intermediates prepared according to known procedures: **SM-1**,[1] cinnamyl bromides,[2] **SM-2**.[3]

General procedure for the synthesis of 1,6-enynes (1)

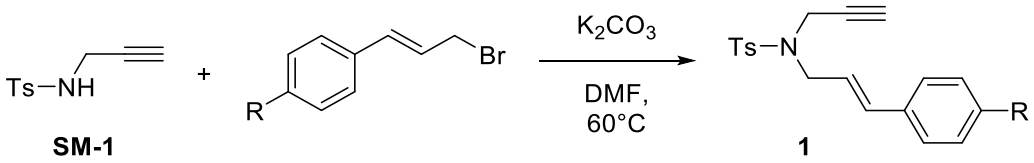

In an oven dried flask under N_2 atmosphere, **SM-1** (314 mg, 1.5 mmol) was dissolved in 5 mL of DMF and followed by addition of K_2CO_3 (414 mg, 3 mmol). The reaction was stirred 15 minutes at room temperature and then a solution of desired cinnamyl bromide (2.25 mmol) in 2 mL of DMF was added dropwise to the mixture. The reaction was heated at 60 °C overnight. Reaction was monitored by TLC (3:1 *n*-hexane:ethyl acetate), quenched with 15 mL of water and diluted with 20 mL of ethyl acetate. Aqueous phase was extracted 2 x 20 mL with ethyl acetate, organic phase washed 2 x 20 mL of water and 1 x 20 mL of brine and dried over Na_2SO_4. Solvent was removed and product was purified by flash chromatography using *n*-hexane:ethyl acetate 4:1.

1a, 91%, White solid, MP: 78.2-80.1 °C.

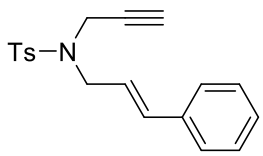

^{1}H NMR (600 MHz, Chloroform-*d*) δ 7.70 – 7.63 (m, 2H), 7.25 – 7.19 (m, 6H), 7.18 – 7.14 (m, 1H), 6.48 (dt, *J* = 15.8, 1.4 Hz, 1H), 5.98 (dt, *J* = 15.8, 6.8 Hz, 1H), 4.04 (d, *J* = 2.5 Hz, 2H), 3.90 (dd, *J* = 6.9, 1.3 Hz, 2H), 2.33 (s, 3H), 1.97 (t, *J* = 2.5 Hz, 1H).^{13}C NMR (150 MHz, Chloroform-*d*) δ 143.69, 136.17, 136.12, 134.96, 129.60, 128.68, 128.13, 127.84, 126.61, 126.61, 122.97, 76.68, 73.96, 48.65, 35.97, 21.61. LC-MS(ESI$^+$): 348.2 [M+Na]$^+$, 673.0 [2M+Na]$^+$. El. Anal. calc. for $C_{19}H_{19}NO_2S$: C, 70.13; H, 5.89; found: C, 70.01; H, 5.70.

1b, 81%, Pale yellow solid. MP: 80.7-83.2 °C.

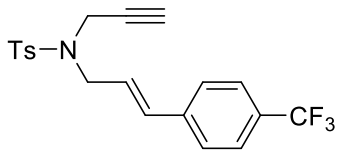

^{1}H NMR (400 MHz, Chloroform-*d*) δ 7.76 (d, *J* = 8.3 Hz, 2H), 7.54 (d, *J* = 8.1 Hz, 2H), 7.41 (d, *J* = 8.1 Hz, 2H), 7.30 (d, *J* = 8.1 Hz, 2H), 6.61 (d, *J* = 15.8 Hz, 1H), 6.19 (dt, *J* = 15.8, 6.6 Hz, 1H), 4.13 (d, *J* = 2.5 Hz, 2H), 4.02 (dd, *J* = 6.7, 1.4 Hz, 2H), 2.41 (s, 3H), 2.08 (t, *J* = 2.5 Hz, 1H). ^{13}C NMR (100 MHz, Chloroform-*d*) δ 143.89, 139.70 (q, J = 1.5 Hz), 135.98, 133.19, 129.76 (q, J = 32.5 Hz), 129.67, 127.83, 126.80, 126.10, 125.61 (q, J = 3.9 Hz), 122.85, 76.56, 74.18, 48.54, 36.30, 21.56. ^{19}F NMR (377 MHz, Chloroform-*d*) δ -62.53. LC-MS(ESI+): 416.0 [M+Na]$^+$, 809.0 [2M+Na]$^+$.El. Anal. calc. for $C_{20}H_{18}F_3NO_2S$: C, 61.06; H, 4.61; found: C, 60.85; H, 4.41.

1c, 58%, White solid, MP: 100.2-102.8 °C.

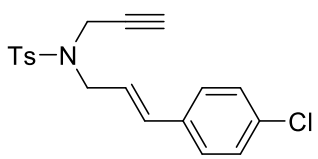

^{1}H NMR (400 MHz, Chloroform-*d*) δ 7.77 – 7.71 (m, 2H), 7.30 – 7.26 (m, 2H), 7.24 (d, *J* = 2.0 Hz, 4H), 6.50 (dt, *J* = 15.8, 1.4 Hz, 1H), 6.04 (dt, *J* = 15.8, 6.8 Hz, 1H), 4.10 (d, *J* = 2.5 Hz, 2H), 3.96 (dd, *J* = 6.8, 1.4 Hz, 2H), 2.40 (s, 3H), 2.04 (t, *J* = 2.4 Hz, 1H). ^{13}C NMR (100 MHz, Chloroform-*d*) δ 143.80, 136.03, 134.71, 133.76, 133.54, 129.65, 128.85, 127.85, 123.85, 76.64, 74.09, 48.58, 36.13, 21.65. LC-MS(ESI$^+$): 423.0 [(^{35}Cl)M+ACN+Na]$^+$, 741.0 [2(^{35}Cl)M+Na]$^+$. El. Anal. calc. for $C_{19}H_{18}ClNO_2S$: C, 63.41; H, 5.04; found: 63.30; H, 4.89.

1d, 78%, White solid, MP: 105.8-106.9 °C.

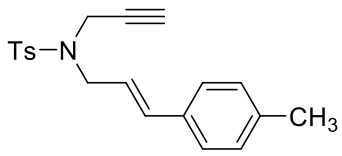

^{1}H NMR (400 MHz, Chloroform-*d*) δ 7.76 (d, *J* = 8.3 Hz, 2H), 7.30 (d, *J* = 8.1 Hz, 2H), 7.23 (d, *J* = 8.2 Hz, 2H), 7.11 (d, *J* = 7.9 Hz, 2H), 6.54 (d, *J* = 15.8 Hz, 1H), 6.02 (dt, *J* = 15.8, 6.9 Hz, 1H), 4.12 (d, *J* = 2.5 Hz, 2H), 3.98 (dd, *J* = 7.0, 1.3 Hz, 2H), 2.42 (s, 3H), 2.33 (s, 3H), 2.06 (t, *J* = 2.4 Hz, 1H). ^{13}C NMR (100 MHz, Chloroform-*d*) δ 143.64, 137.98, 136.07, 134.89, 133.36, 129.56, 129.34, 127.80, 126.50, 121.77, 76.65, 73.95, 48.67, 35.86, 21.57, 21.24. LC-MS(ESI$^+$): 362.2 [M+Na]$^+$, 701.2 [2M+Na]$^+$. El. Anal. calc. for $C_{20}H_{21}NO_2S$: C, 70.77; H, 6.24; found: C, 70.58; H, 6.15.

1e, 75%, White solid, MP: 68.6-71.8 °C.

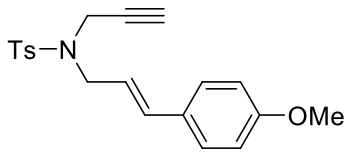

^{1}H NMR (400 MHz, Chloroform-*d*) δ 7.83 – 7.69 (m, 2H), 7.31 – 7.27 (m, 2H), 7.27 – 7.22 (m, 2H), 6.90 – 6.73 (m, 2H), 6.50 (d, *J* = 15.8 Hz, 1H), 5.91 (dt, *J* = 15.8, 6.9 Hz, 1H), 4.11 (d, *J* = 2.5 Hz, 2H), 3.95 (dd, *J* = 6.9, 1.3 Hz, 2H), 3.78 (s, 3H), 2.41 (s, 3H), 2.04 (t, *J* = 2.4 Hz, 1H). ^{13}C NMR (100 MHz, Chloroform-*d*) δ 159.56, 143.57, 136.09, 134.45, 129.50, 128.88, 127.77, 120.48, 114.01, 76.68, 73.81, 55.29, 48.67, 35.77, 21.53. LC-MS(ESI+): 378.0 [M+Na]$^+$, 733.2 [2M+Na]$^+$. El. Anal. calc. for $C_{20}H_{21}NO_3S$: C, 67.58; H, 5.96; found: 67.41; H, 5.77.

General procedure for gold(I) catalysed 1,6-enyne cycloisomerization

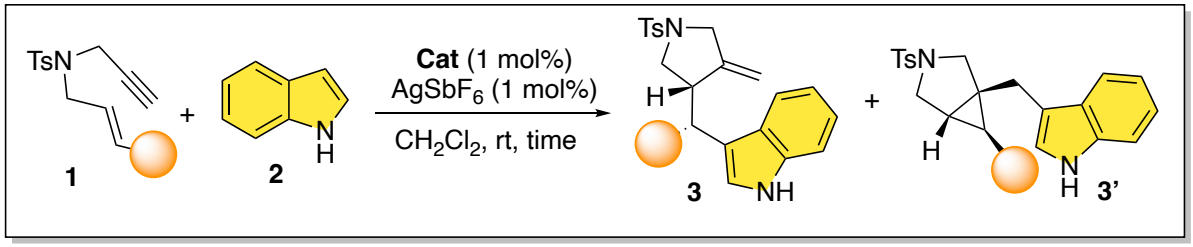

In an oven dried flask under N_2 atmosphere, **Cat1** (1.3 mg, 2 µmol) was dissolved in 1 mL of DCM and to this solution 100 µL of $AgSbF_6$ in DCM (6.8 mg/mL) were added. The mixture was stirred for 10 minutes and then **1** (0.2 mmol) and indole **2** (28 mg, 0.24 mmol) were added on portion. After complete consumption of **1** (reaction time is given for each substrate), DCM was evaporated and product purified by flash chromatography using *n*-hexane:ethyl acetate 4:1 to 3:1. Isomers **3** were isolated as a single detectable diastereoisomer for the reaction crude.

3a. Off-wite solid, 95% (1 h, **3a**/**3a'** > 25:1), MP: 92.6-95.2 °C.

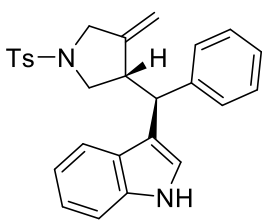

^{1}H NMR (600 MHz, Chloroform-*d*) δ 8.21 – 8.07 (m, 1H), 7.65 – 7.61 (m, 2H), 7.36 (dd, *J* = 8.0, 1.0 Hz, 1H), 7.31 (dt, *J* = 8.1, 0.9 Hz, 1H), 7.27 – 7.23 (m, 2H), 7.23 – 7.18 (m, 4H), 7.16 (ddd, *J* = 8.2, 7.0, 1.1 Hz, 1H), 7.14 – 7.10 (m, 1H), 7.04 (ddd, *J* = 8.0, 7.0, 1.0 Hz, 1H), 6.97 (d, *J* = 2.5 Hz, 1H), 4.77 (q, *J* = 1.8 Hz, 1H), 4.26 (q, *J* = 2.0 Hz, 1H), 3.97 (d, *J* = 10.1 Hz, 1H), 3.90 (qt, *J* = 13.7, 1.8 Hz, 2H), 3.52 – 3.41 (m, 2H), 3.39 – 3.31 (m, 1H), 2.44 (s, 3H). ^{13}C NMR (151 MHz, $CDCl_3$) δ 145.10, 143.71, 143.29, 136.46, 132.79, 129.84, 128.35, 128.26, 127.80, 126.87, 126.37, 122.20, 121.29, 119.46, 119.38, 117.80, 111.34, 110.31, 53.21, 52.44, 47.88, 45.85, 21.65. LC-MS(ESI$^+$): 443.2 [M+H]$^+$, 465.2 [M+Na]$^+$, 907.0 [2M+Na]$^+$.El. Anal. calc. for $C_{27}H_{26}N_2O_2S$: C, 73.27; H, 5.92; found: C, 73.15; H, 5.71.

3b, Off-white solid, 85% (22 h, **3b**/**3b'** >25:1), MP: 97.3-99.8 °C.

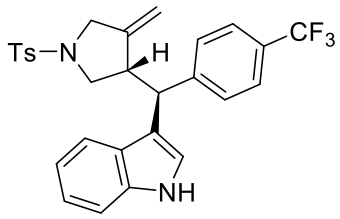

^{1}H NMR (600 MHz, Chloroform-*d*) δ 8.25 – 8.17 (m, 1H), 7.65 – 7.58 (m, 2H), 7.45 (d, *J* = 8.1 Hz, 2H), 7.35 (dd, *J* = 8.2, 0.9 Hz, 1H), 7.29 (td, *J* = 5.0, 2.5 Hz, 4H), 7.26 – 7.22 (m, 2H), 7.18 (ddd, *J* = 8.2, 7.0, 1.1 Hz, 1H), 7.07 – 7.02 (m, 2H), 4.77 (q, *J* = 1.9 Hz, 1H), 4.21 (q, *J* = 2.0 Hz, 1H), 4.03 (d, *J* = 10.6 Hz, 1H), 3.94 (dq, *J* = 13.9, 2.1 Hz, 1H), 3.83 (dt, *J* = 13.8, 1.9 Hz, 1H), 3.45 (dtd, *J* = 12.1, 5.2, 1.4 Hz, 1H), 3.40 (d, *J* = 5.4 Hz, 2H), 2.43 (s, 3H). ^{13}C NMR (151 MHz, Chloroform-*d*) δ 147.26, 144.64, 143.74, 136.45, 132.69, 129.80, 128.63, 128.59 (q, *J* = 32.2 Hz), 127.73, 126.55, 125.18 (q, *J* = 3.8 Hz), 124.17 (q, *J* = 271.9 Hz), 122.49, 121.30, 119.62, 119.20, 116.94, 111.39, 110.70, 52.99, 52.13, 47.75, 45.61, 21.58. ^{19}F NMR (565 MHz, Chloroform-*d*) δ -62.35 (s, 6F). LC-MS(ESI$^+$): 533.0 [M+Na]$^+$, 1044.0 [2M+Na]$^+$. El. Anal. calc. for $C_{28}H_{25}F_3N_2O_2S$: C, 65.87; H, 4.94; found: C, 65.71; H, 4.75.

3c, White solid, 85% (5 h, **3c**/**3c'** >25:1), MP: 188.7-191.1 °C.

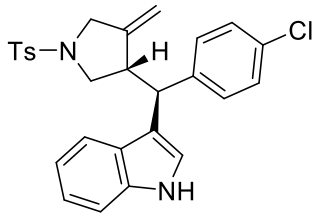

^{1}H NMR (600 MHz, Chloroform-*d*) δ 8.18 (s, 1H), 7.61 (d, *J* = 8.2 Hz, 2H), 7.33 (dd, *J* = 8.2, 0.9 Hz, 1H), 7.29 – 7.27 (m, 1H), 7.24 (d, *J* = 8.0 Hz, 2H), 7.18 – 7.14 (m, 3H), 7.10 – 7.07 (m, 2H), 7.03 (ddd, *J* = 8.0, 7.0, 1.0 Hz, 1H), 7.00 (d, *J* = 2.4 Hz, 1H), 4.78 (q, *J* = 1.6 Hz, 1H), 4.25 (q, *J* = 1.8 Hz, 1H), 3.96 – 3.88 (m, 2H), 3.84 (dt, *J* = 13.8, 1.9 Hz, 1H), 3.44 – 3.33 (m, 3H), 2.43 (s, 3H). ^{13}C NMR (151 MHz, $CDCl_3$) δ 144.82, 143.79, 141.80, 136.54, 132.79, 132.03, 129.88, 129.74, 128.40, 127.81, 126.71, 122.46, 121.27, 119.58, 119.38, 117.40, 111.43, 110.72, 53.12, 52.29, 47.93, 45.26, 21.68. LC-MS(ESI$^+$): 477.0 [(^{35}Cl)M+H]$^+$, 499.0[(^{35}Cl)M+Na]$^+$. El. Anal. calc. for $C_{27}H_{25}ClN_2O_2S$: C, 67.98; H, 5.28; found: C, 67.81; H, 5.11.

3d, White solid, 93% (1 h, **3d**/**3d'** > 25:1), MP: 171.3-172.2 °C.

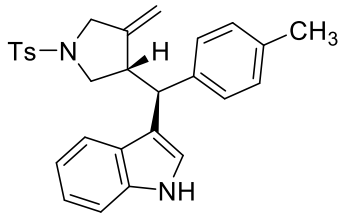

^{1}H NMR (600 MHz, Chloroform-*d*) δ 8.04 (s, 1H), 7.63 – 7.57 (m, 2H), 7.33 (dd, *J* = 18.4, 8.1 Hz, 2H), 7.24 (d, *J* = 8.0 Hz, 2H), 7.15 (t, *J* = 7.6 Hz, 1H), 7.07 (d, *J* = 7.8 Hz, 2H), 7.04 – 6.98 (m, 4H), 4.76 (t, *J* = 1.9 Hz, 1H), 4.30 (t, *J* = 2.0 Hz, 1H), 3.94 (d, *J* = 10.3 Hz, 1H), 3.89 – 3.84 (m, 2H), 3.48 – 3.39 (m, 2H), 3.31 (dd, *J* = 9.8, 4.5 Hz, 1H), 2.43 (s, 3H), 2.24 (s, 3H). ^{13}C NMR (151 MHz, $CDCl_3$) δ 145.34, 143.65, 140.24, 136.49, 135.85, 132.91, 129.83, 129.01, 128.20, 127.87, 126.93, 122.29, 121.17, 119.59, 119.47, 118.26, 111.27, 110.24, 53.22, 52.53, 47.84, 45.43, 21.70, 21.10. LC-MS(ESI+): 457.2 [M+H]$^+$, 479.0 [M+Na]$^+$, 935.2 [2M+Na]$^+$. El. Anal. calc. for $C_{28}H_{28}N_2O_2S$: C, 73.65; H, 6.18; found: C, 73.50; H, 6.05.

3e, White solid, 99% (1 h, **3e**/**3e'** > 25:1), MP: 171.9-173.3 °C.

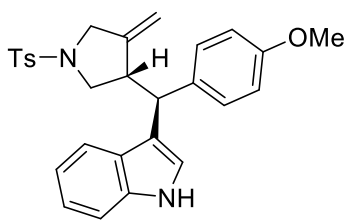

^{1}H NMR (600 MHz, Chloroform-*d*) δ 8.08 (s, 1H), 7.63 – 7.58 (m, 2H), 7.34 – 7.30 (m, 2H), 7.24 (d, *J* = 7.9 Hz, 2H), 7.15 (ddd, *J* = 8.2, 7.0, 1.1 Hz, 1H), 7.09 – 7.06 (m, 2H), 7.02 (ddd, *J* = 7.9, 7.0, 1.0 Hz, 1H), 6.99 (d, *J* = 2.4 Hz, 1H), 6.77 – 6.70 (m, 2H), 4.77 (q, *J* = 1.8 Hz, 1H), 4.28 (q, *J* = 1.9 Hz, 1H), 3.92 (d, *J* = 9.4 Hz, 1H), 3.91 – 3.83 (m, 2H), 3.72 (s, 3H), 3.46 – 3.38 (m, 2H), 3.33 (dd, *J* = 7.7, 5.9 Hz, 1H), 2.43 (s, 3H). ^{13}C NMR (151 MHz, $CDCl_3$) δ 158.05, 145.24, 143.67, 136.53, 135.47, 132.87, 129.84, 129.28, 127.85, 126.91, 122.29, 121.11, 119.60, 119.45, 118.29, 113.65, 111.29, 110.35, 55.27, 53.22, 52.49, 48.04, 45.03, 21.69. LC-MS(ESI+): 495.0 [M+Na]$^+$, 967.2 [2M+Na]$^+$ El. Anal. calc. for $C_{28}H_{28}N_2O_3S$: C, 71.16; H, 5.97; found: C, 71.00; H, 5.71.

Synthesis of N-tosyl-N-propargyl tryptamine (8)

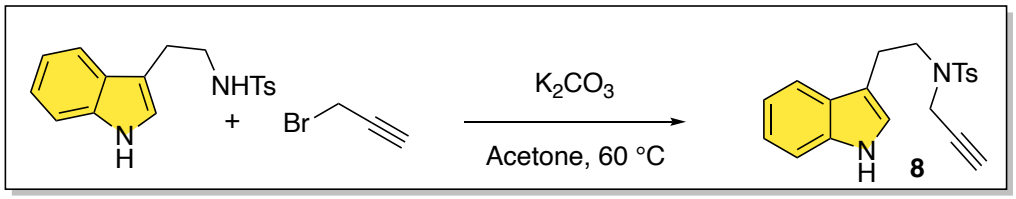

In an oven dried Schlenk tube under N_2 atmosphere, *N*-tosyl tryptamine (**SM-2**, 441 mg, 1.4 mmol) was dissolved in 4.5 mL of acetone. Subsequently, K_2CO_3 (212 mg, 1.54 mmol) and propargyl bromide (170 µL, 80% wt in toluene,) were added and the reaction heated to 60 °C. After complete consumption of starting material, the reaction was cooled to room temperature and volatile compounds evaporated. Water (15 mL) and 15 mL of ethyl acetate were added, and the aqueous phase extracted 2 x 15 mL with ethyl acetate. Organic phase dried over Na_2SO_4 and evaporated. Product **8** was purified by flash chromatography using *n*-hexane:ethyl acetate 2:1.

8, 93%, Off-white solid, MP: 122.5-125.1 °C.

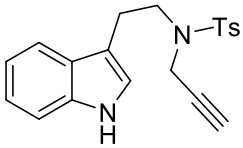

^{1}H NMR (600 MHz, Chloroform-*d*) δ 8.05 (s, 1H), 7.77 – 7.69 (m, 2H), 7.62 (dd, *J* = 7.9, 1.1 Hz, 1H), 7.36 (dd, *J* = 8.2, 0.9 Hz, 1H), 7.28 – 7.24 (m, 2H), 7.20 (ddd, *J* = 8.1, 7.0, 1.2 Hz, 1H), 7.12 (ddd, *J* = 8.0, 7.0, 1.0 Hz, 1H), 7.09 (d, *J* = 2.4 Hz, 1H), 4.18 (d, *J* = 2.5 Hz, 2H), 3.57 – 3.48 (m, 2H), 3.13 – 3.06 (m, 2H), 2.40 (s, 3H), 2.08 (t, *J* = 2.5 Hz, 1H). ^{13}C NMR (151 MHz, $CDCl_3$) δ 143.59, 136.34, 136.01, 129.59, 127.79, 127.39, 122.34, 122.23, 119.58, 118.77, 112.38, 111.34, 73.90, 47.08, 36.83, 24.42, 21.64. LC-MS(ESI$^+$): 375.0 $[M+Na]^+$, 727.2 $[2M+Na]^+$.El. Anal. calc. for $C_{20}H_{20}N_2O_2S$: C, 68.16; H, 5.72; found: C, 68.01; H, 5.85.

<u>General procedure for gold(I) catalysed N-tosyl-N-propargyl tryptamine cyclization (11)</u>

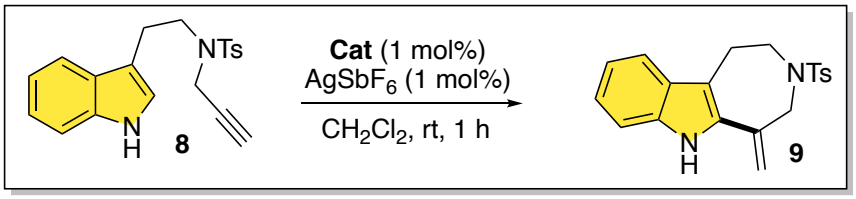

In an oven dried flask under N_2 atmosphere, **Cat1** (1.3 mg, 1 mol%) was dissolved in 1 mL of DCM and to this solution 100 µL of $AgSbF_6$ in DCM (6.8 mg/mL) were added. The mixture was stirred for 10 minutes and then **8** (70.4 mg, 0.2 mmol) was added one portion. Reaction monitoring was done by TLC *n*-hexane:ethyl acetate 10/1 (NOTE: the same TLC was ran 3 times to appreciate different Rf. Higher polarities of the eluent were unsuccessful). Compound **9** was isolated as a single regioisomer from the reaction crude.

9, White solid, 84%, MP: 69.3-72.9 °C.

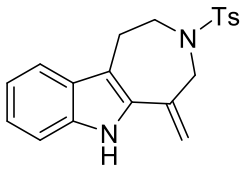

^{1}H NMR (600 MHz, Chloroform-*d*) δ 7.93 (s, 1H), 7.55 (d, *J* = 7.8 Hz, 2H), 7.33 (d, *J* = 7.9 Hz, 1H), 7.16 (d, *J* = 7.8 Hz, 1H), 7.05 (t, *J* = 8.0 Hz, 3H), 6.98 (t, *J* = 7.6 Hz, 1H), 5.16 (s, 1H), 5.10 (s, 1H), 4.21 (s, 2H), 3.61 (t, *J* = 5.9 Hz, 2H), 2.93 (t, *J* = 5.9 Hz, 2H), 2.23 (s, 3H). ^{13}C NMR (151 MHz, $CDCl_3$) δ 143.11, 137.60, 136.92, 135.95, 133.11, 129.45, 128.44, 127.12, 123.16, 119.64, 118.51, 113.13, 111.73, 110.74, 52.72, 48.93, 24.22, 21.46. LC-MS(ESI$^+$): 375.1 $[M+Na]^+$. El. Anal. calc. for $C_{20}H_{20}N_2O_2S$: C, 68.16; H, 5.72; found: C, 69.05; H, 6.22.

Synthesis of ortho-biaryl bromides (A1-3)

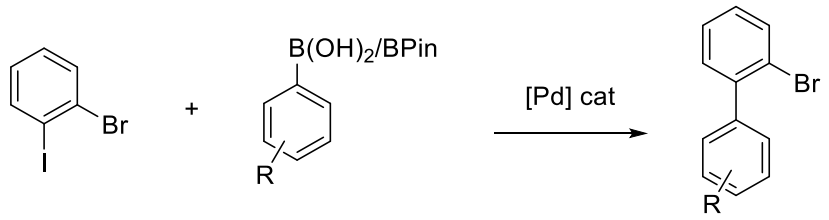

Procedure A:

In a Schlenk tube, under inert atmosphere of N_2, Cs_2CO_3 (975 mg, 3 mmol), desired phenyl boronic acid/ester (1.1 mmol) and 2-bromoiodobenzene (128 µl, 1 mmol) were dissolved in 5 mL of reagent grade 1,4-dioxane. The solution was degassed by purging with N_2 for 3 minutes under vigorous stirring, then $Pd(dppf)Cl_2$ (37 mg, 0.05 mmol, 5 mol%) was added and the mixture heated at 90 °C. The reaction was monitored by GC-MS. After complete consumption of 2-bomoiodobenzene, the reaction was cooled to room temperature, 10 mL of water and 15 mL of ethyl acetate were added. Aqueous phase was extracted 3 x 15 mL with ethyl acetate and the combined organic phases washed with water (x 2) and brine, dried over Na_2SO_4 and volatile compounds evaporated under vacuum. Final products were purified by flash chromatography using indicated eluent.

Procedure B:

In a Schlenk tube, under inert atmosphere of N_2, CsF (91 mg, 0.6 mmol), aryl boronic acid (0.55 mmol) and $Pd(dppf)Cl_2$ (20 mg, 0.025 mmol, 5 mol%) were dissolved in 2 mL of toluene. Then, 2-bromoiodobenzene (65 µl, 0.5 mmol), 0.5 mL of methanol and 0.5mL of K_2CO_3 (2.2 M in H_2O) were added and the mixture degassed by purging with N_2 for 3 minutes under vigorous stirring. The reaction was stirred under reflux for 16 h. After complete consumption of 2-bromoiodobenzene the reaction was cooled to room temperature 10 mL of water and 15 mL of ethyl acetate were added. Aqueous phase was extracted 3 x 15 mL with ethyl acetate and the combined organic phases washed with water (x 2) and brine, dried over Na_2SO_4 and volatile compounds evaporated under vacuum. Final products were purified by flash chromatography using indicated eluent.

A1, Procedure A, colourless liquid, 89%, FC 100% *n*-hexane.

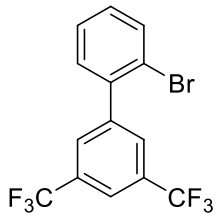

^{1}H NMR ^{1}H NMR (400 MHz, Chloroform-*d*) δ 7.92 – 7.89 (m, 1H), 7.88 (s, 2H), 7.71 (dd, *J* = 8.0, 1.2 Hz, 1H), 7.42 (td, *J* = 7.5, 1.2 Hz, 1H), 7.33 (dd, *J* = 7.7, 1.8 Hz, 1H), 7.29 (td, *J* = 7.8, 1.8 Hz, 1H).^{13}C NMR (100 MHz, Chloroform-*d*) δ 142.95, 139.68, 133.69, 131.58 (q, *J* = 33.3 Hz), 131.18, 130.28, 130.04 – 129.80 (m), 128.03, 123.44 (q, *J* = 272.5 Hz), 122.38, 121.88 – 121.49 (m). ^{19}F NMR (377 MHz, Chloroform-*d*) δ -62.86 (s, 6F). El. Anal. calc. for $C_{14}H_7BrF_6$: C, 45.56; H, 1.91; found: C, 45.32; H, 1.70.

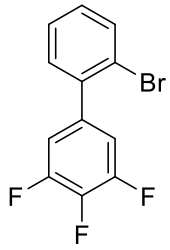

A2, Procedure B, colourless liquid, 84% (purity 96%),[1] FC 100% *n*-hexane.

^{1}H NMR (600 MHz, Chloroform-*d*) δ 7.70 – 7.66 (m, 1H), 7.38 (tdd, *J* = 7.5, 2.1, 1.2 Hz, 1H), 7.31 – 7.22 (m, 2H), 7.04 (ddd, *J* = 8.1, 6.5, 1.5 Hz, 2H). ^{13}C NMR (150 MHz, Chloroform-*d*) δ 150.74 (ddd, *J* = 250.1, 10.0, 4.2 Hz), 139.65, 139.44 (dt, *J* = 252.3, 15.3 Hz), 136.97 – 136.66 (m), 133.42, 130.93, 129.74, 127.67, 122.23, 113.88 (dd, *J* = 17.0, 4.8 Hz). ^{19}F NMR (565 MHz, Chloroform-*d*) δ -134.60 (dt, *J* = 20.9, 7.3 Hz, 2F), -161.70 (tt, *J* = 20.4, 6.6 Hz, 1F). El. Anal. calc. for $C_{12}H_6BrF_3$: C, 50.21; H, 2.11; found: C, 50.11; H, 2.00.

A3, Procedure A, colourless liquid, 84%, FC 30:1 *n*-hexane:ethyl acetate.

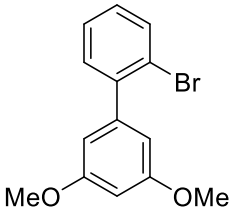

^{1}H NMR (400 MHz, Chloroform-*d*) δ 7.68 (dt, *J* = 8.0, 0.9 Hz, 1H), 7.42 – 7.33 (m, 2H), 7.22 (dt, *J* = 8.0, 4.6 Hz, 1H), 6.59 (d, *J* = 2.3 Hz, 2H), 6.53 (t, *J* = 2.3 Hz, 1H), 3.85 (s, 6H). ^{13}C NMR (100 MHz, Chloroform-*d*) δ 160.36, 143.05, 142.59, 133.19, 131.17, 128.90, 127.38, 122.50, 107.69, 99.83, 55.47. El. Anal. calc. for $C_{14}H_{13}BrO_2$: C, 57.36; H, 4.47; found: C, 57.21; H, 4.35.

Synthesis of biaryl phosphines

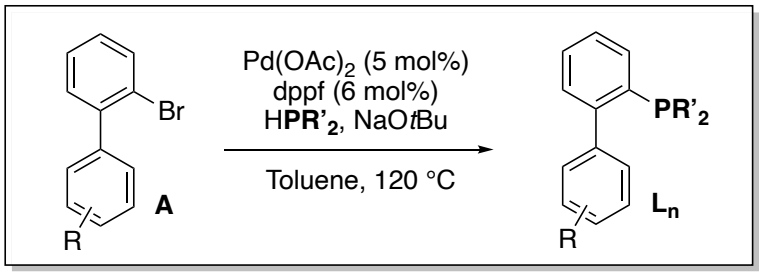

In an oven dried Schlenk tube under inert atmosphere of N_2, **A** (0.25 mmol) was dissolved in 1 mL of toluene. Subsequently, $Pd(OAc)_2$ (2.8 mg, 5 mol%), dppf (8.3 mg, 0.015 mmol, 6 mol%) and NaO*t*Bu (29 mg, 0.3 mmol) were added and the mixture was stirred at room temperature for 30 minutes. The desired dialkyl phosphine (0.3 mmol) was added to the reaction and heated to 120° C overnight. The reaction was cooled to room temperature, 5 mL of water and 5 mL of ethyl acetate were added, aqueous phase extracted 3 x 5 mL with ethyl acetate, organic phases collected, dried over Na_2SO_4 and solvent evaporated. The final phosphine ligands were purified by flash chromatography.

L1, Viscous colourless liquid, crystalize over time to colourless crystals, 77%, FC 100% *n*-hexane to 30:1 *n*-hexane:ethyl acetate, MP: 44-46 °C.

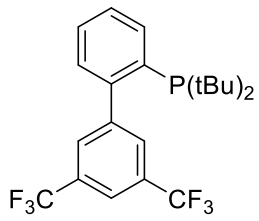

^{1}H NMR (40 MHz, Chloroform-*d*) δ 8.01 – 7.97 (m, 1H), 7.87 – 7.84 (m, 1H), 7.76 (d, *J* = 1.7 Hz, 2H), 7.48 – 7.44 (m, 2H), 7.33 – 7.28 (m, 1H), 1.16 (d, *J* = 11.8 Hz, 18H). ^{13}C NMR (100 MHz, Chloroform-*d*) δ 148.49 (d, *J* = 32.8 Hz), 145.87 (d, *J* = 7.6 Hz), 136.20 (d, *J* = 29.5 Hz), 135.91 (d, *J* = 3.0 Hz), 131.32 – 130.93 (m), 130.46 (q, *J* = 33.1 Hz), 130.18 (d, *J* = 6.0 Hz), 129.14 (d, *J* = 1.2 Hz), 127.36, 123.81 (q, *J* = 272.4 Hz), 120.40 (hept, *J* = 3.9 Hz), 33.17 (d, *J* = 24.8 Hz), 30.73 (d, *J* = 15.2 Hz). ^{19}F NMR (377 MHz,

[1] 2-Bromoiodobenzene and the product cannot be perfectly separated by flash chromatography. **A2** containing small percentage of SM was utilized in the next steps.

Chloroform-*d*) δ -62.88 (s, 6F). ^{31}P NMR (162 MHz, Chloroform-*d*) δ 17.37. LC-MS(ESI$^+$): 435.0 [M+H]$^+$. El. Anal. calc. for $C_{22}H_{25}F_6P$: C, 60.83; H, 5.80; found: C, 60.69; H, 5.91.

L2, White powder, 48%, FC 100% *n*-hexane to 30:1 *n*-hexane:ethyl acetate, MP: 180.0-182.3 °C.

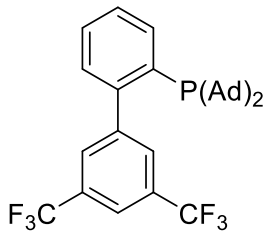

^{1}H NMR (600 MHz, Chloroform-*d*) δ 7.96 – 7.92 (m, 1H), 7.82 (s, 1H), 7.70 (s, 2H), 7.46 – 7.42 (m, 2H), 7.29 (q, *J* = 4.2 Hz, 1H), 1.92 – 1.76 (m, 18H), 1.70 – 1.59 (m, 12H). ^{13}C NMR (151 MHz, Chloroform-*d*) δ 147.66 (d, *J* = 32.4 Hz), 144.66, 135.92, 132.47, 129.98, 129.12 (q, *J* = 32.3 Hz) partially overlapped with 128.99, 127.76, 125.75, 122.59 (q, *J* = 272.6 Hz), 119.12, 40.83 (d, *J* = 12.5 Hz), 35.82, 27.73 (d, *J* = 8.6 Hz). ^{19}F NMR (565 MHz, Chloroform-*d*) δ -62.75 (s, 6F). ^{31}P NMR (243 MHz, Chloroform-*d*) δ 20.05. LC-MS(ESI$^+$): 591.3 [M+H]$^+$. El. Anal. calc. for $C_{34}H_{37}F_6P$: C, 69.14; H, 6.31; found: C, 69.22; H, 6.39.

L3, Colourless crystals, 57%, FC 100% *n*-hexane to 30:1 *n*-hexane:DCM, MP: 111.0-113.0 °C.

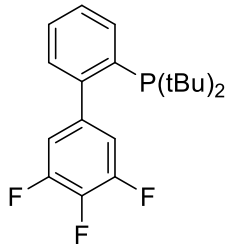

^{1}H NMR (400 MHz, Chloroform-*d*) δ 7.94 (ddd, *J* = 6.3, 3.0, 1.7 Hz, 1H), 7.45 – 7.35 (m, 2H), 7.22 (dt, *J* = 5.8, 3.8 Hz, 1H), 6.97 – 6.82 (m, 2H), 1.17 (d, *J* = 11.8 Hz, 18H). ^{13}C NMR (100 MHz, Chloroform-*d*) δ 150.29 (ddd, *J* = 249.1, 9.9, 4.2 Hz), 148.42 (dt, *J* = 32.0, 1.9 Hz), 139.92 (qd, *J* = 7.9, 5.0 Hz), 138.88 (dt, *J* = 250.2, 15.3 Hz), 135.95, 135.64 (d, *J* = 3.1 Hz), 130.25 (dd, *J* = 5.9, 1.0 Hz), 128.90 (d, *J* = 1.4 Hz), 126.94, 114.84 (ddd, *J* = 15.6, 5.6, 3.9 Hz), 33.01 (d, *J* = 24.0 Hz), 30.79 (d, *J* = 15.2 Hz). ^{19}F NMR (377 MHz, Chloroform-*d*) δ -135.30 – -136.63 (m, 2F), -163.85 (tt, *J* = 20.5, 6.5 Hz, 1F). ^{31}P NMR (162 MHz, Chloroform-*d*) δ 17.92. LC-MS(ESI$^+$): 353.2 [M+H]$^+$. El. Anal. calc. for $C_{20}H_{24}F_3P$: C, 68.17; H, 6.87; found: C, 68.08; H, 6.70.

L4, White powder, 53%, FC 100% *n*-hexane to 30:1 *n*-hexane:ethyl acetate, MP: 187.1-190.0 °C.

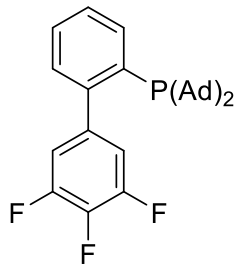

^{1}H NMR (600 MHz, Chloroform-*d*) δ 7.89 (tt, *J* = 5.3, 2.8 Hz, 1H), 7.41 – 7.36 (m, 2H), 7.23 – 7.18 (m, 1H), 6.87 – 6.79 (m, 2H), 1.92 – 1.87 (m, 12H), 1.86 – 1.79 (m, 6H), 1.70 – 1.63 (m, 12H). ^{13}C NMR (151 MHz, Chloroform-*d*) δ 150.09 (ddd, *J* = 248.8, 10.0, 4.2 Hz), 148.82 (d, *J* = 32.4 Hz), 140.11 – 139.78 (m), 138.70 (dt, *J* = 250.0, 15.3 Hz), 136.76 (d, *J* = 2.8 Hz), 133.17 (d, *J* = 27.9 Hz), 130.22 (d, *J* = 6.0 Hz), 128.54, 126.35, 114.73 (dt, *J* = 16.5, 3.9 Hz), 41.92 (d, *J* = 12.6 Hz), 37.50 (d, *J* = 24.6 Hz), 36.86, 28.80 (d, *J* = 8.5 Hz). ^{19}F NMR (565 MHz, Chloroform-*d*) δ -136.09 – -136.19 (m, 2F), -163.99 (tt, *J* = 20.9, 6.8 Hz, 1F). ^{31}P NMR (243 MHz, $CDCl_3$) δ 20.78. LC-MS(ESI$^+$): 509.3 [M+H]$^+$. El. Anal. calc. for $C_{32}H_{36}F_3P$: C, 75.57; H, 7.13; found: C, 75.70; H, 7.01.

L5, White powder, 73%, FC 30:1 *n*-hexane:ethyl acetate, MP: 98.0-100.0 °C.

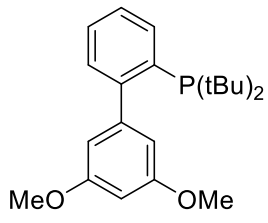

^{1}H NMR (400 MHz, Chloroform-*d*) δ 7.89 (dt, *J* = 7.9, 1.8 Hz, 1H), 7.39 – 7.30 (m, 2H), 7.26 (ddd, *J* = 8.8, 4.4, 2.2 Hz, 1H), 6.43 (t, *J* = 2.3 Hz, 1H), 6.40 (d, *J* = 2.3 Hz, 2H), 3.78 (s, 6H), 1.17 (d, *J* = 11.6 Hz, 18H). ^{13}C NMR (100 MHz, Chloroform-*d*) δ 159.60, 151.32 (d, *J* = 33.5 Hz), 146.03 (d, *J* = 7.3 Hz), 135.57 (d, *J* = 27.8 Hz), 135.32 (d, *J* = 3.4 Hz), 130.27 (d, *J* = 6.2 Hz), 128.42 (d, *J* = 1.2 Hz), 125.95, 108.92 (d, *J* = 3.5 Hz), 98.86, 55.33, 32.77 (d, *J* = 25.2 Hz), 30.91 (d, *J* = 15.6 Hz). ^{31}P NMR (162 MHz, Chloroform-*d*) δ 18.50. LC-MS(ESI$^+$): 359.2 [M+H]$^+$. El. Anal. calc. for $C_{22}H_{31}O_2P$: C, 73.72; H, 8.72; found: C, 73.61; H, 8.55.

Synthesis of gold complexes

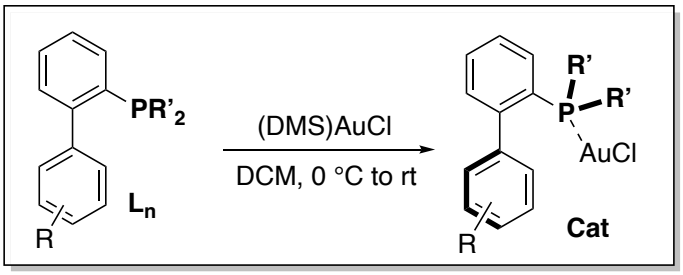

In an oven-dried three neck flask under inert atmosphere of N_2, equipped with a dropping funnel, gold chloride dimethylsulfide (14.7 mg, 0.05 mmol) was dissolved in 3 mL of DCM and cooled to 0 °C. A solution of phosphine (0.05mmol, 1eq, in 3mL of DCM) was added dropwise. Once the dropping was completed, the reaction was warmed to room temperature and let stirring for 20 minutes. Reaction monitoring was done by TLC *n*-hexane:ethyl acetate 2/1. The reaction mixture was transferred in a vial, the solvent was evaporated, the gold complex washed 3 x 1 mL with *n*-hexane and then dried under high vacuum. Gold complexes were used in catalysis without further purification.

Cat1, Off-white powder, 96%, MP: decomposition above 260 °C.

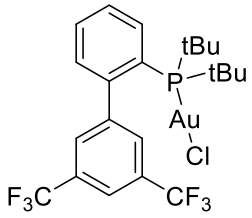

^{1}H NMR (600 MHz, Chloroform-*d*) δ 8.06 (s, 1H), 7.94 (ddd, *J* = 9.4, 4.6, 2.5 Hz, 1H), 7.60 (ddd, *J* = 5.9, 4.4, 2.6 Hz, 2H), 7.54 (d, *J* = 1.8 Hz, 2H), 7.34 – 7.30 (m, 1H), 1.41 (d, *J* = 15.8 Hz, 18H). ^{13}C NMR (151 MHz, Chloroform-*d*) δ 146.94 (d, *J* = 12.6 Hz), 144.07 (d, *J* = 6.4 Hz), 134.26 (d, *J* = 2.4 Hz), 133.08 (d, *J* = 7.2 Hz), 131.67 (q, *J* = 33.3 Hz), 131.34, 129.48 (q, *J* = 3.5 Hz), 128.20 (d, *J* = 6.6 Hz), 126.77 (d, *J* = 43.6 Hz), 123.36 (q, *J* = 273.0 Hz), 122.66 (hept, *J* = 3.9 Hz), 38.20 (d, *J* = 25.7 Hz), 30.88 (d, *J* = 6.4 Hz). ^{19}F NMR (565 MHz, Chloroform-*d*) δ -62.81 (s, 6F). ^{31}P NMR (243 MHz, Chloroform-*d*) δ 61.23. El. Anal. calc. for $C_{22}H_{25}AuClF_6P$: C, 39.63; H, 3.78; found: C, 39.50; H, 3.61.

Cat2, White powder, 95%, MP: decomposition above 230 °C.

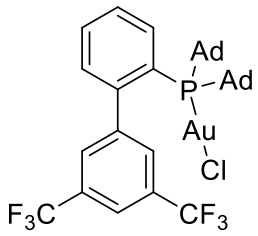

^{1}H NMR (600 MHz, Chloroform-*d*) δ 8.08 (s, 1H), 7.97 – 7.89 (m, 1H), 7.62 – 7.57 (m, 2H), 7.54 (s, 2H), 7.34 – 7.30 (m, 1H), 2.20 – 2.14 (m, 6H), 2.13 – 2.08 (m, 6H), 2.05 – 1.97 (m, 6H), 1.69 (s, 12H). ^{13}C NMR (151 MHz, Chloroform-*d*) δ 147.52 (d, *J* = 12.1 Hz), 144.02 (d, *J* = 6.3 Hz), 135.03 (d, *J* = 2.1 Hz), 133.21 (d, *J* = 7.0 Hz), 131.47 (q, *J* = 33.4 Hz), 130.91 (d, *J* = 2.4 Hz), 129.43 (q, *J* = 3.8 Hz), 127.46 (d, *J* = 6.5 Hz), 124.59 (d, *J* = 41.9 Hz), 123.30 (q, *J* = 273.1 Hz), 122.57 (hept, *J* = 3.8 Hz), 42.90 (d, *J* = 23.4 Hz), 42.19 (d, *J* = 2.3 Hz), 36.20, 28.56 (d, *J* = 10.1 Hz). ^{19}F NMR (565 MHz, Chloroform-*d*) δ -62.79 (s, 6F). ^{31}P NMR (243 MHz, $CDCl_3$) δ 61.5. El. Anal. calc. for $C_{34}H_{37}AuClF_6P$: C, 49.62; H, 4.53; found: C, 49.77; H, 4.40.

Cat3, white powder, 97%, MP: decomposition above 215 °C.

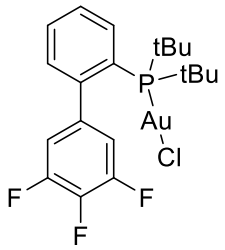

^{1}H NMR (600 MHz, Chloroform-*d*) δ 7.87 (ddt, *J* = 11.1, 7.6, 3.4 Hz, 1H), 7.58 – 7.53 (m, 2H), 7.28 (dt, *J* = 5.6, 4.1 Hz, 1H), 6.76 – 6.68 (m, 2H), 1.40 (d, *J* = 15.8 Hz, 18H). ^{13}C NMR (151 MHz, Chloroform-*d*) δ 151.46 (ddd, *J* = 252.3, 10.2, 4.7 Hz), 146.81 (d, *J* = 12.5 Hz), 141.35 (dt, *J* = 252.9, 15.0 Hz), 137.42 (ddd, *J* = 13.7, 8.1, 5.7 Hz), 133.89 (d, *J* = 2.7 Hz), 132.93 (d, *J* = 7.3 Hz), 131.15 (d, *J* = 2.3 Hz), 127.95 (d, *J* = 6.7 Hz), 126.17 (d, *J* = 44.2 Hz), 114.08 (dd, *J* = 16.3, 5.0 Hz), 38.03 (d, *J* = 25.6 Hz), 30.88 (d, *J* = 6.6 Hz). ^{19}F NMR (565 MHz, Chloroform-*d*) δ -131.36 – -134.81 (m, 2F), -161.01 (tt, *J* = 20.9, 6.6 Hz, 1F). ^{31}P NMR (243 MHz, Chloroform-*d*) δ 61.16. El. Anal. calc. for $C_{20}H_{24}AuClF_3P$: C, 41.08; H, 4.14; found: C, 40.85; H, 4.01.

Cat4, White powder, 96%, MP: decomposition above 255 °C.

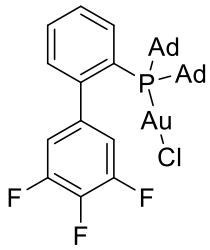

^{1}H NMR (600 MHz, Chloroform-*d*) δ 7.90 – 7.83 (m, 1H), 7.57 – 7.52 (m, 2H), 7.31 – 7.26 (m, 1H), 6.75 – 6.68 (m, 2H), 2.19 – 2.14 (m, 6H), 2.12 – 2.06 (m, 6H), 2.02 – 1.98 (m, 6H), 1.68 (s, 12H). ^{13}C NMR (151 MHz, Chloroform-*d*) δ 150.32 (ddd, *J* = 252.1, 10.2, 4.7 Hz), 146.39 (d, *J* = 12.1 Hz), 140.29 (dt, *J* = 253.1, 15.0 Hz), 136.71 – 136.22 (m), 133.64 (d, *J* = 2.4 Hz), 132.03 (d, *J* = 7.0 Hz), 129.72 (d, *J* = 2.4 Hz), 126.23 (d, *J* = 6.4 Hz), 122.94 (d, *J* = 42.5 Hz), 113.01 (dt, *J* = 16.1, 4.9 Hz), 41.71 (d, *J* = 23.4 Hz), 41.10, 35.16, 27.53 (d, *J* = 9.9 Hz). ^{19}F NMR (565 MHz, Chloroform-*d*) δ -133.01 – -133.18 (m, 2F), -161.14 (tt, *J* = 21.0, 6.1 Hz, 1F). ^{31}P NMR (243 MHz, $CDCl_3$) δ 61.51. El. Anal. calc. for $C_{32}H_{36}AuClF_3P$: C, 51.87; H, 4.90; found: C, 51.99; H, 4.76.

Cat5, white powder, 98%, MP: decomposition above 278 °C.

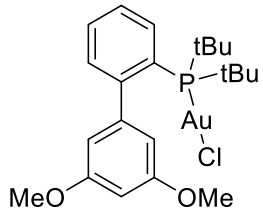

^{1}H NMR (600 MHz, Chloroform-*d*) δ 7.83 (td, *J* = 7.7, 1.5 Hz, 1H), 7.57 – 7.42 (m, 2H), 7.32 (ddd, *J* = 7.6, 4.3, 1.6 Hz, 1H), 6.62 (t, *J* = 2.3 Hz, 1H), 6.27 (d, *J* = 2.2 Hz, 2H), 3.83 (s, 6H), 1.40 (d, *J* = 15.5 Hz, 18H). ^{13}C NMR (151 MHz, Chloroform-*d*) δ 160.82, 149.94 (d, *J* = 13.5 Hz), 143.47 (d, *J* = 6.6 Hz), 133.49 (d, *J* = 2.6 Hz), 132.82 (d, *J* = 7.4 Hz), 130.65 (d, *J* = 2.4 Hz), 126.84 (d, *J* = 6.9 Hz), 126.06 (d, *J* = 45.2 Hz), 108.98, 99.50, 55.55, 37.76 (d, *J* = 25.6 Hz), 30.99 (d, *J* = 6.7 Hz). ^{31}P NMR (243 MHz, $CDCl_3$) δ 60.94. El. Anal. calc. for $C_{22}H_{31}AuClO_2P$: C, 44.72; H, 5.29; found: C, 44.90; H, 5.07.

Preparation of L1Au(ACN)SbF$_6$

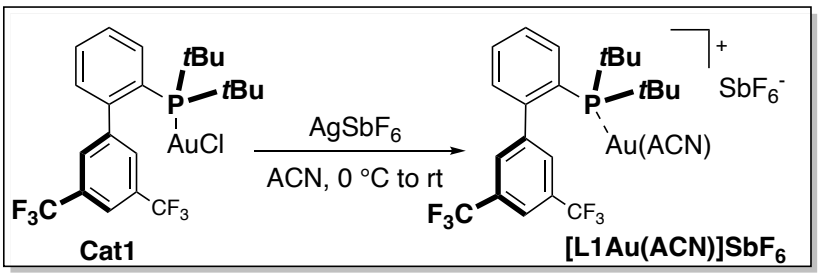

In an oven dried two-necked flask under inert atmosphere of N_2, **Cat1** (6.6 mg, 0.01 mmol) was dissolved in 2 mL of ACN and cooled at 0 °C. The flask was covered with an aluminium foil and $AgSbF_6$ (3.4

mg, 0.01 mmol) was added. The reaction was let stirring for 2 h, then the solvent evaporated. Then, the residue was redissolved in DCM, filtered through a plug of Celite® and washed with DCM. The filtrated is concentred and dried under vacuum prior to use.

L1Au(ACN)SbF$_6$, off-white powder, 96%, MP: decomposition above 255 °C

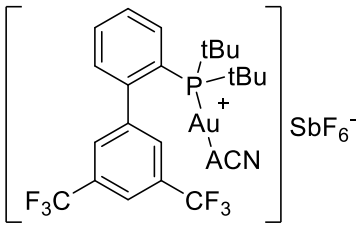

^{1}H NMR (400 MHz, Chloroform-*d*) δ 8.03 (s, 1H), 7.96 (tt, *J* = 6.8, 2.0 Hz, 1H), 7.70 (ddt, *J* = 5.6, 3.7, 2.0 Hz, 2H), 7.67 (d, *J* = 1.6 Hz, 2H), 7.37 – 7.32 (m, 1H), 2.37 (s, 3H), 1.44 (d, *J* = 16.6 Hz, 18H). ^{19}F NMR (377 MHz, Chloroform-*d*) δ -62.83 (s, 6F). ^{31}P NMR (162 MHz, Chloroform-*d*) δ 57.26. El. Anal. calc. for $C_{24}H_{28}AuF_{12}NPSb$: C, 44.72; H, 5.29; found: C, 44.60; H, 5.15.

Kinetic experiments

NOTE: $CDCl_3$ was filtered over basic alumina before use. NMR tubes were washed with aqua regia, water and acetone, dried under vacuum prior to use.

Standard NMR tube loading: **1a** (45.6 mg, 0.14 mmol, 1 eq, 0.2 M), **2** (16.4 mg, 0.14 mmol, 1 eq, 0.2 M), ca. exactly 2 mg of dimethyl sulfone and 0.6 mL of $CDCl_3$.

Preparation of the catalyst solutions: a 2 mL vial with PTFE septum equipped with stirring bar was charged with 0.015 mmol of desired complex (**Cat1** or **Cat5**) and dissolved in 215 µL of $CDCl_3$ (0.07 M). Then, 215 µL of an equimolar solution of $AgSbF_6$ in $CDCl_3$ were added and the mixture stirred for 10 min in the dark. This mother solution, Solution A, was then used for the preparation of the other solution by the principle of dilution in other vials.

Solution A: prepared as described. [$LAuSbF_6$] = 0.035 M
Solution B: 140 µL of Solution A + 60 µL of $CDCl_3$ [**L**$AuSbF_6$] = 0.0245M.
Solution C: 60 µL of Solution A + 90 µL of $CDCl_3$ [**L**$AuSbF_6$] = 0.014 M.
Solution D: 50 µL of Solution C + 50 µL of $CDCl_3$ [**L**$AuSbF_6$] = 0.007 M.

For [JohnPhosAu(ACN)]SbF_6 the same approach is adopted, but 0.015 mmol of it are dissolved directly in 430 µL of $CDCl_3$ without addition of any Ag salt.

NMR acquisition: The ^{1}H NMR of the pre-mixed reagent is acquired prior to the addition of the catalyst. Then 100 µL of catalyst solution (A for 2.5 mol%, B for 1.75 mol%, C for 1 mol% and D for 0.5 mol%) are added and time started (t = 0). The sample is placed in the instrument and several ^{1}H acquisition were done 30-40 seconds apart. For each spectra acquired, the time elapsed was noted.

The procedure was repeated for each catalyst **Cat1**, [JohnPhosAu(ACN)]SbF_6 and **Cat5** at each mol% of the catalyst.

Data analysis: for each spectrum, the product **3a** is integrated and converted, by the internal standard, in its concentration into the sample. Molarity of **3a** vs. time is plotted for each catalyst at the four different loadings.

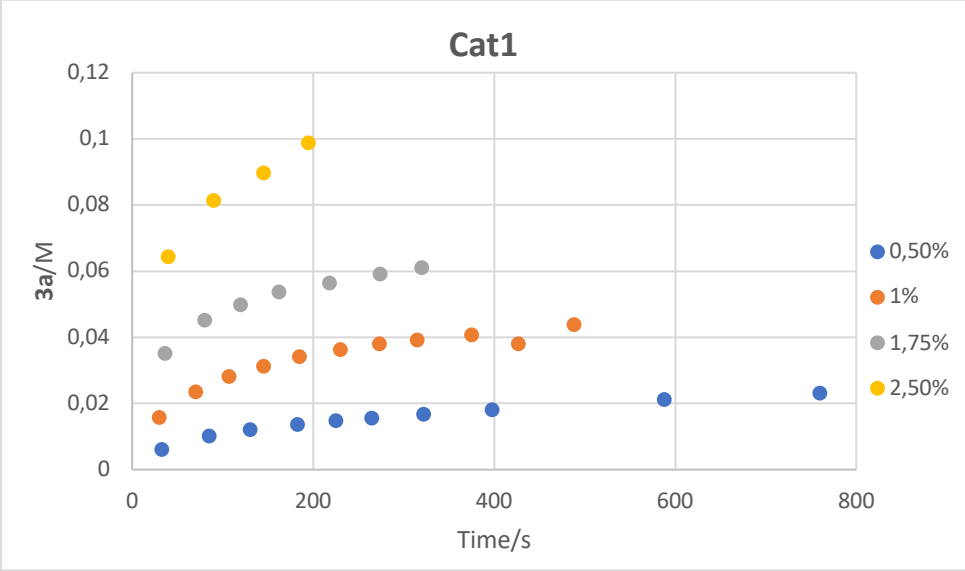

0.5 mol%		1 mol%		1.75 mol%		2.5 mol%	
Time (s)	**3a (M)**	**Time (s)**	**3a (M)**	**Time (s)**	**3a (M)**	**Time (s)**	**3a (M)**
33	0,0059	30	0,0156	36	0,0351	40	0,0642

85	0,0101
130	0,0119
183	0,0136
225	0,0147
265	0,0155
322	0,0167
398	0,0180
588	0,0211
760	0,0230

70	0,0235
107	0,0280
145	0,0312
185	0,0340
230	0,0361
273	0,0379
315	0,0392
375	0,0406
427	0,0378
488	0,0438

80	0,0450
120	0,0496
162	0,0536
218	0,0564
274	0,0590
320	0,0610

90	0,0814
145	0,0896
195	0,0987

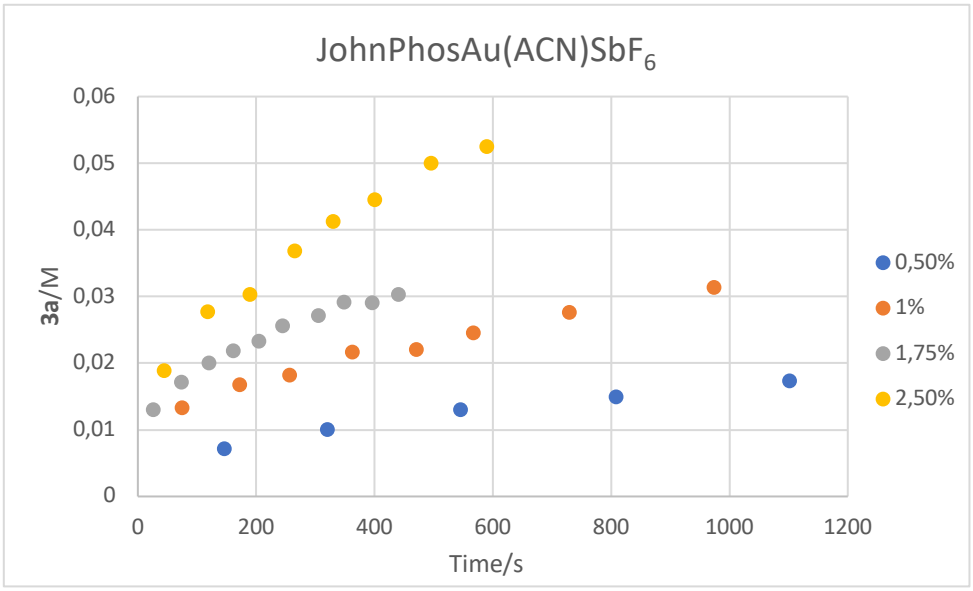

0.5 mol%	
Time (s)	**3a (M)**
146	0,0071
320	0,0100
546	0,0130
808	0,0149
1102	0,0172
1425	0,0194
1775	0,0219
2105	0,0234

1 mol%	
Time (s)	**3a (M)**
75	0,0132
172	0,0166
257	0,0181
363	0,0216
471	0,0219
567	0,0245
729	0,0275
974	0,0313

1.75 mol%	
Time (s)	**3a (M)**
26	0,0129
74	0,0171
120	0,0200
161	0,0218
205	0,023
245	0,0255
305	0,0270
348	0,0290
396	0,0290
440	0,0302

2.5 mol%	
Time (s)	**3a (M)**
45	0,0188
118	0,0277
190	0,0303
265	0,0367
330	0,0412
400	0,0445
496	0,0499
590	0,0524

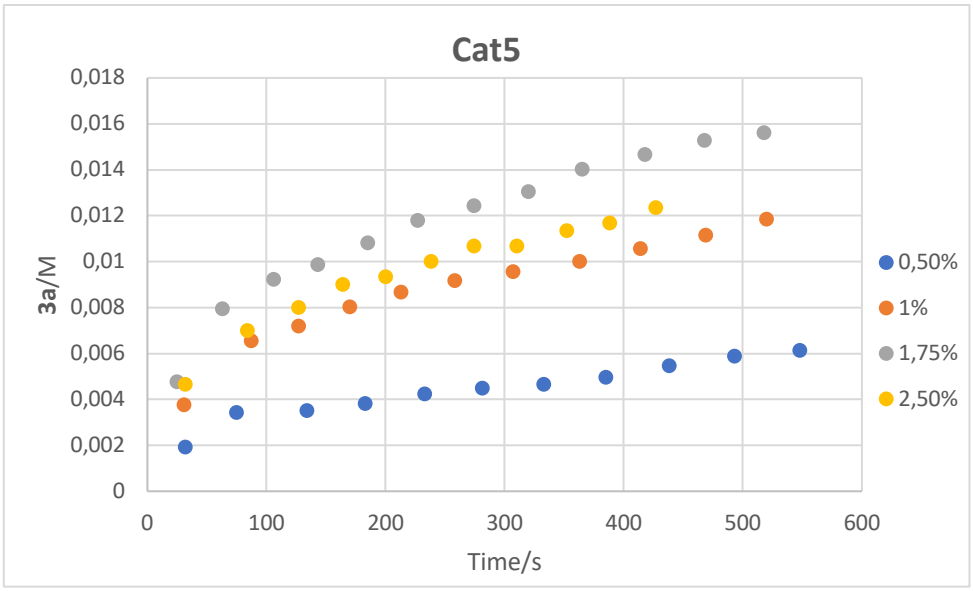

0.5 mol%		1 mol%		1.75 mol%		2.5 mol%	
Time (s)	**3a (M)**	**Time (s)**	**3a (M)**	**Time (s)**	**3a (M)**	**Time (s)**	**3a (M)**
32	0,001935	31	0,003761	25	0,004781	32	0,004674
75	0,003437	87	0,006565	63	0,007968	84	0,007012
134	0,003529	127	0,007203	106	0,009243	127	0,008013
183	0,003824	170	0,008031	143	0,00988	164	0,009015
233	0,004257	213	0,008669	185	0,010836	200	0,009349
281	0,004485	258	0,009179	227	0,011792	238	0,010017
333	0,004667	307	0,009561	274	0,01243	274	0,010684
385	0,004963	363	0,010007	320	0,013067	310	0,010684
438	0,005486	414	0,010581	365	0,014023	352	0,011352
493	0,005896	469	0,011155	418	0,014661	388	0,011686
548	0,006147	520	0,011856	468	0,015298	427	0,012354
				518	0,015617		

The points of each curve where the linearity is maintained are then linearly fitted and the slopes of the linear regression (initial velocity V_0) and reported in the table below:

		V_0 *(M/sec)*	
Au loading	**Cat1 (R^2)**	**JohnphosAu(ACN)SbF_6 (R^2)**	**Cat5(R^2)**
0,5mol%	5,03E-05 (0.94)	1,18E-05 (0.97)	1,06E-05 (0.97)
1mol%	1,35E-04 (0.96)	2,27E-05 (0.94)	2,39E-05 (0.97)
1,75mol%	1,74E-04 (0.97)	5,46E-05 (0.97)	4,74E-05 (0.99)
2,50mol%	2,15E-04 (0.96)	7,52E-05 (0.98)	6,38E-05 (0.97)

These data are further linearly fitted to give V_0 dependence on catalysts loading.

Catalyst	V_0/cat. loading (R^2)
Cat1	9,48E-05 (0.98)
JPAu(ACN)SbF$_6$	2,95E-05 (0.99)
Cat5	2,57E-05 (0.99)

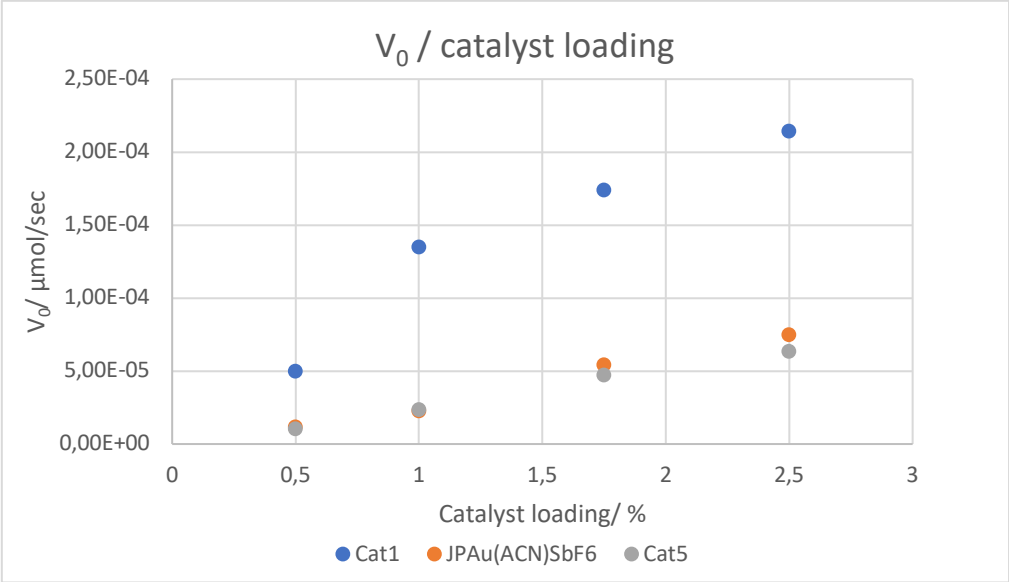

Crystallographic data

The X-ray intensity data for **L1** and **Cat1**-**5** were collected on a Bruker APEX-II CCD diffractometer using Mo-Kα radiation. All data were processed using the Bruker suite of programs[4,5,6] and all structures were solved by direct methods and refined with the SHELX program suite.[7] All non-hydrogen atoms were assigned anisotropic displacement parameters. Most of the hydrogen atoms were located in the Fourier map, placed in idealized positions and included as riding with constrained isotropic displacement parameters (C—H = 0.98, 0.95 Å for methyl, and aromatic protons, respectively, and refined as riding with U_{iso}(H) = 1.5 or 1.2U_{eq}(C)). In the asymmetric unit of **Cat3** two independent molecules are present. Molecular graphics were generated using the program Mercury.[8]

The X-ray intensity data were measured on a Bruker Apex II CCD diffractometer. Cell dimensions and the orientation matrix were initially determined from a least-squares refinement on reflections measured in three sets of 20 exposures, collected in three different ω regions, and eventually refined against all data. A full sphere of reciprocal space was scanned by 0.5° ω steps. The software SMART[3] was used for collecting frames of data, indexing reflections and determination of lattice parameters. The collected frames were then processed for integration by the SAINT program, and an empirical absorption correction was applied using SADABS. The structures were solved by direct methods (SIR 2014) and subsequent Fourier syntheses and refined by full-matrix least-squares on F^2 (SHELXTL) using anisotropic thermal parameters for all non-hydrogen atoms. The aromatic and methyl hydrogen atoms were placed in calculated positions, refined with isotropic thermal parameters *U(H)* = 1.2 *Ueq*(C) and allowed to ride on their carrier carbons. Molecular drawings were generated using Mercury.

Crystallographic data have been deposited with the Cambridge Crystallographic Data Centre (CCDC) as supplementary publication number CCDC 2327551-2327556. Copies of the data can be obtained free of charge via www.ccdc.cam.ac.uk/getstructures .

Table S1. Crystal data and structure refinement for compounds **L1**, **Cat1-2**.

Compound	**L1**	**Cat1**	**Cat2**
Formula	$C_{22}H_{25}F_6P$	$C_{22}H_{25}AuClF_6P$	$C_{34}H_{37}AuClF_6P$
Fw	434.39	666.80	823.02
T, K	296 (2)	296(2)	296 (2)
λ, Å	0.71073	0.71073	0.71073
Crystal symmetry	Monoclinic	Monoclinic	Monoclinic
Space group	*$P2_1/c$*	*C2/c*	*C2/c*
***a*, Å**	8.3722(3)	28.889(2)	24.4231(9)
***b*, Å**	14.9231(5)	8.6259(6)	10.6355(4)
***c*, Å**	19.0155(6)	20.032(2)	24.3200(9)
α	90	90	90
β	100.601(1)	101.026(2)	103.117(1)
γ	90	90	90
Cell volume, Å^3	2335.2(1)	4899.6(6)	6152.3(4)
Z	4	8	8
Dc, Mg m^{-3}	1.236	1.808	1.777
μ(Mo-K$_\alpha$), mm^{-1}	0.169	6.232	4.982
F(000)	904	2576	3248
Crystal size/ mm	0.34 x 0.18 x 0.14	0.36 x 0.24 x 0.20	0.27 x 0.18 x 0.14
θ limits, °	1.746 to 25.248	2.623 to 25.249	1.712 to 25.499
Reflections collected	37090	29141	50603
Unique obs. Reflections [$F_o > 4\sigma(F_o)$]	4214 [R(int) = 0.0609]	4366 [R(int) = 0.0267]	5727 [R(int) = 0.0568]
Goodness-of-fit-on F^2	0.956	1.056	1.191
R_1 (F)[a], wR_2 (F^2)[b] [$I > 2\sigma(I)$]	R1 = 0.0476, wR2 = 0.1415	R1 = 0.0333, wR2 = 0.0874	R1 = 0.0226, wR2 = 0.0497
Largest diff. peak and hole, e. Å^{-3}	0.259 and -0.193	0.995 and -1.167	0.687 and -0.753
CCDC	2327551	2327552	2327553

[a] $R_1 = \Sigma||F_o|-|F_c||/\Sigma|F_o|$. [b] $wR_2 = [\Sigma w(F_o^2-F_c^2)^2/\Sigma w(F_o^2)^2]^{1/2}$ where $w = 1/[\sigma^2(F_o^2) + (aP)^2 + bP]$ where $P = (F_o^2 + F_c^2)/3$.

Figure S1. ORTEP molecular drawing of **L1** and **Cat1**. Thermal ellipsoids are draw at 30% of probability level. Hydrogen atoms and disordered -CF_3 moieties are omitted for clarity.

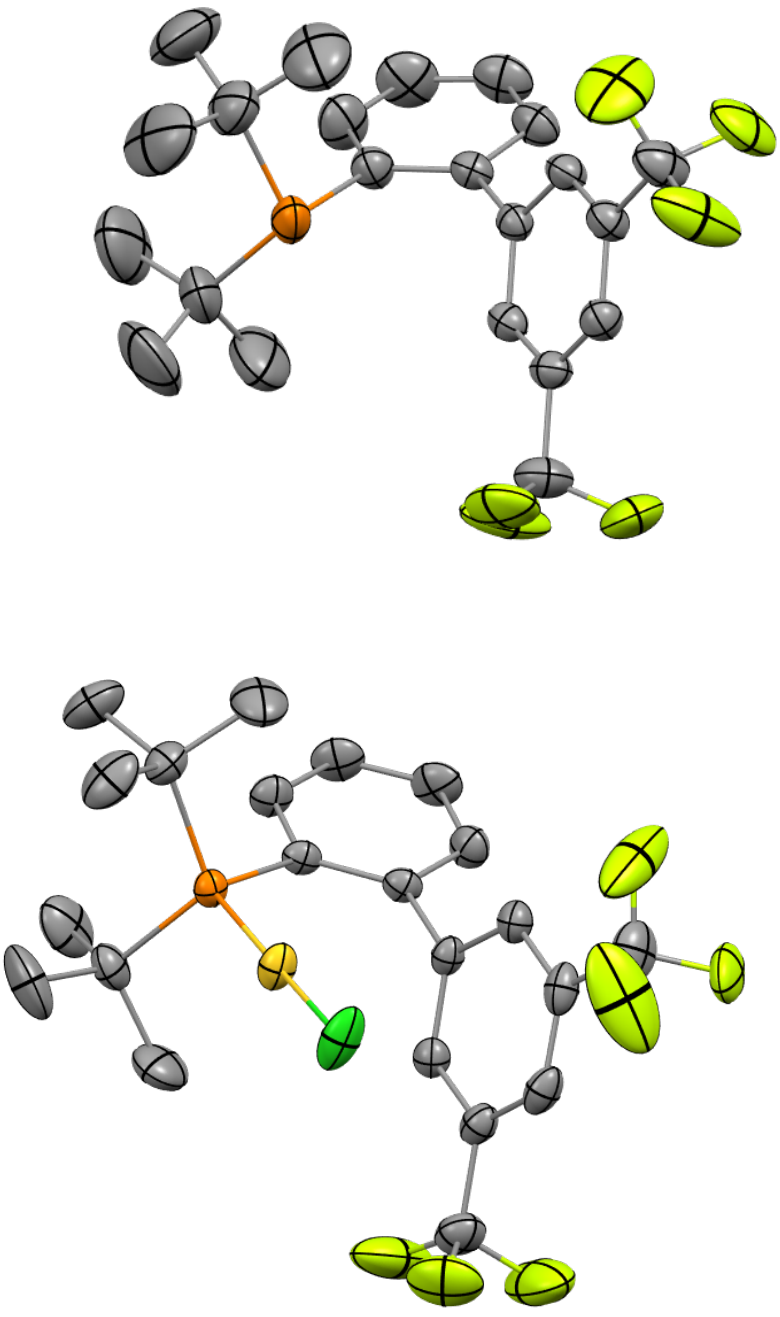

Figure S2. ORTEP molecular drawing of **Cat2**. Thermal ellipsoids are draw at 30% of probability level. Hydrogen atoms and disordered -CF_3 moieties are omitted for clarity.

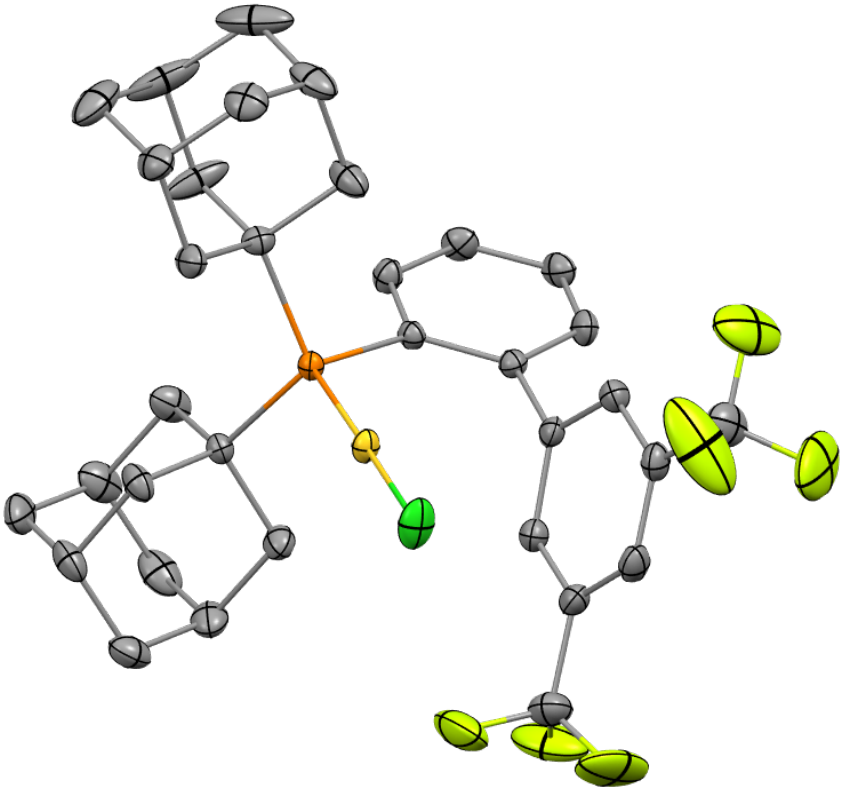

Table S2. Crystal data and structure refinement for compounds **Cat3-5**.

Compound	**Cat3**	**Cat4**	**Cat5**
Formula	$C_{20}H_{24}AuClF_3P$	$C_{32}H_{36}AuClF_3P$	$C_{22}H_{31}AuClO_2P$
Fw	584.78	740.99	590.85
T, K	296 (2)	296(2)	296 (2)
λ, Å	0.71073	0.71073	0.71073
Crystal symmetry	Triclinic	Monoclinic	Monoclinic
Space group	*P-1*	$P2_1/c$	$P2_1/n$
***a*, Å**	10.3440(9)	10.1009(6)	8.530(2)
***b*, Å**	14.739(1)	27.464(2)	10.205(3)
***c*, Å**	15.695(1)	11.0036(7)	26.581(8)
α	80.768(2)	90	90
β	86.013(2)	100.449(2)	97.56(1)
γ	74.571(2)	90	90
Cell volume, Å^3	2275.9(3)	3001.9(3)	2293.9(1)
Z	4	4	4
Dc, Mg m^{-3}	1.707	1.640	1.711
μ(Mo-K$_\alpha$), mm^{-1}	6.677	5.081	6.613
F(000)	1128	1464	1160
Crystal size/ mm	0.31 x 0.21 x 0.18	0.22 x 0.17 x 0.11	0.28 x 0.12 x 0.08
θ limits, °	1.807 to 25.500	2.396 to 25.998	1.546 to 25.495
Reflections collected	28269	37886	25188
Unique obs. Reflections [$F_o > 4\sigma(F_o)$]	8251 [R(int) = 0.0382]	5896 [R(int) = 0.0374]	4253 [R(int) = 0.0432]
Goodness-of-fit-on F^2	1.060	1.315	1.215
R_1 (F)[a], wR_2 (F^2)[b] [I > 2σ(I)]	R1 = 0.0324, wR2 = 0.0664	R1 = 0.0508, wR2 = 0.1027	R1 = 0.0409, wR2 = 0.0885
Largest diff. peak and hole, e. Å^{-3}	0.895 and -1.052	1.310 and -2.451	2.215 and -3.625
CCDC	2327554	2327555	2327556

[a] $R_1 = \Sigma||F_o|-|F_c||/\Sigma|F_o|$. [b] $wR_2 = [\Sigma w(F_o^2-F_c^2)^2/\Sigma w(F_o^2)^2]^{1/2}$ where $w = 1/[\sigma^2(F_o^2) + (aP)^2 + bP]$ where $P = (F_o^2 + F_c^2)/3$.

Figure S3. ORTEP molecular drawing of **Cat3** and **Cat4**. Thermal ellipsoids are draw at 30% of probability level. Hydrogen atoms are omitted for clarity. For **Cat3** only one of the two molecules in the asymmetric unit is shown.

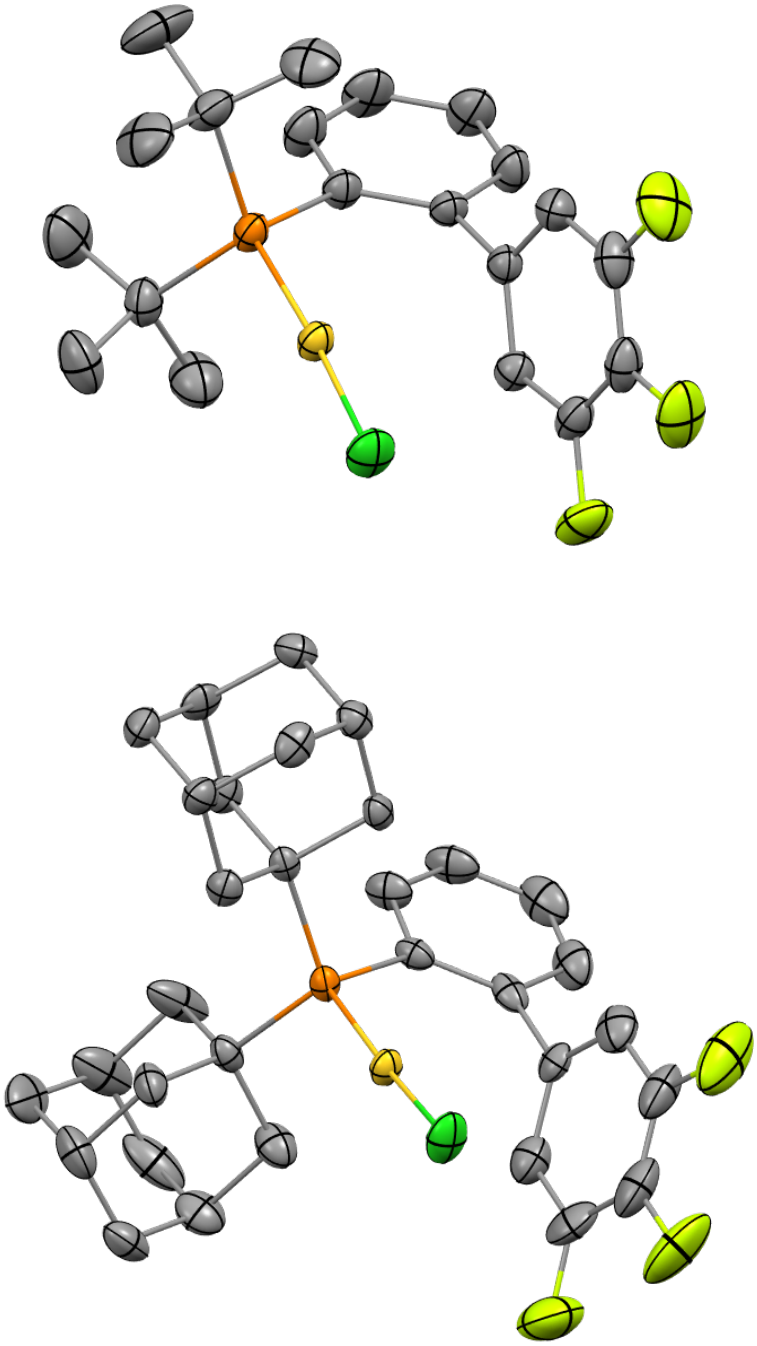

Figure S4. ORTEP molecular drawing of **Cat5**. Thermal ellipsoids are draw at 30% of probability level. Hydrogen atoms are omitted for clarity.

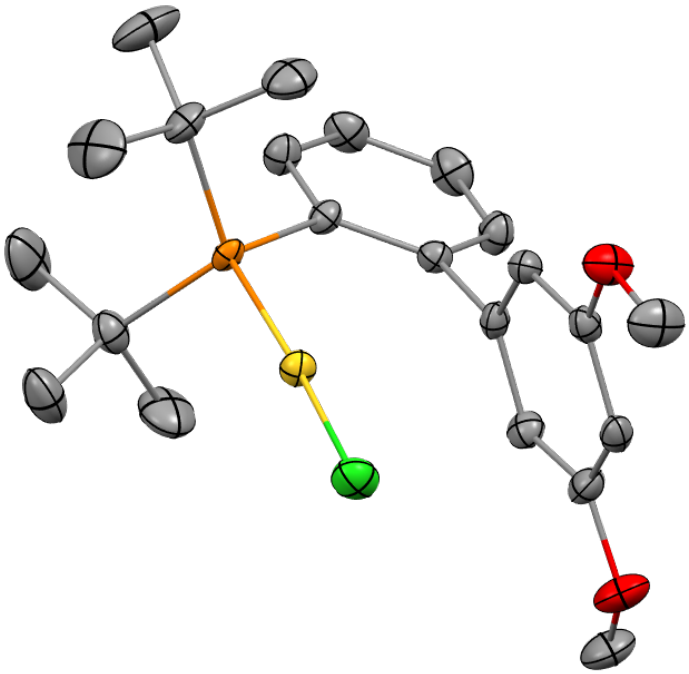

Computational Study

The B3LYP[9]/6-31+G(d,p) level of theory was used for the reactivity investigation, while the inner electrons of Au were described by the SDD effective core potential.[10] This is not the optimal DFT combination for gold catalysis but, considering the size and complexity of the structures at hand, it is a good cost effective model according to ad-hoc benchmarks.[11]

The SCF convergence was conducted using an ultrafine grid. The nature of the stationary points as minima or TSs was characterized by analysis of the normal modes via diagonalization of the Hessian matrix. In challenging cases, IRC calculations were performed to connect the minima that are associated with a TS without ambiguity. The geometry optimizations were carried out at the gas phase, due to high computational cost of the involved structures, while the final energies that are reported are electronic energies acquired by performing single point calculations with a dichloromethane (DCM) solvent environment on the gas phase optimized geometry. The solvation effects were considered using the PCM implicit solvation model.[12]

Table S3. *DFT calculated bond distances at the ωB97XD/6-31+G(d,p)+SDD level.*

Catalyst	Bond Distance (Å)		
	Ar---Au	Au-P	Au-Cl
JohnPhosAuCl	3.344	2.316	2.359
Cat1	3.274	2.317	2.354
Cat3	3.293	2.315	2.355
Cat5	3.267	2.318	2.362

Table S4. Inter-arene dihedral angle values for the computed and the X-ray structures of the catalysts.

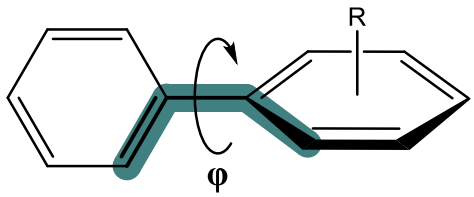

Structure	**Computational Dihedral (degrees)**	**X-Ray Dihedral (degrees)**
JohnPhos	93.0	90.0
PedroPhos	93.6	72.3
Cat3	94.7	81.0
Cat5	97.0	69.9

Alternative path to *endo* isomer

To investigate the excellent stereoselectivity of the reaction, we performed additional calculations to model the path that would lead to the *endo* isomer **3a''**. This excellent control in stereoselectivity that is observed

experimentally can be explained by the thermodynamic instability of the intermediate that would lead to the endo product. Due to the flatness of the potential energy surface (PES) we were unable to locate the transition state leading to this intermediate. Instead, we approximated it using a relaxed scan calculation. Specifically, we initiated the scan from the optimized structure **10**, and varied the distance leading to the opening of the three-carbon ring. We used the highest point of this scan as an approximation of the transition state, which in fact lays only 0.3 kcal/mol higher from **10**. Such an unstable intermediate (**10**) would allow the reverse reaction to take place, *i.e.* return to **5** (which is 4.8 kcal/mol more stable) and then proceed through one of the observable paths, leading either to product **3a** or **3a'.** The full reaction mechanism, including the unobserved endo product is presented in Scheme S1.

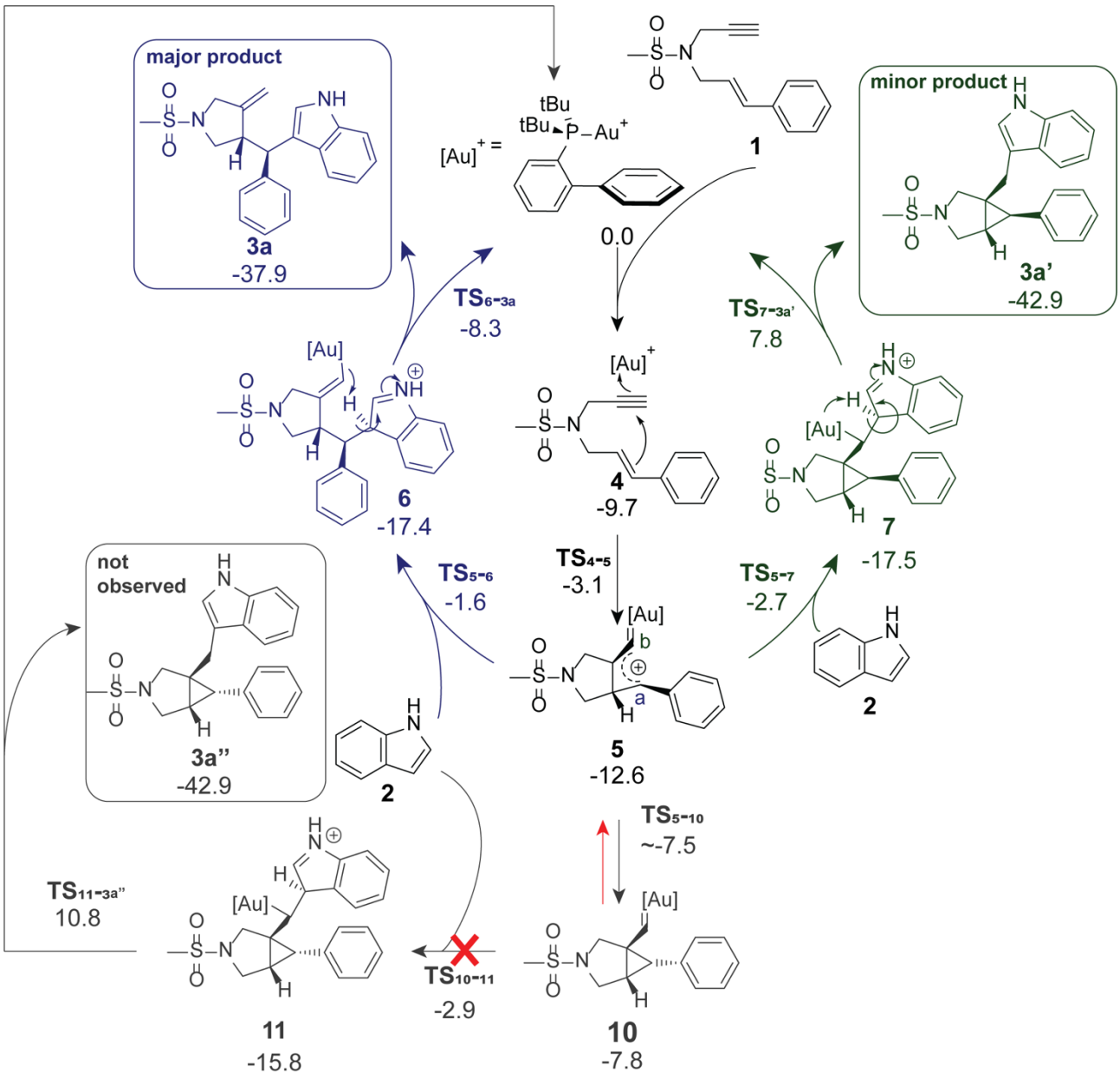

Scheme S1. Schematic representation of the suggested reaction mechanism using the JohnPhosAu catalyst. SCF energies in a dichloromethane solvent environment have been obtained as single point calculations on the gas phase geometry optimized structures at B3LYP/6-31+G(d,p) + SDD level. The energy differences are reported in kcal/mol.

Theoretical investigation of a possible poisoning effect of the final product to the catalyst

The kinetic studies suggested faster initial cycles, when compared to the following ones, which led us to assume that the final product invokes a deleterious effect on the catalyst. In order to assess our hypothesis, we performed additional calculations that allowed us to compare the thermodynamic difference between the final complex ([JohnPhosAu + **3a** or **3a'**) and the precomplex constituted by [JohnPhosAu] + **1a** + **2**. In both cases, the final complex proved to be significantly more stable than the precomplex, which explains the slowdown of the reaction as the concentration of **3a**/**3a'** increases. Furthermore, as a means to investigate whether this effect is even stronger for the lowest performing **Cat5**, we conducted the same calculation using this catalyst as well. In fact, we observed that the complexation between **Cat5** and the major product **3a** is indeed stronger than the one for JohnPhos (-35.1 kcal/mol), which may contribute to the fact that the OMe substituted catalyst provides lower yields.

The results are presented in Scheme S2.

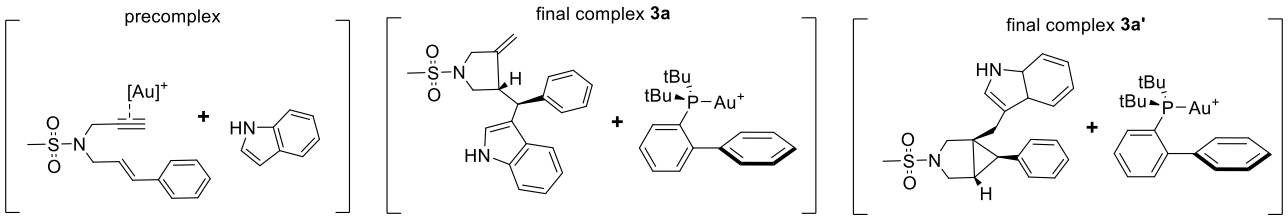

Catalyst	**ΔG_{3a}**	**$\Delta G_{3a'}$**
JohnPhos	-34.3	-21.7
Cat5	-35.1	-21.3

Scheme S2. Theoretical investigation of the putative catalyst poisoning invoked by the final products.

Geometrical Characteristics of the computed catalysts

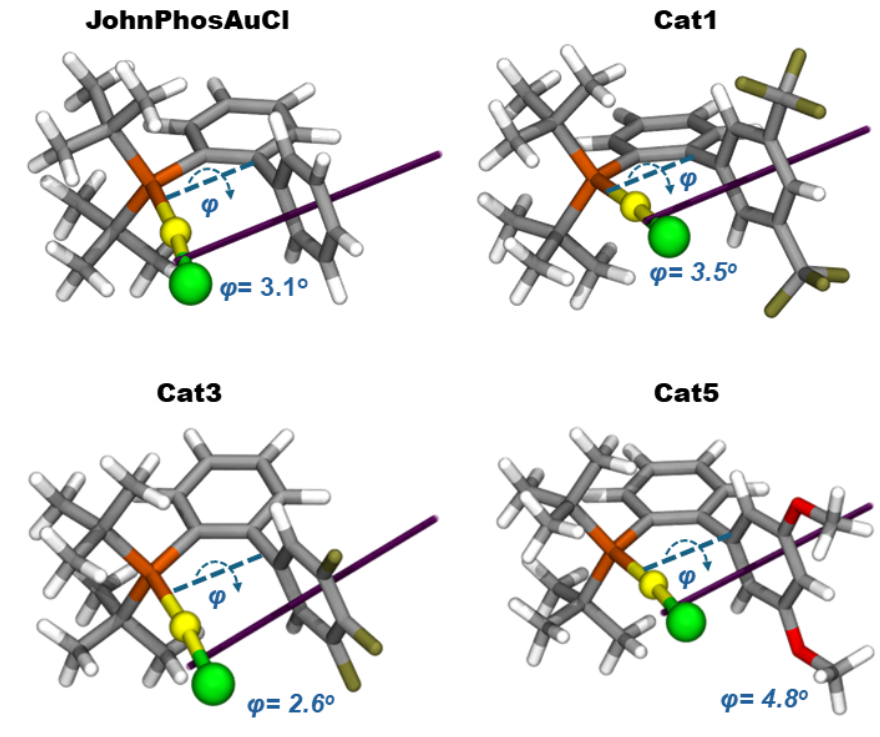

Scheme S3. DFT structures of JohnPhosAuCl, **Cat1**, **Cat3** and **Cat5** at the ωB97XD/ 6-31+G(d,p) + SDD level showing the parallel orientation between the P-Au-Cl bond and the biaryl, with dihedral values of ϕ ranging from 2.6 to 4.8 degrees. The distal aromatic ring axis in purple helps visualize the relative position of this ring and the gold atom.

Non-covalent Interactions (NCI) and Atoms In Molecules (AIM) Topology analysis of the computed catalysts

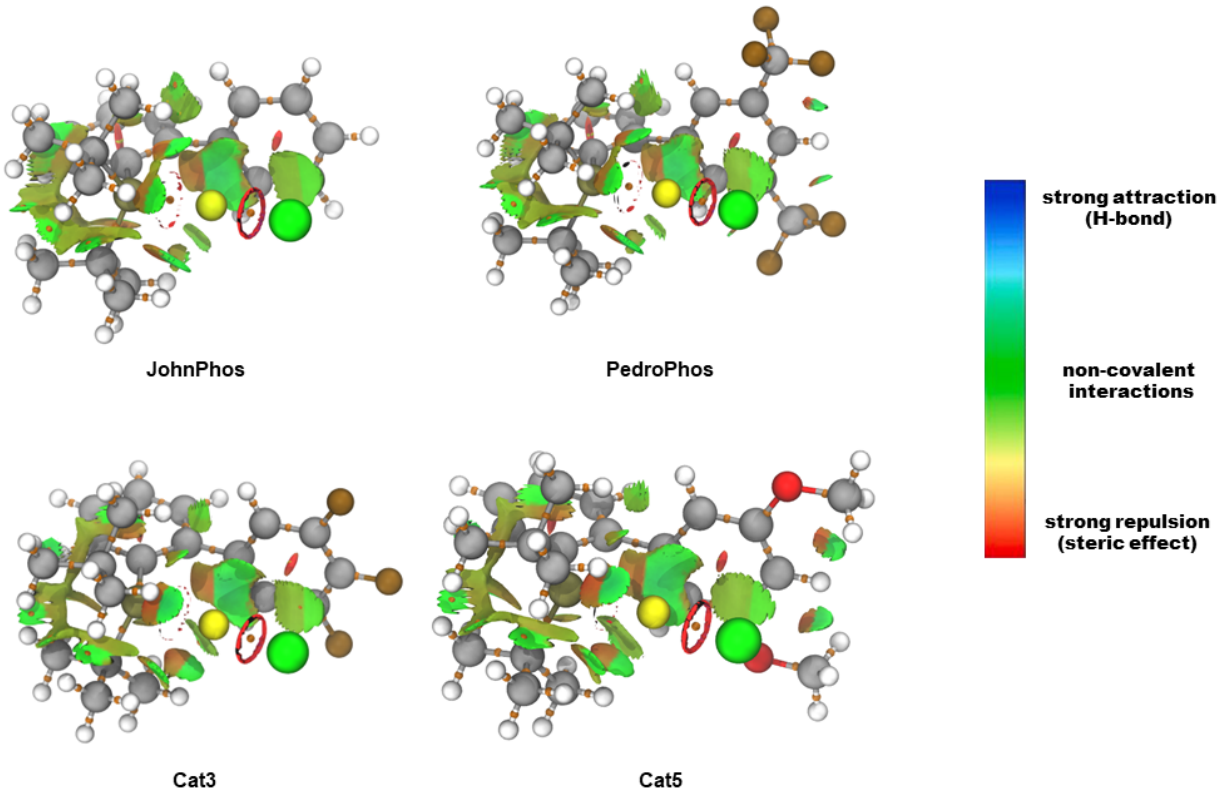

Scheme S4. NCI and AIM analyses of JohnPhos, PedroPhos, **Cat3** and **Cat5**, as implemented in the MultiWfn 3.8 software.[13] Geometry optimizations and wavefunction calculations were performed at the ωB97XD/ 6-31+G(d,p) + SDD level of theory. The critical bond points are represented with orange dots. The non-covalent interactions are represented as per the figure's legend. No covalent bonds are detected between the Au atom and the arene ring, but attractive, non-covalent interactions can be observed.

Non-covalent Interactions (NCI) of the intermediate 5 with JohnPhos, PedroPhos and Cat5

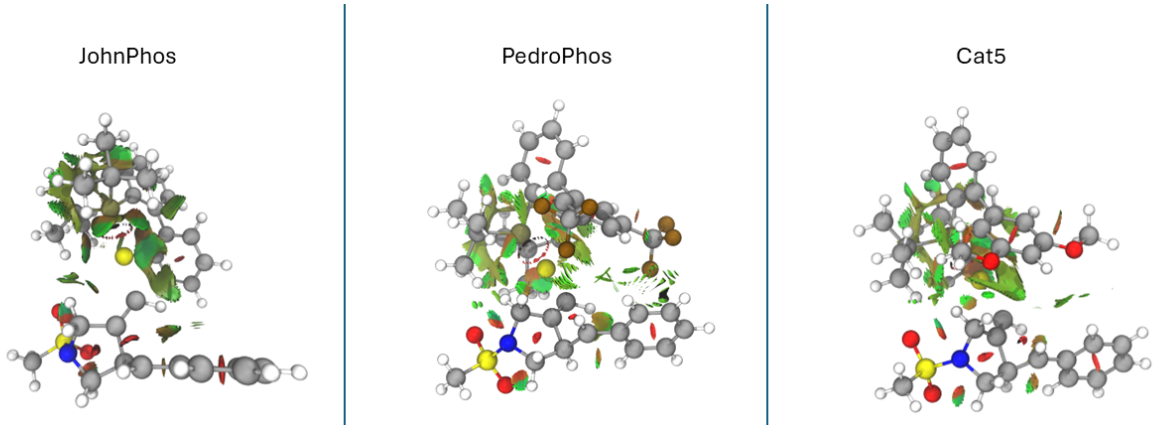

Scheme S5. NCI analysis of the non-classical cationic intermediate **5** with JohnPhos, PedroPhos and Cat5. In the substituted catalysts, PedroPhos and **Cat5**, non-covalent interactions are established with the terminal phenyl of the substrate and the catalyst. These interactions stabilize the conformation of the complex while their absence, as in the case of JohnPhos, makes the reacting complex more flexible, leading to a loss of selectivity.

All the computed structures in this work have been uploaded to the ioChem-BD repository where Cartesian coordinates, energies and frequencies are made publicly available by using the following doi: http://dx.doi.org/10.19061/iochem-bd-6-329

NMR Spectra

^{1}H NMR

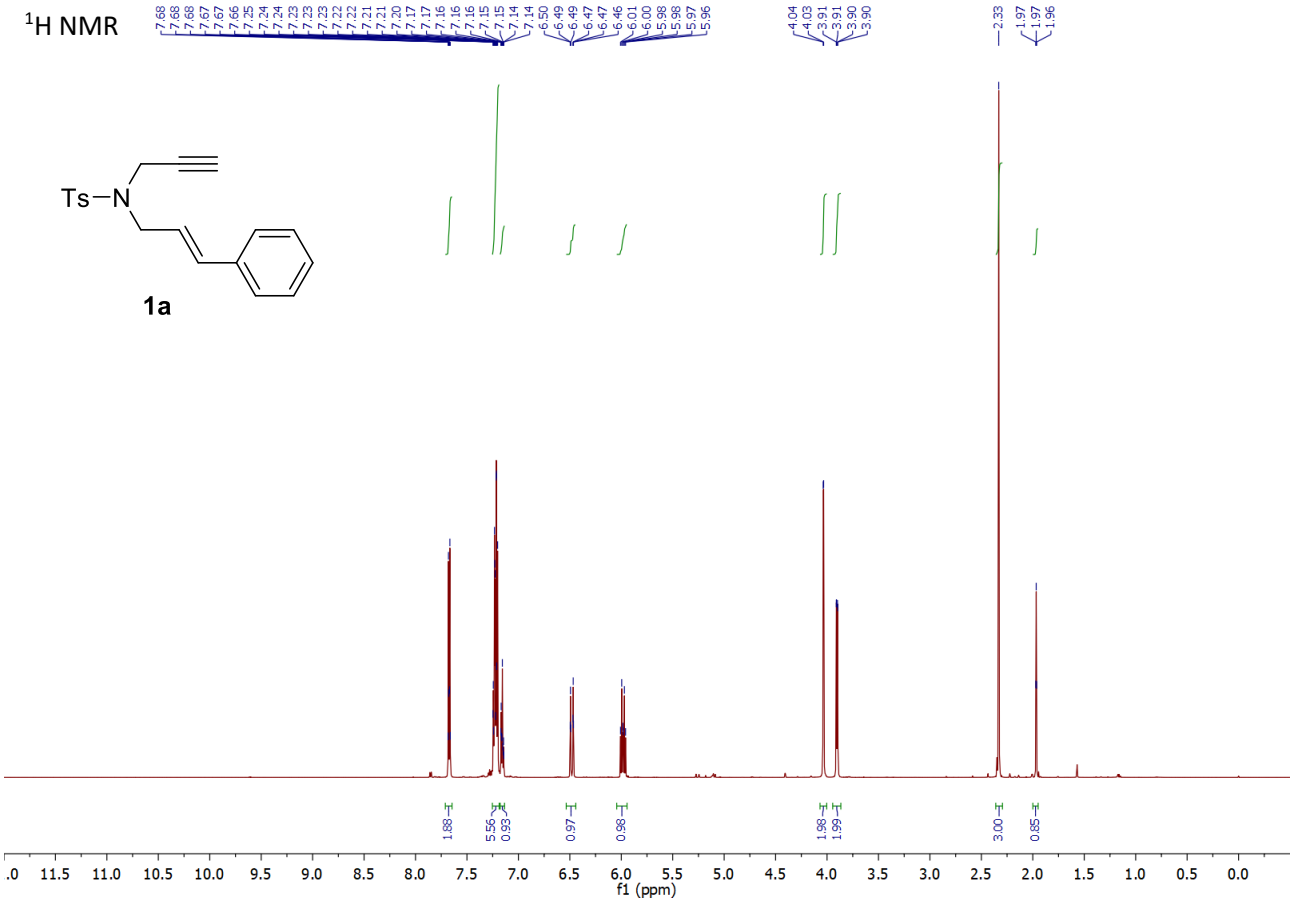

^{13}C NMR

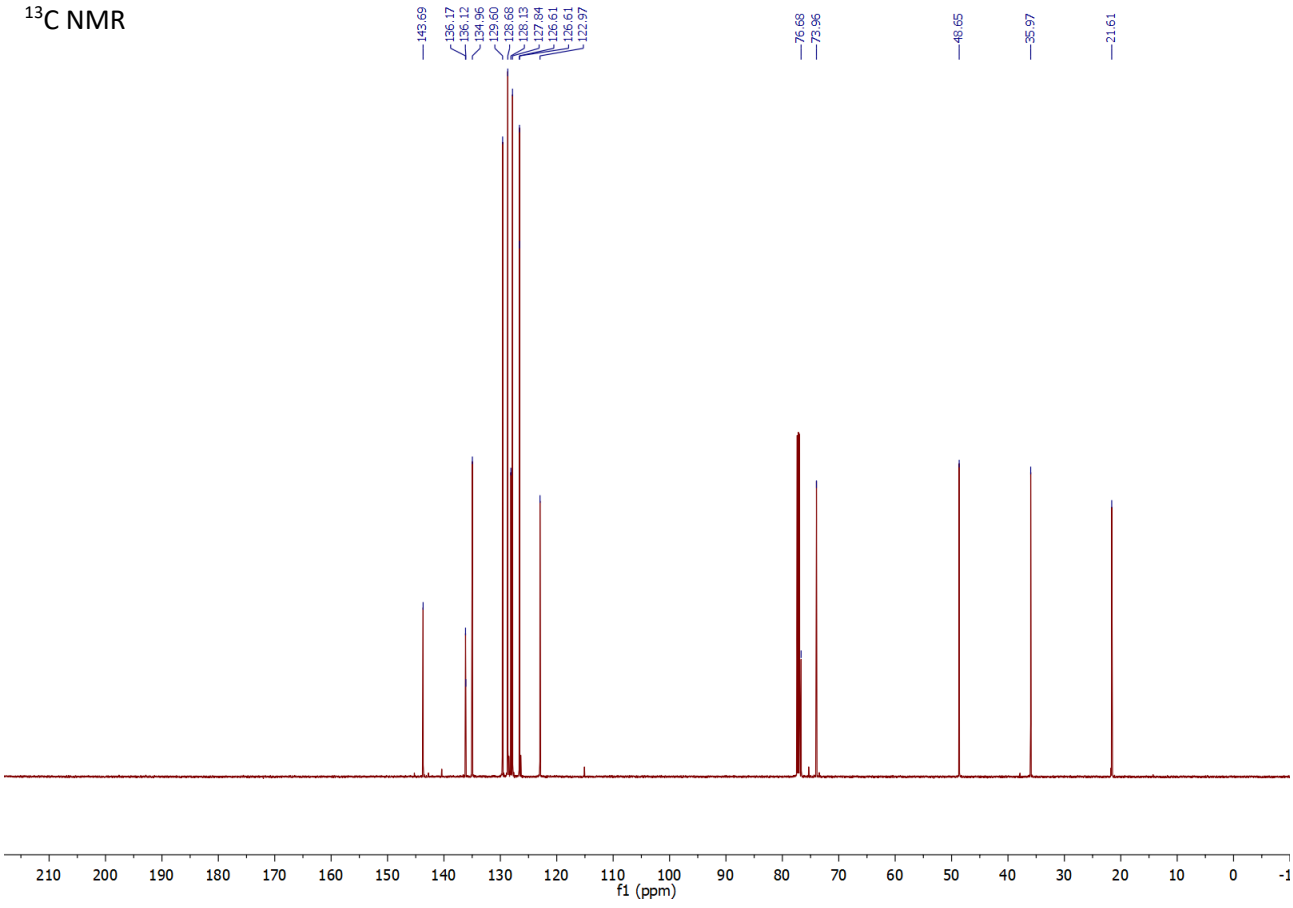

^{1}H NMR

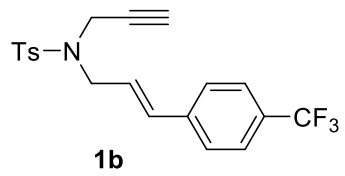

1b

^{13}C NMR

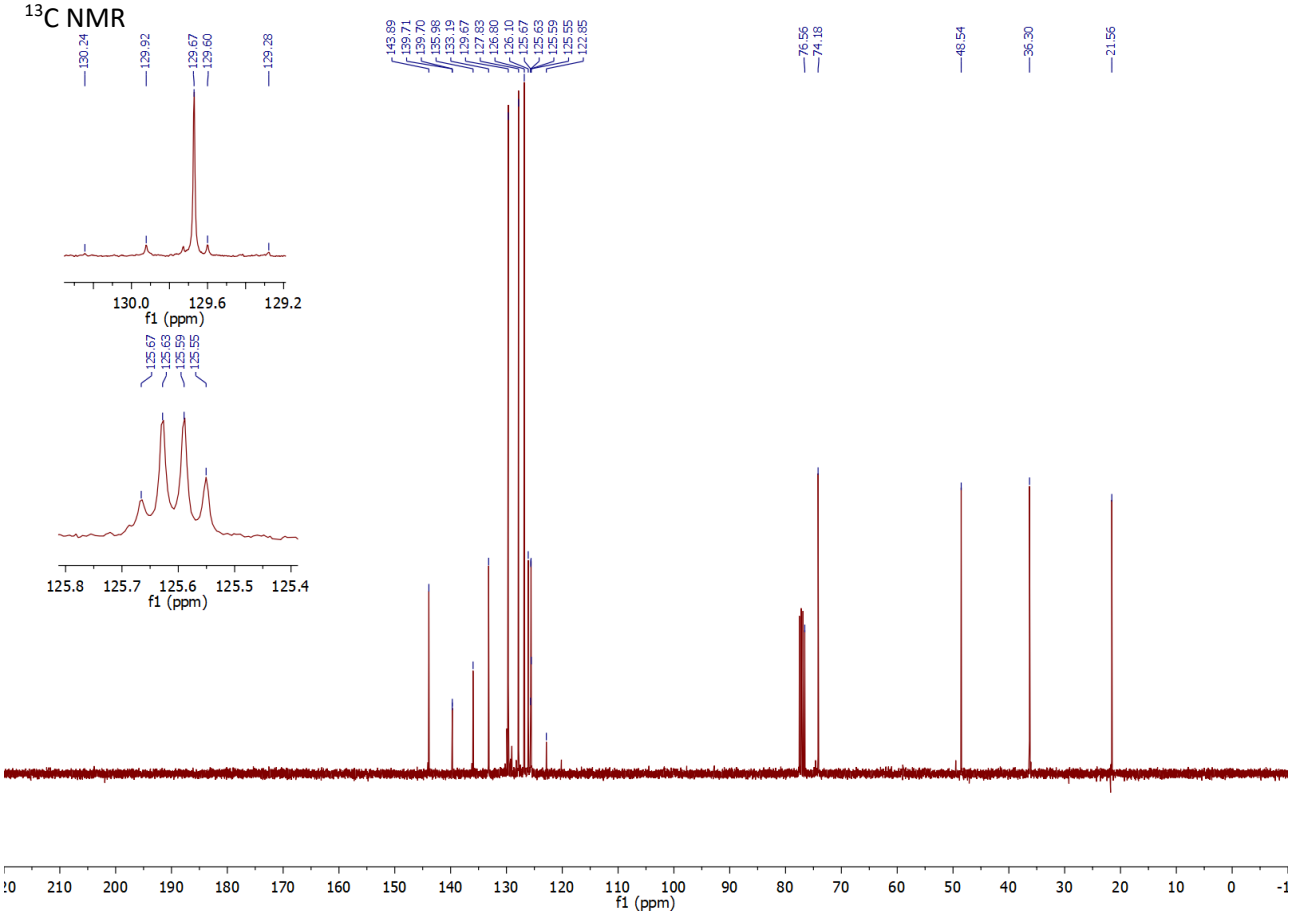

^{19}F NMR

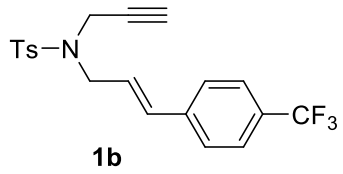
Ts—N
CF3

1b

-62.53
6.00
30 20 10 0 -10 -20 -30 -40 -50 -60 -70 -80 -90 -100 -110 -120 -130 -140 -150 -160 -170 -180 -190 -200
f1 (ppm)

^{1}H NMR

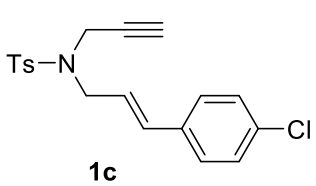

1c

^{13}C NMR

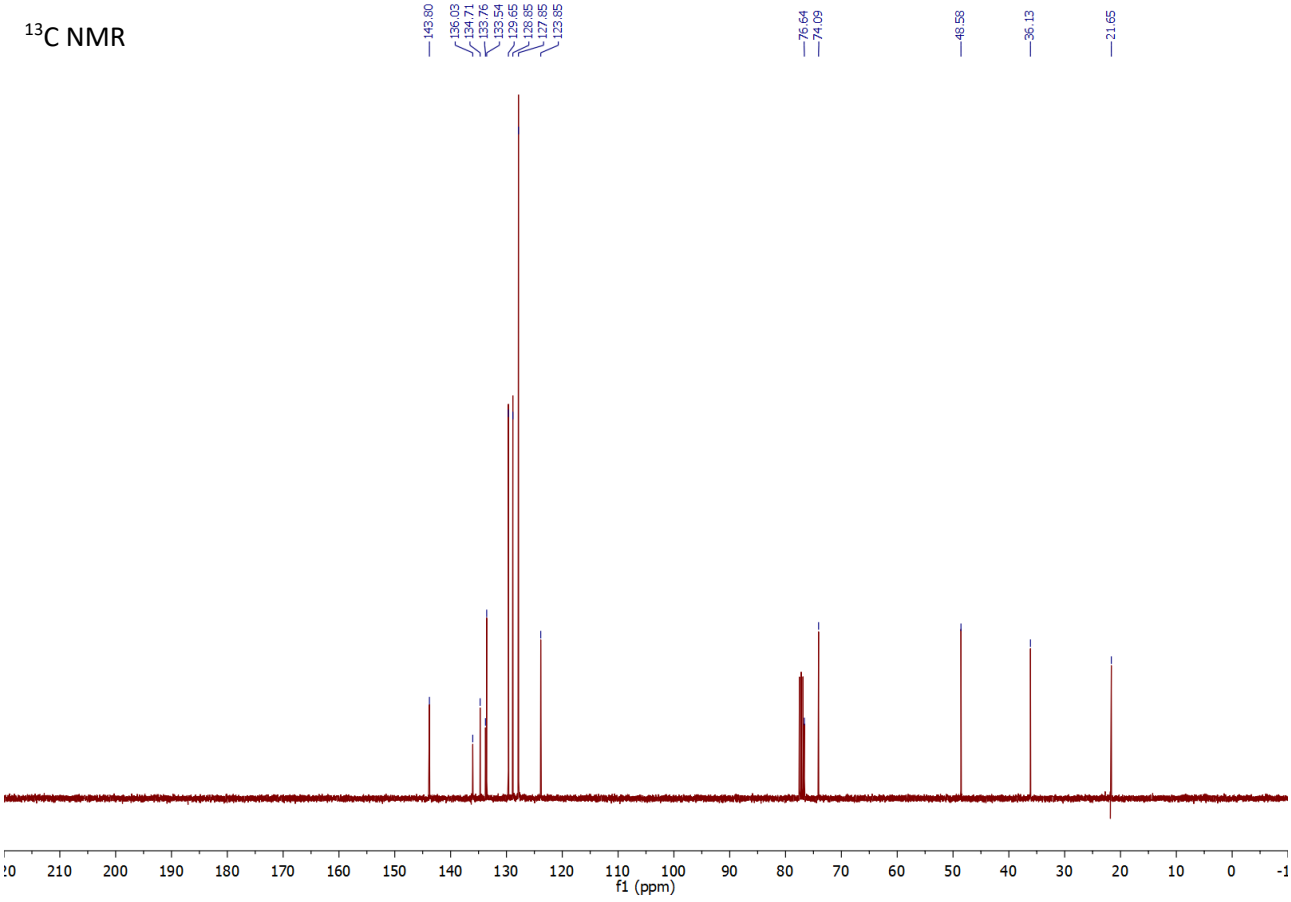

^{1}H NMR

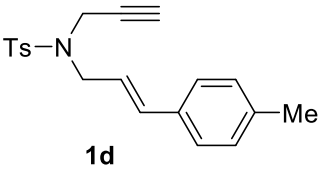

1d

^{13}C NMR

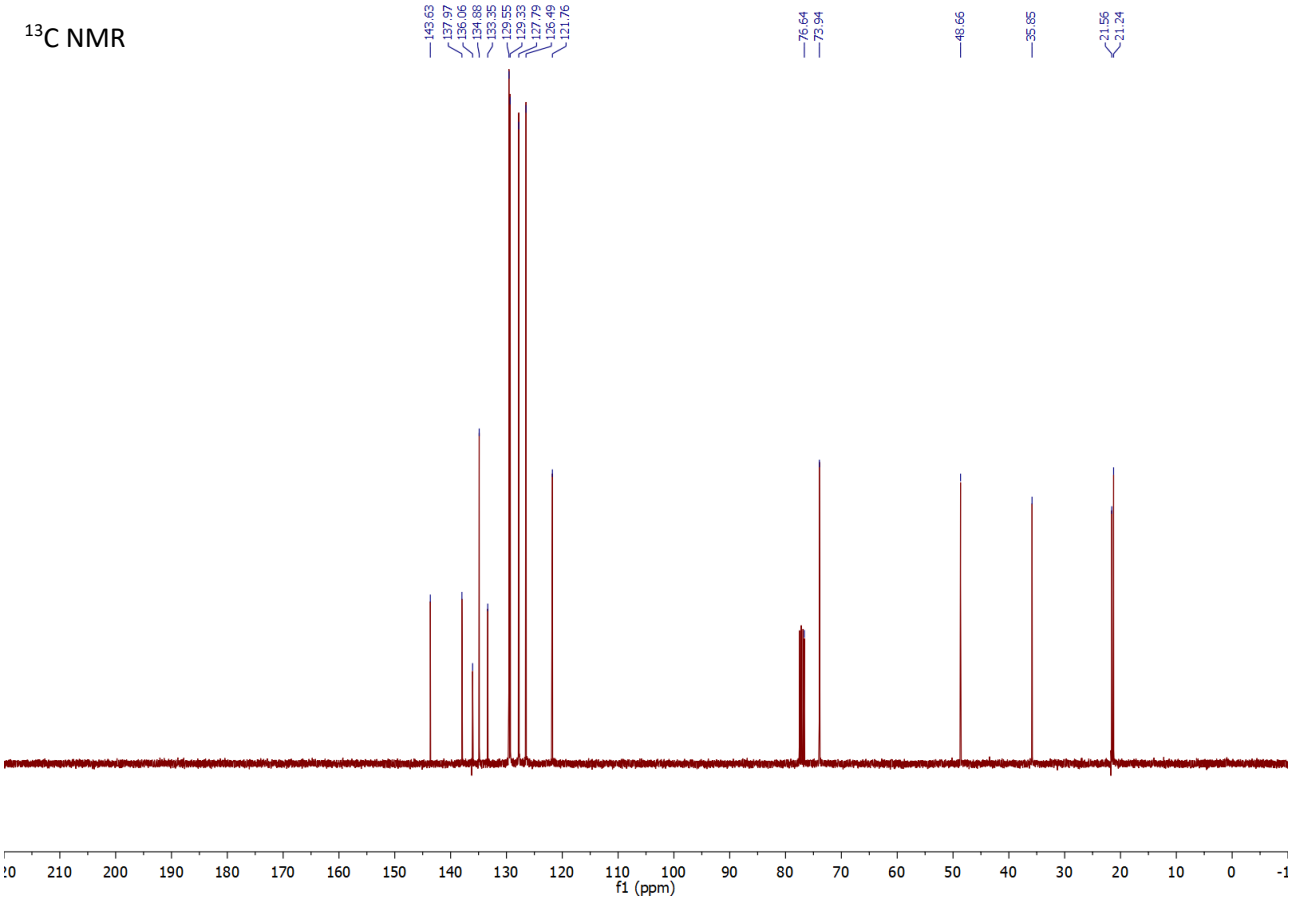

^{1}H NMR

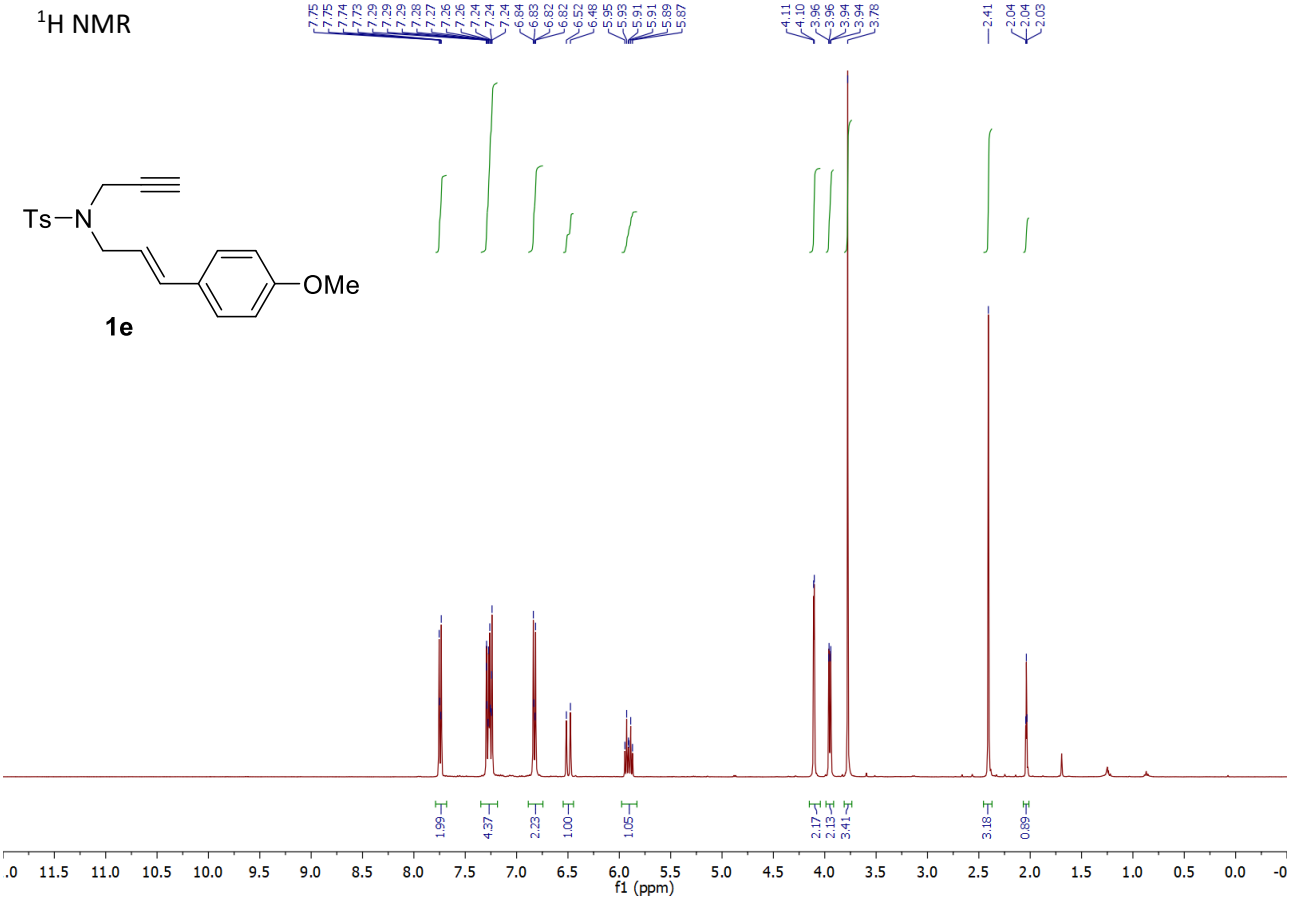

^{13}C NMR

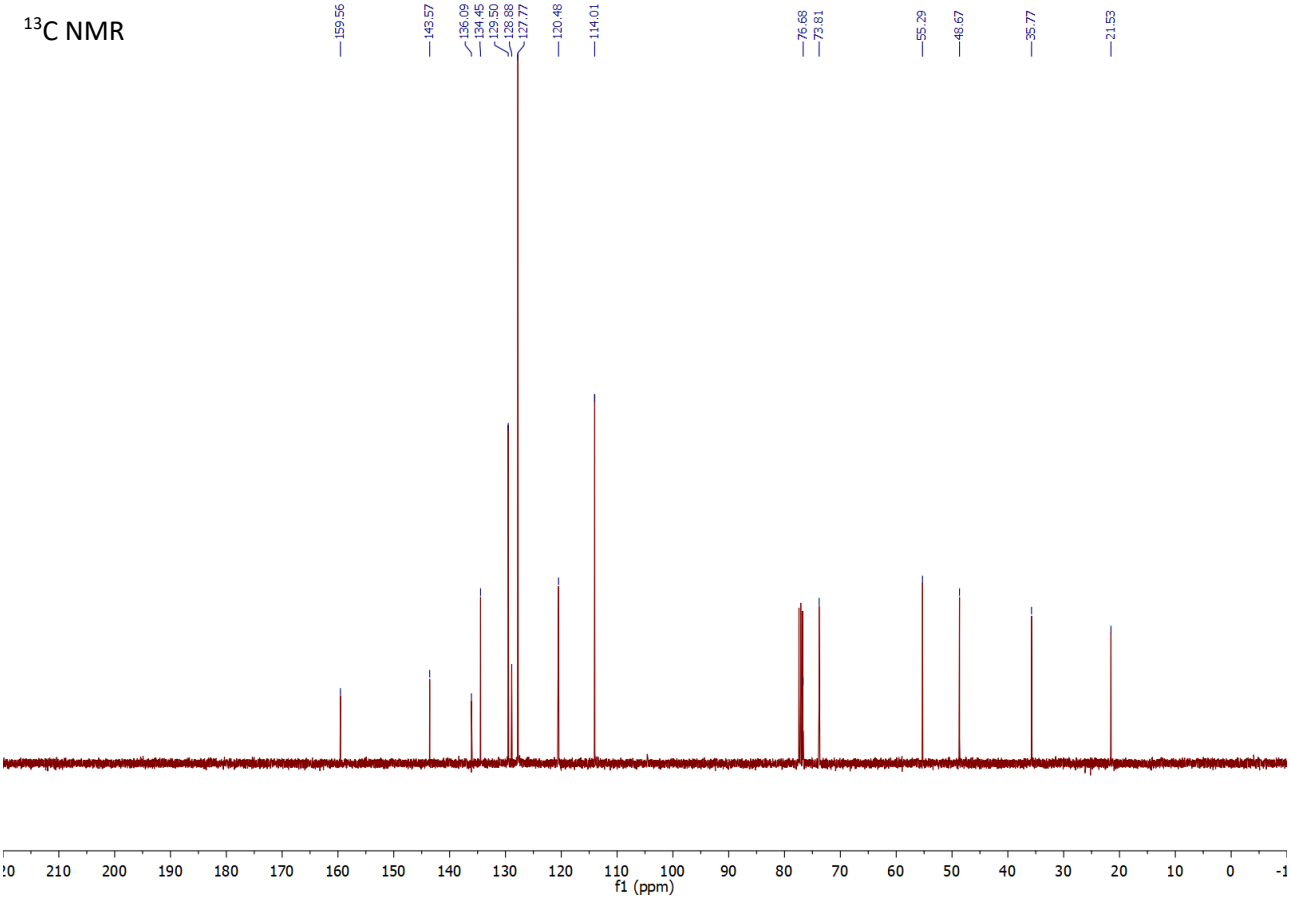

^{1}H NMR

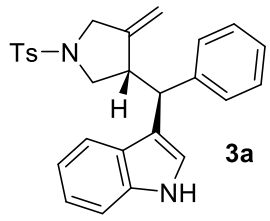

3a

^{13}C NMR

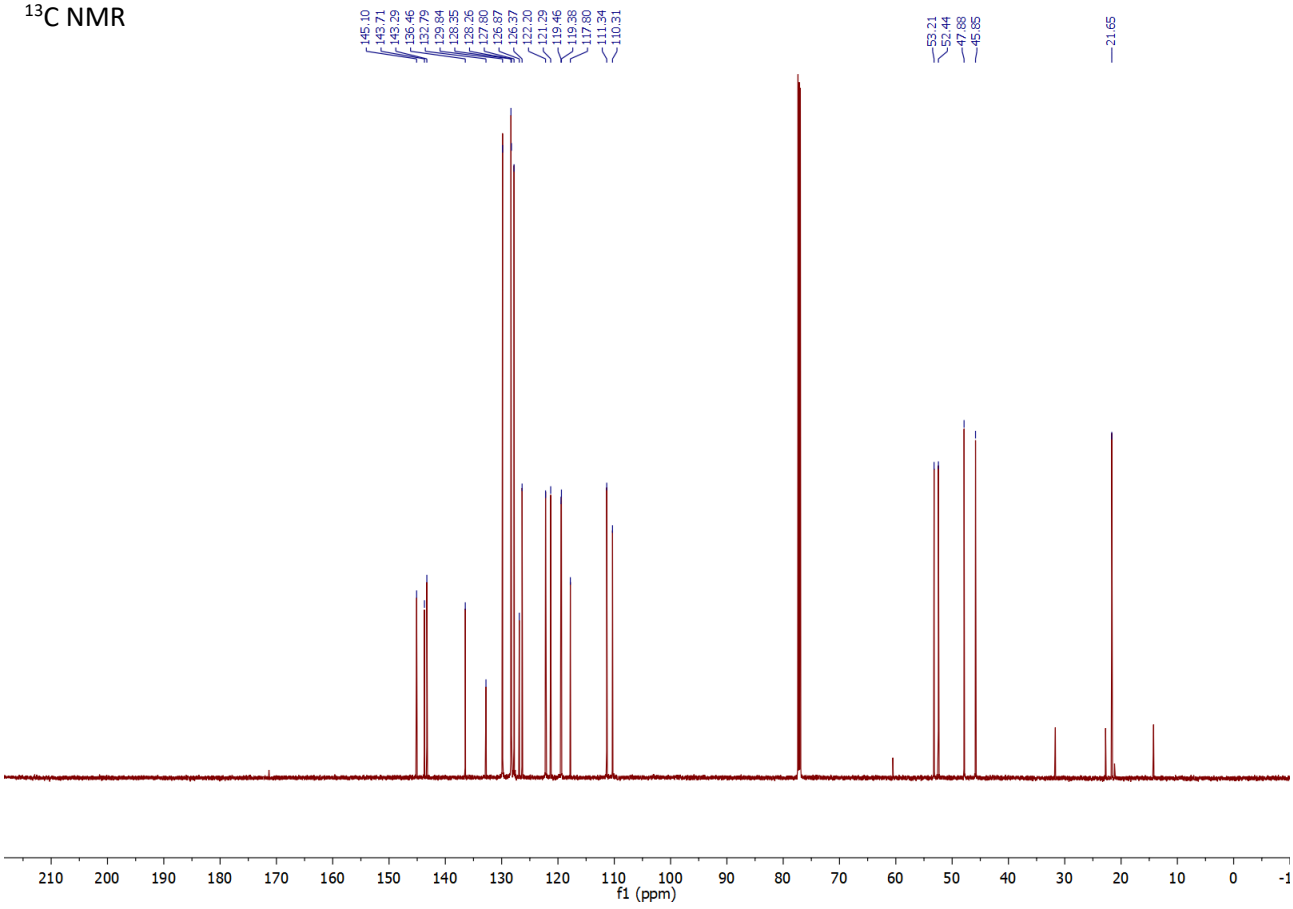

^{1}H NMR

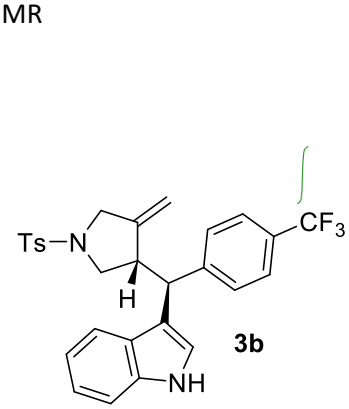

3b

^{13}C NMR

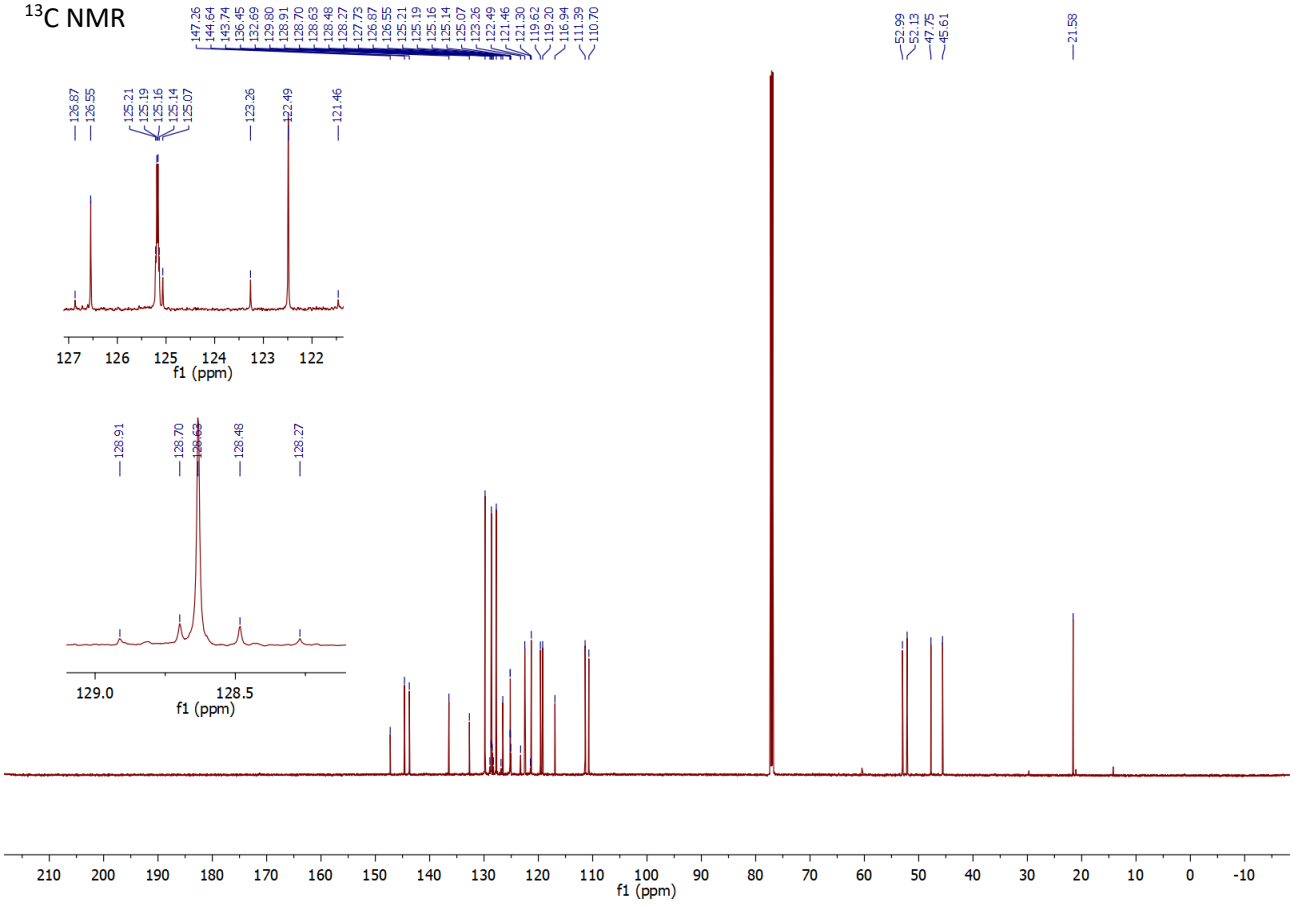

^{19}F NMR

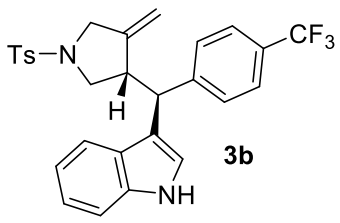
Ts
N
H
CF3
NH

3b

-62.35
6.00
10
0
-10
-20
-30
-40
-50
-60
-70
-80
-90
-100
-110
-120
-130
-140
-150
-160
-170
-180
-190
-200
-210
f1 (ppm)

^{1}H NMR

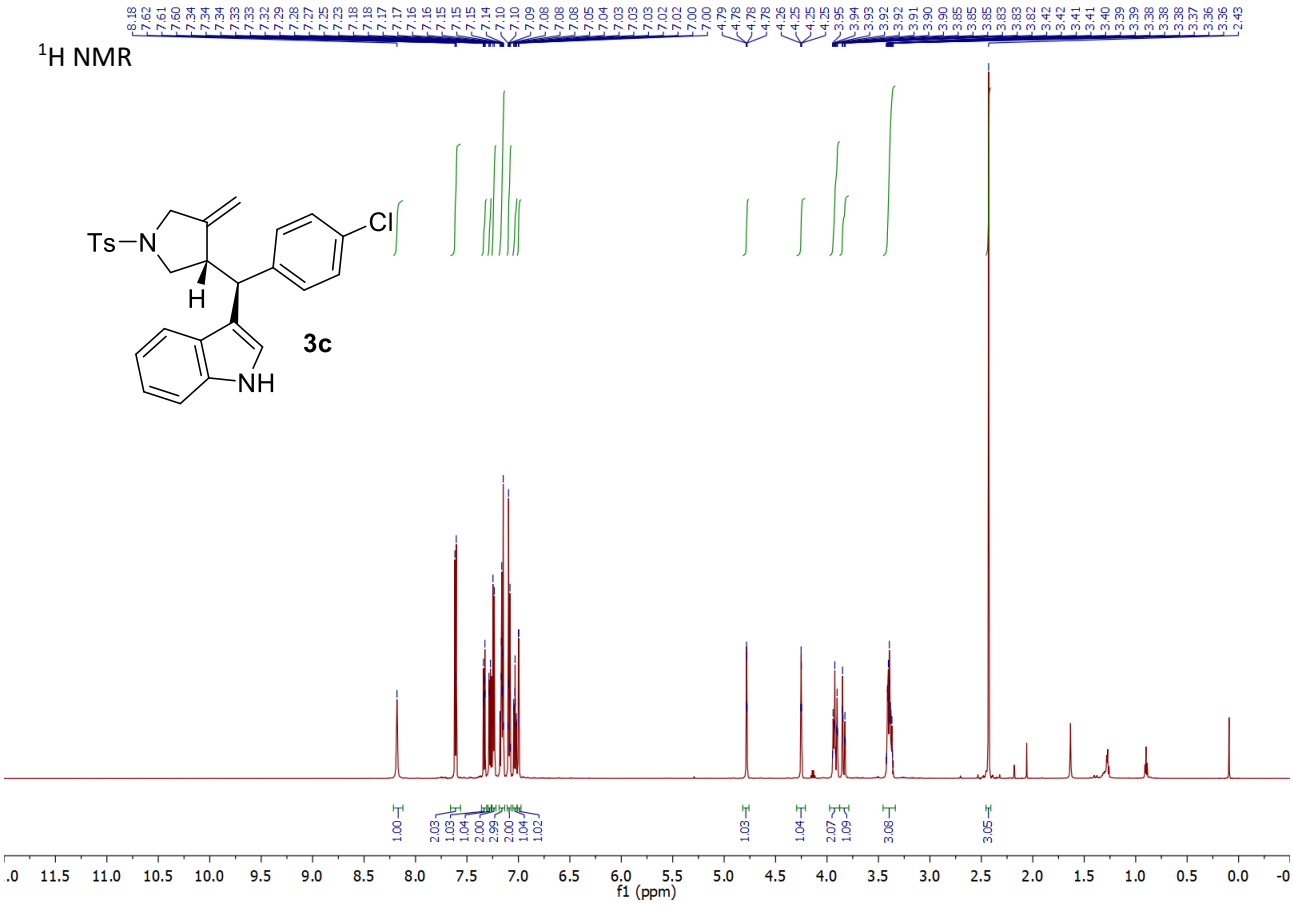

^{13}C NMR

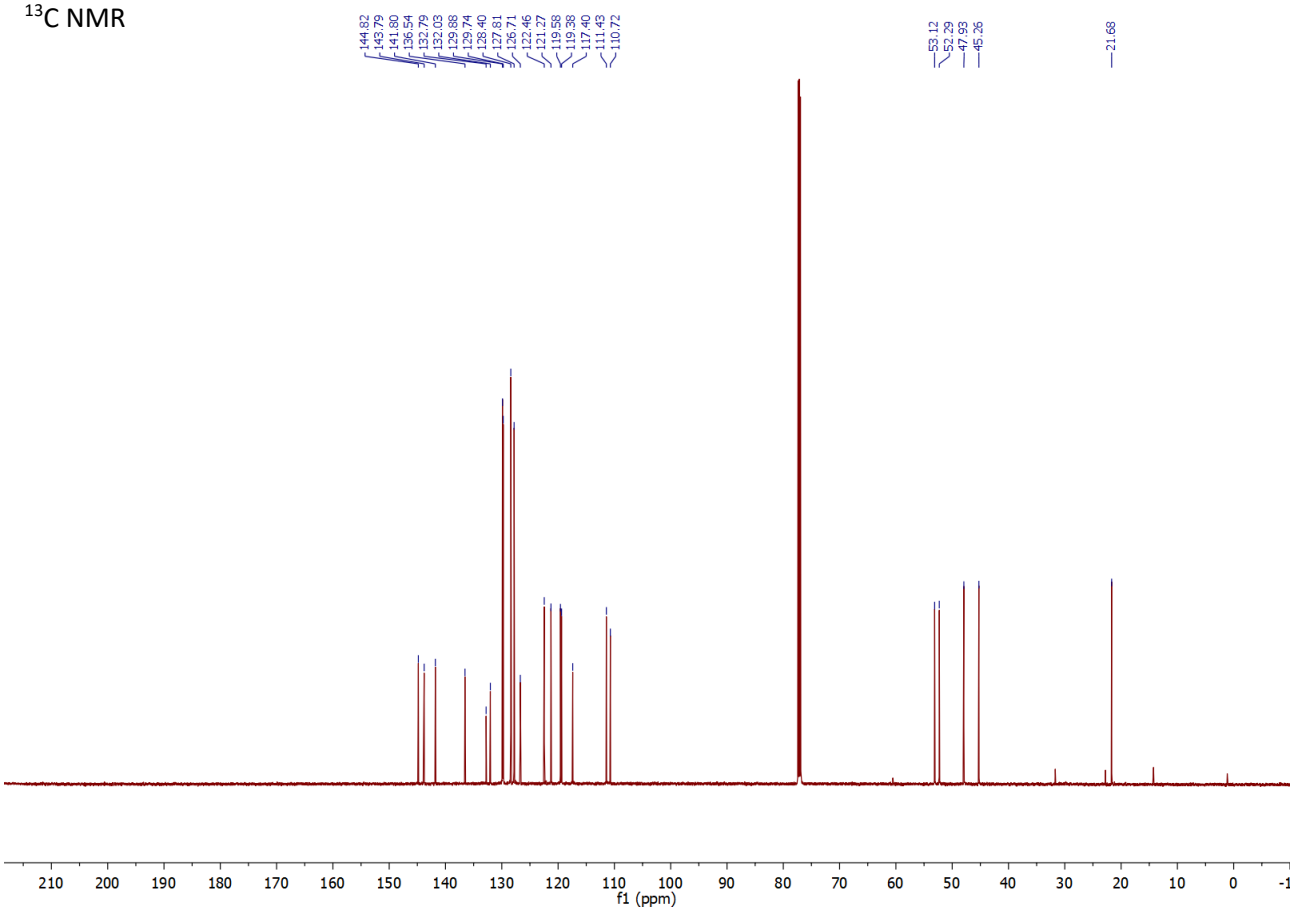

^{1}H NMR

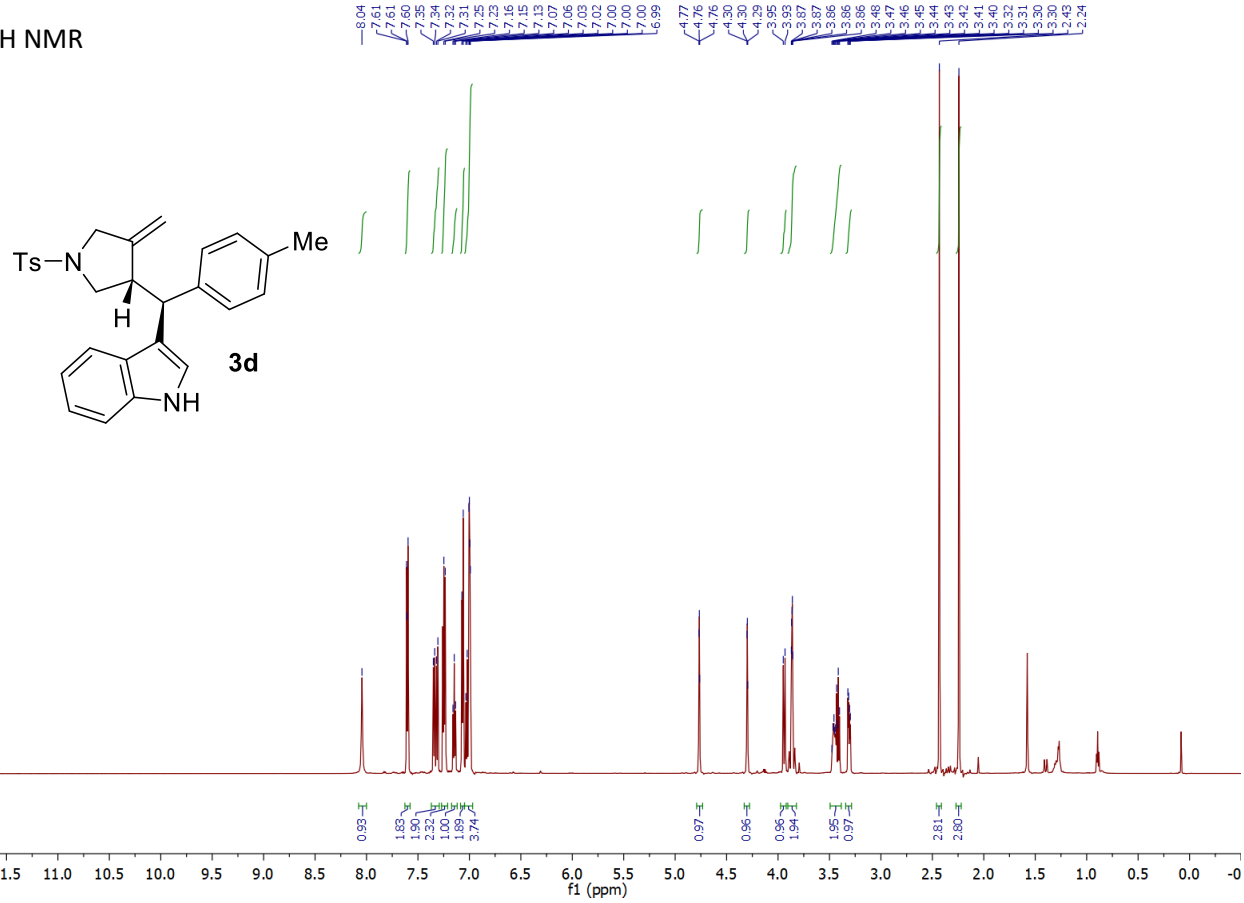

^{13}C NMR

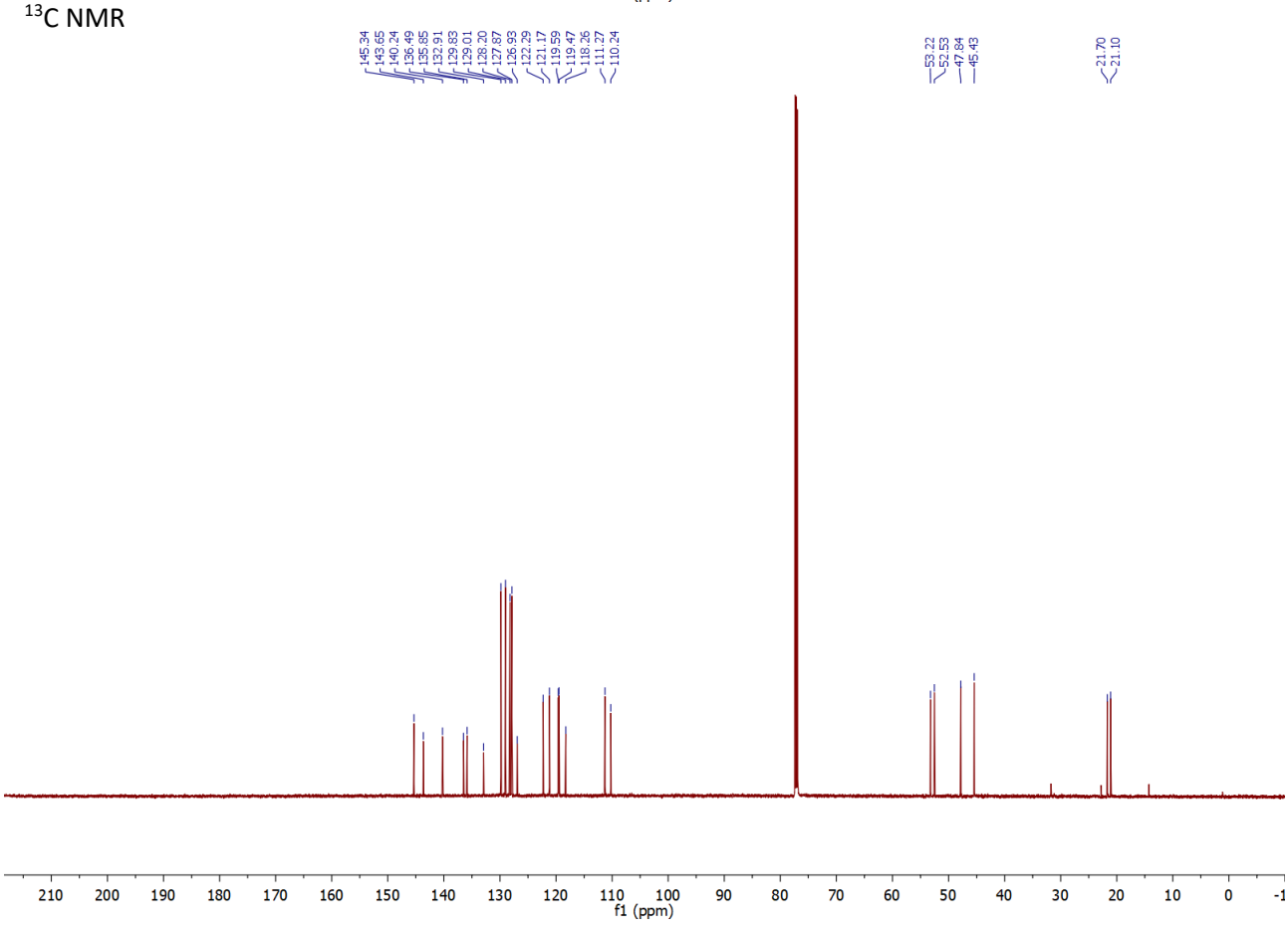

^{1}H NMR

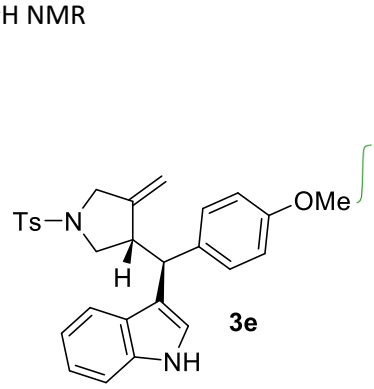

3e

^{13}C NMR

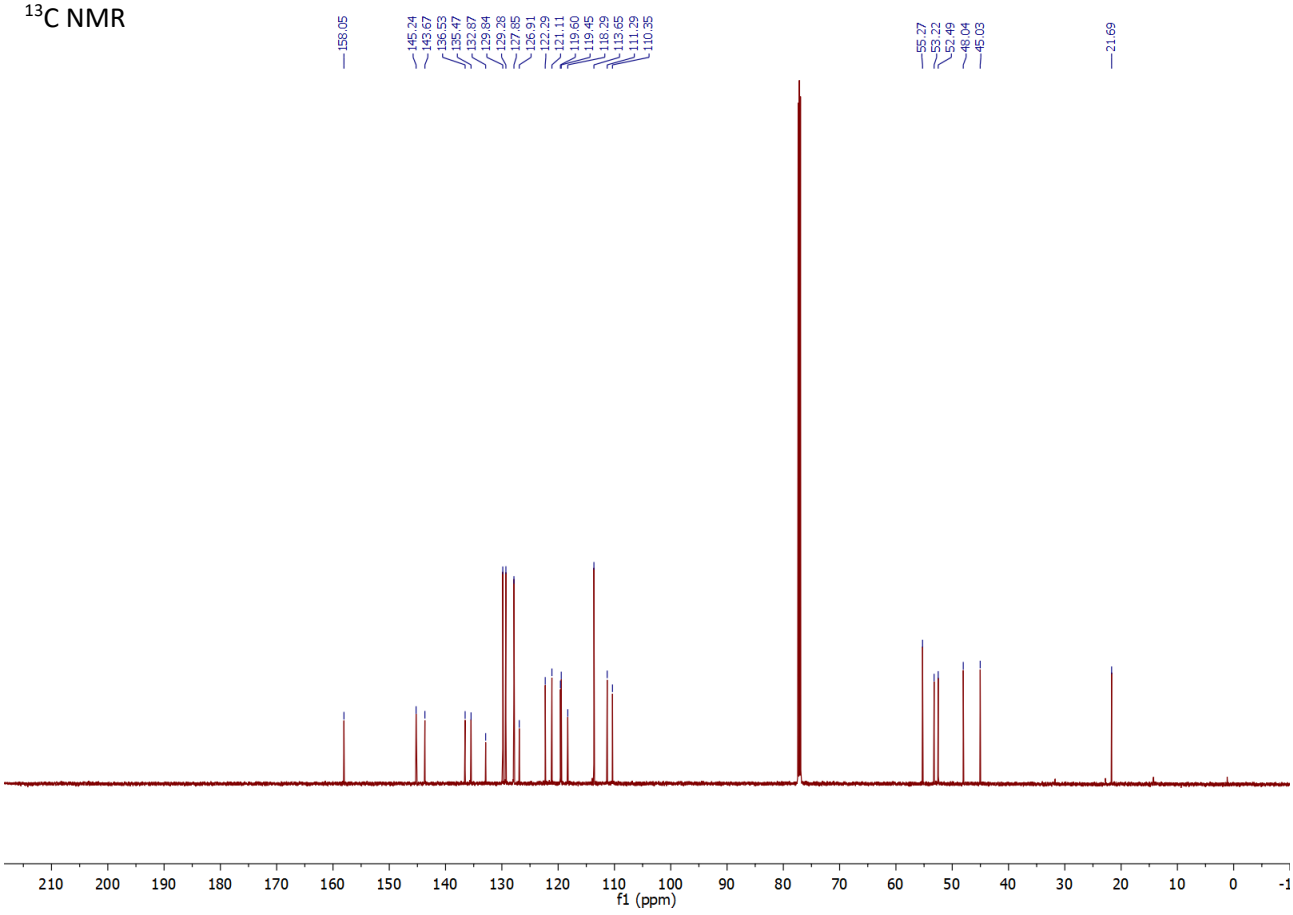

^{1}H NMR

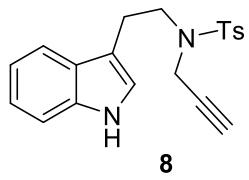

8

^{13}C NMR

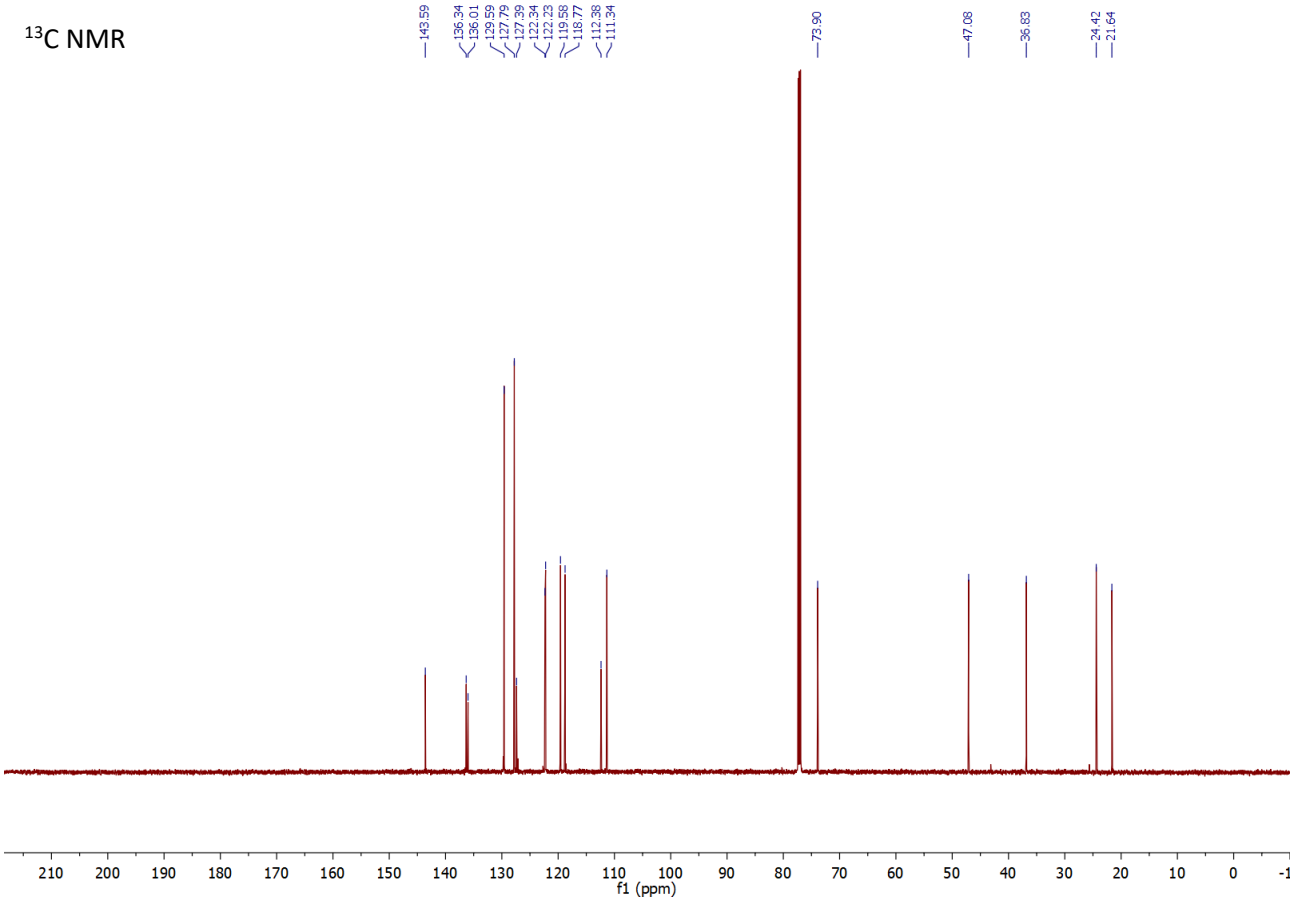

^{1}H NMR

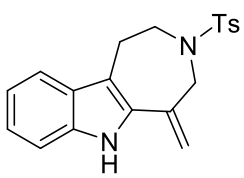

9

^{13}C NMR

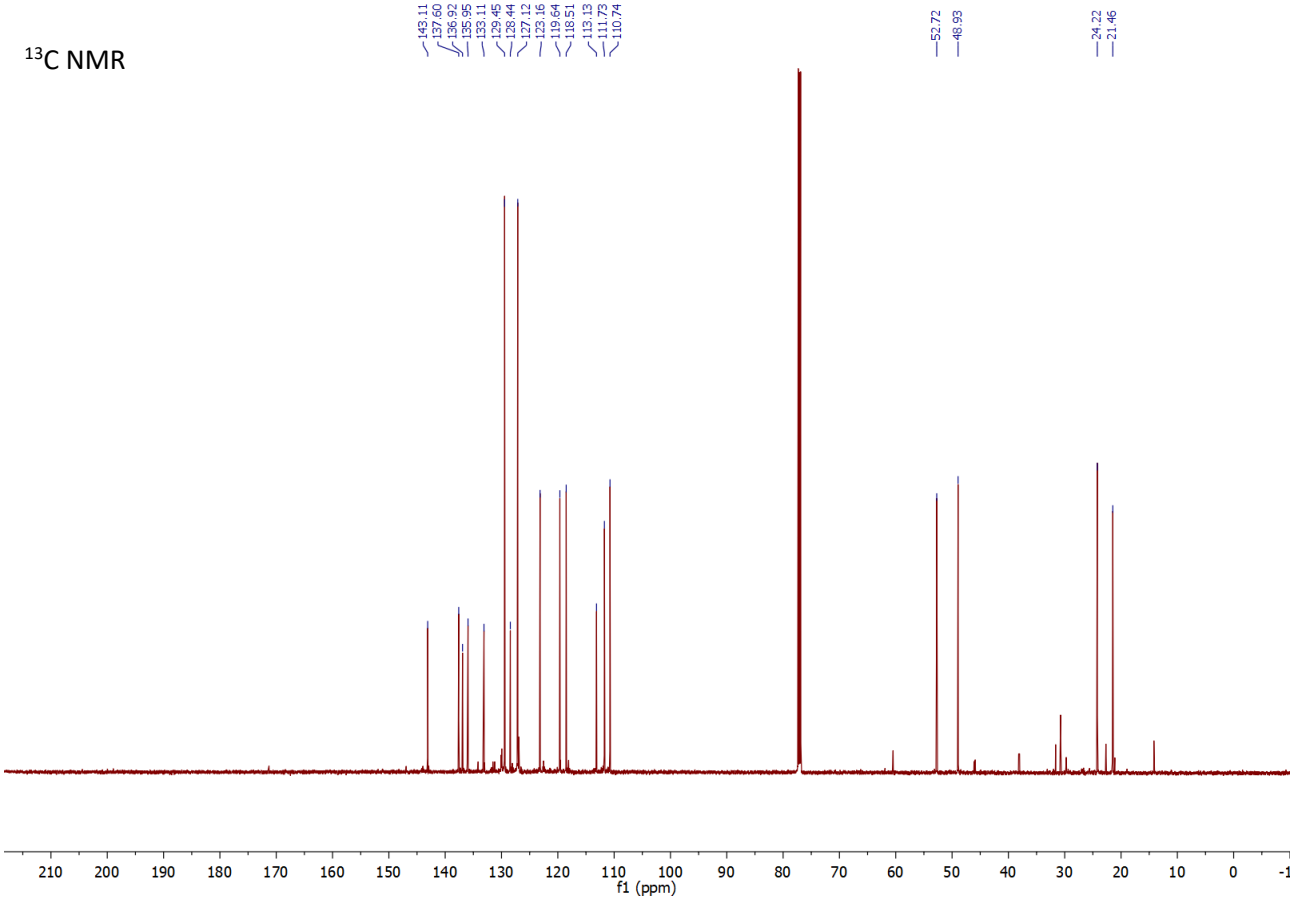

^{1}H NMR

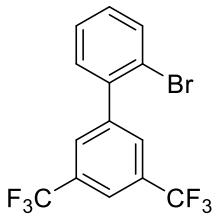

A1

^{13}C NMR

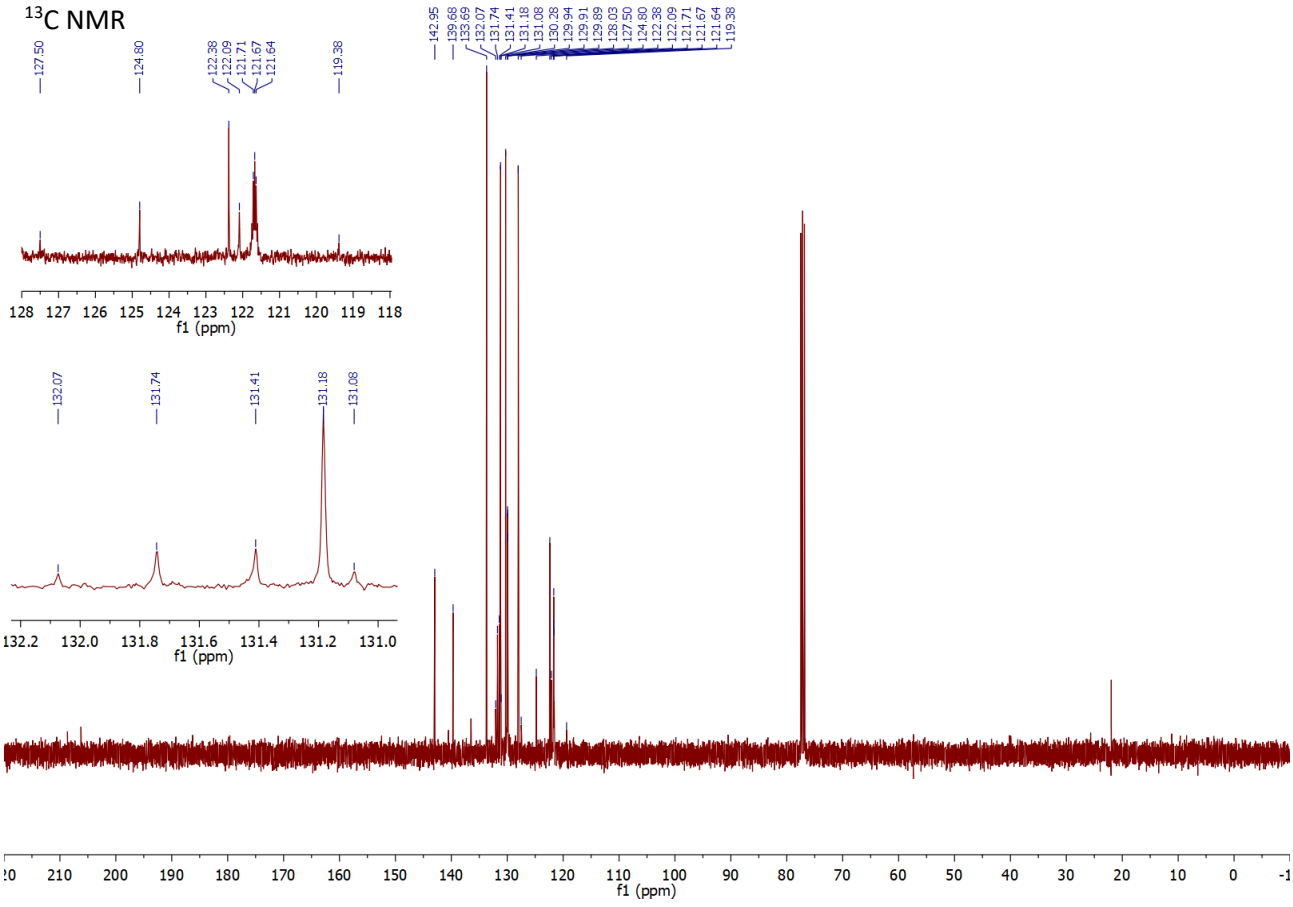

^{19}F NMR

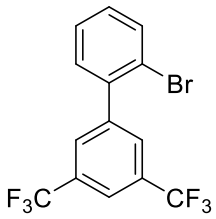
Br
F3C
CF3

A1

-62.86
6.00
30 20 10 0 -10 -20 -30 -40 -50 -60 -70 -80 -90 -100 -110 -120 -130 -140 -150 -160 -170 -180 -190 -200
f1 (ppm)

^{1}H NMR

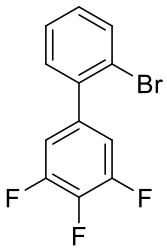

A2

^{13}C NMR

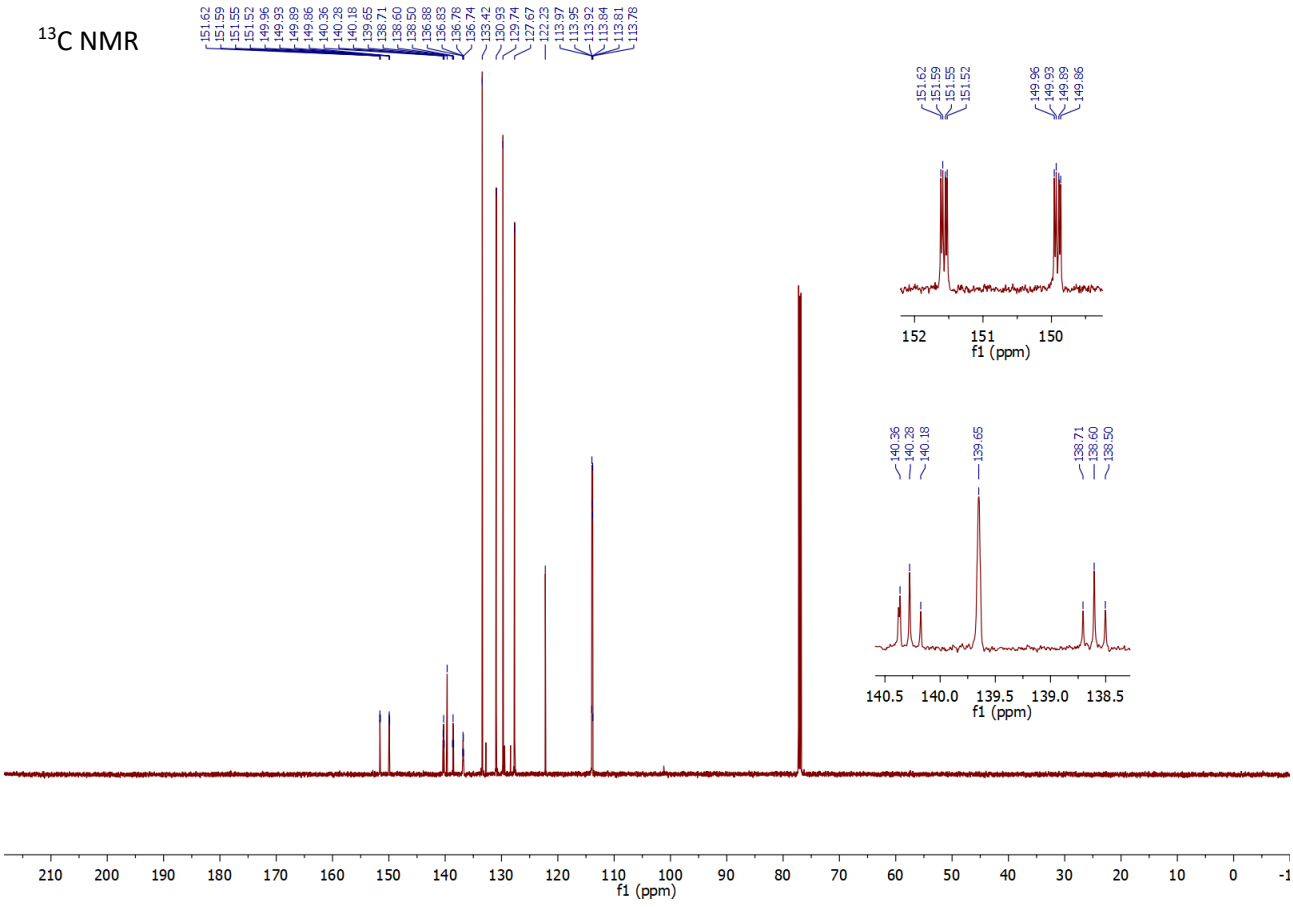

^{19}F NMR

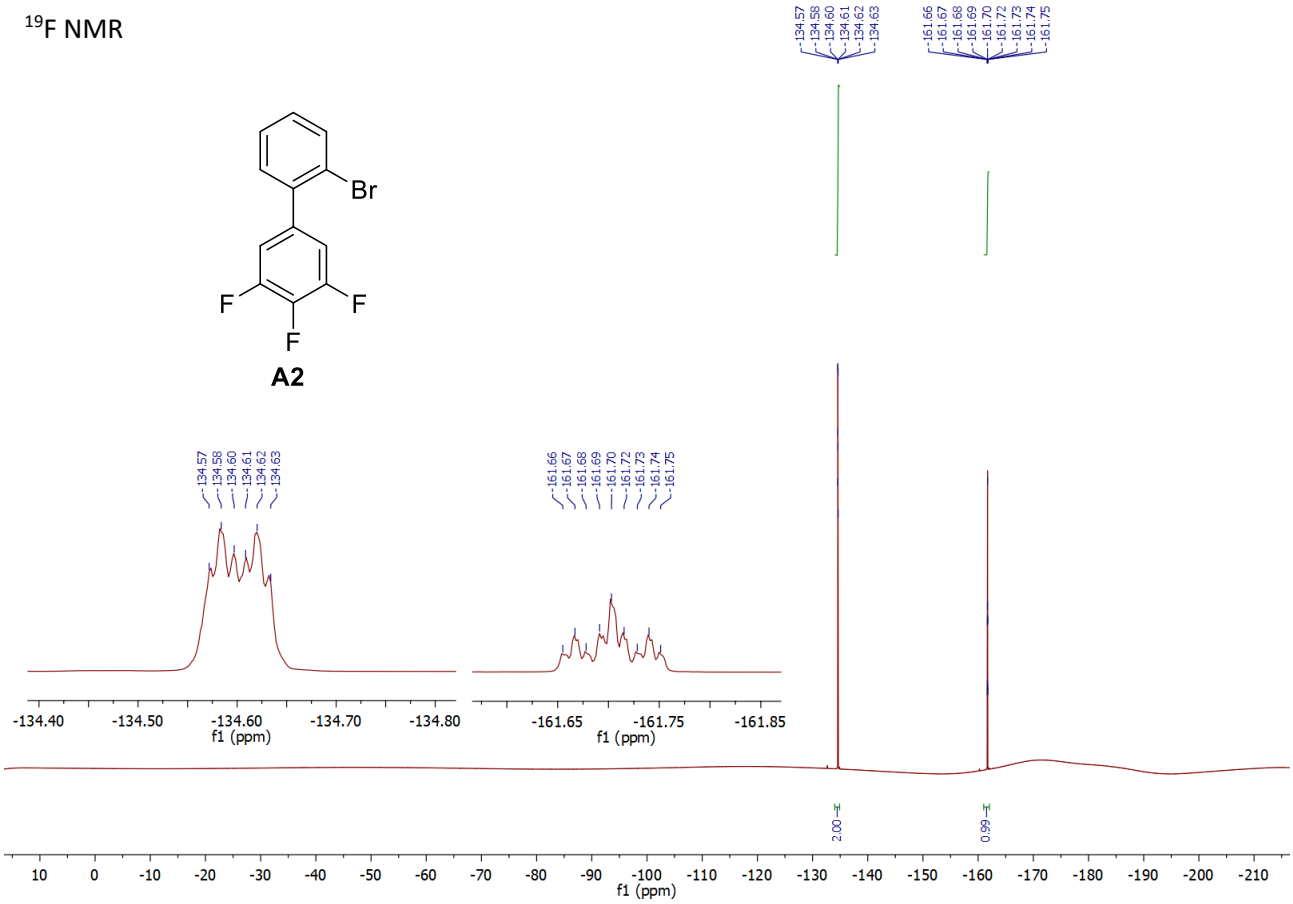
Br
F
F
F
A2
-134.57
-134.58
-134.60
-134.61
-134.62
-134.63
-161.66
-161.67
-161.68
-161.69
-161.70
-161.72
-161.73
-161.74
-161.75
2.00
0.99
f1 (ppm)

^{1}H NMR

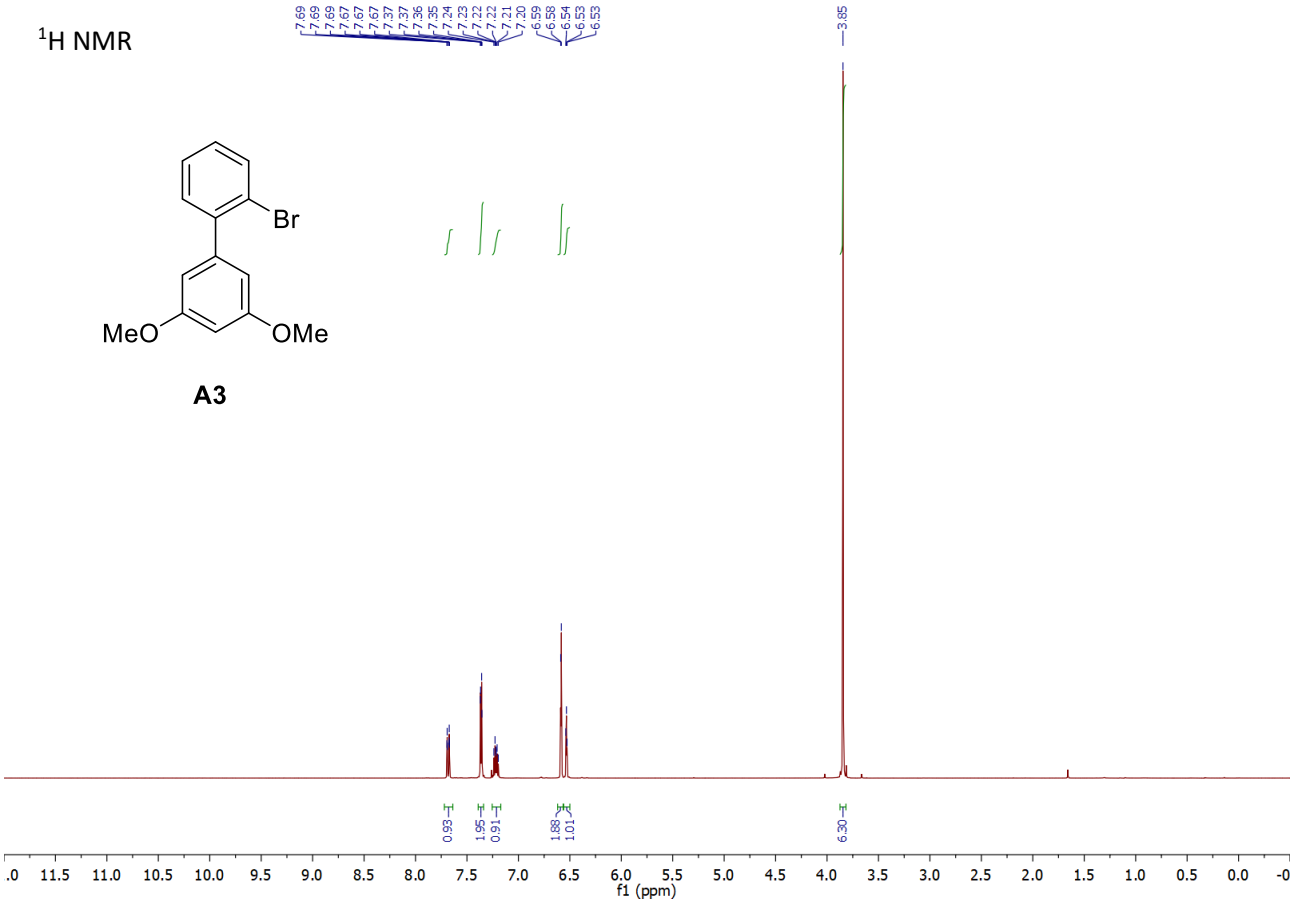

A3

^{13}C NMR

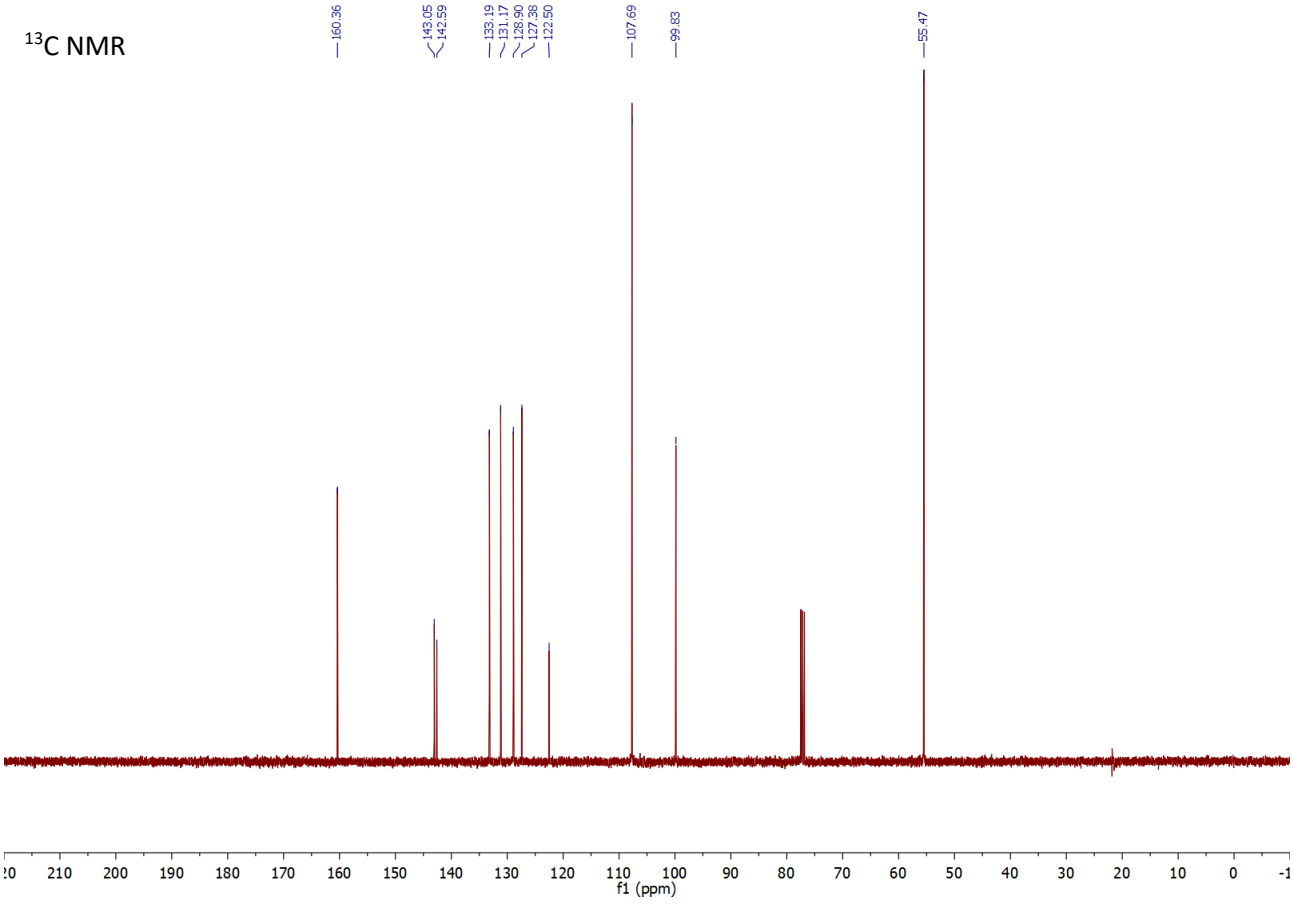

^{1}H NMR

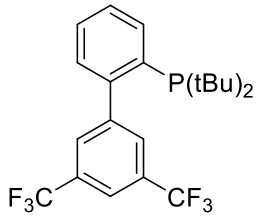

L1

^{13}C NMR

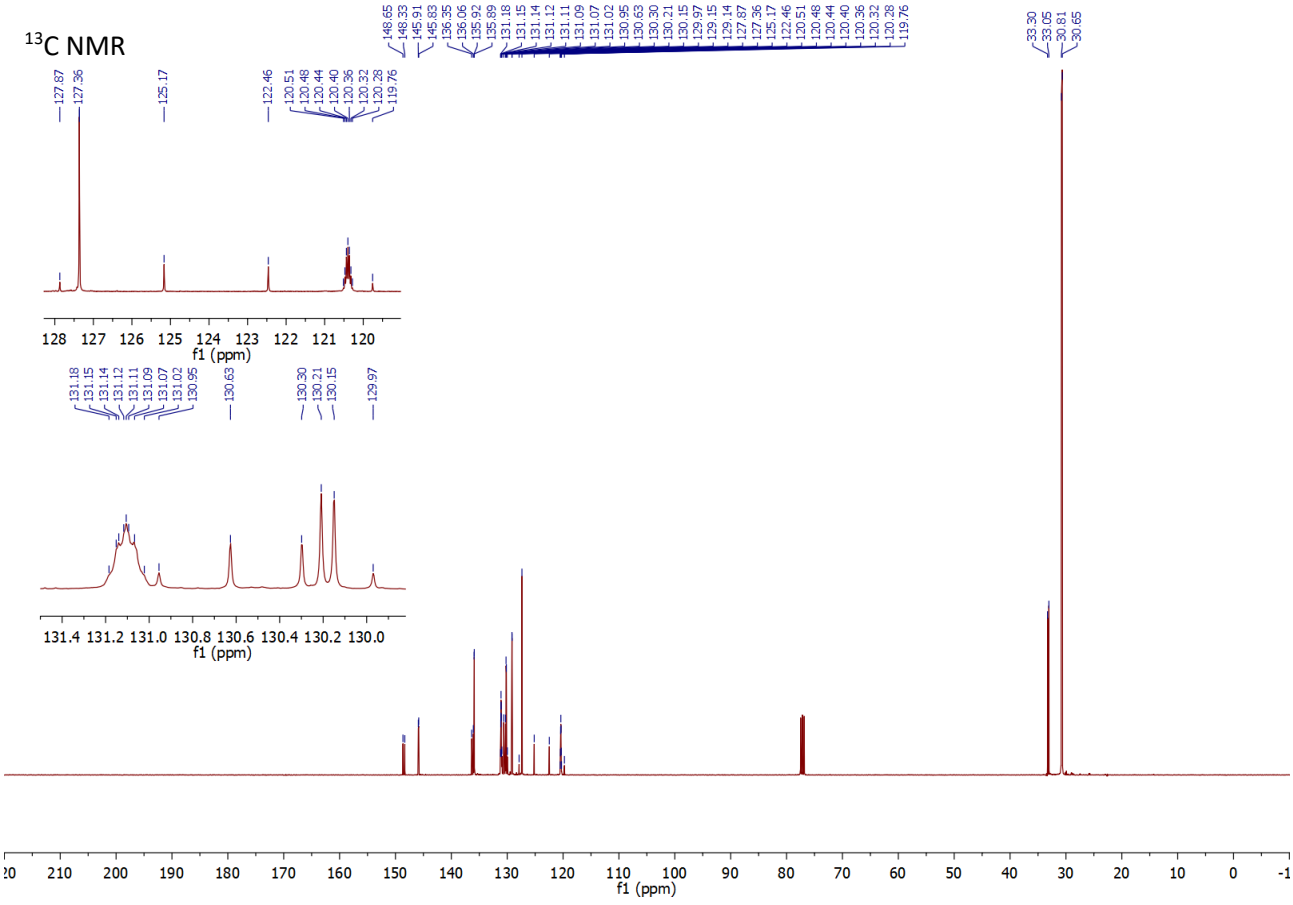

^{19}F NMR

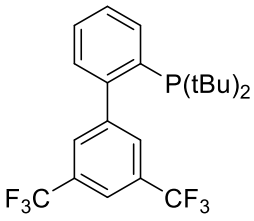

L1

^{31}P NMR

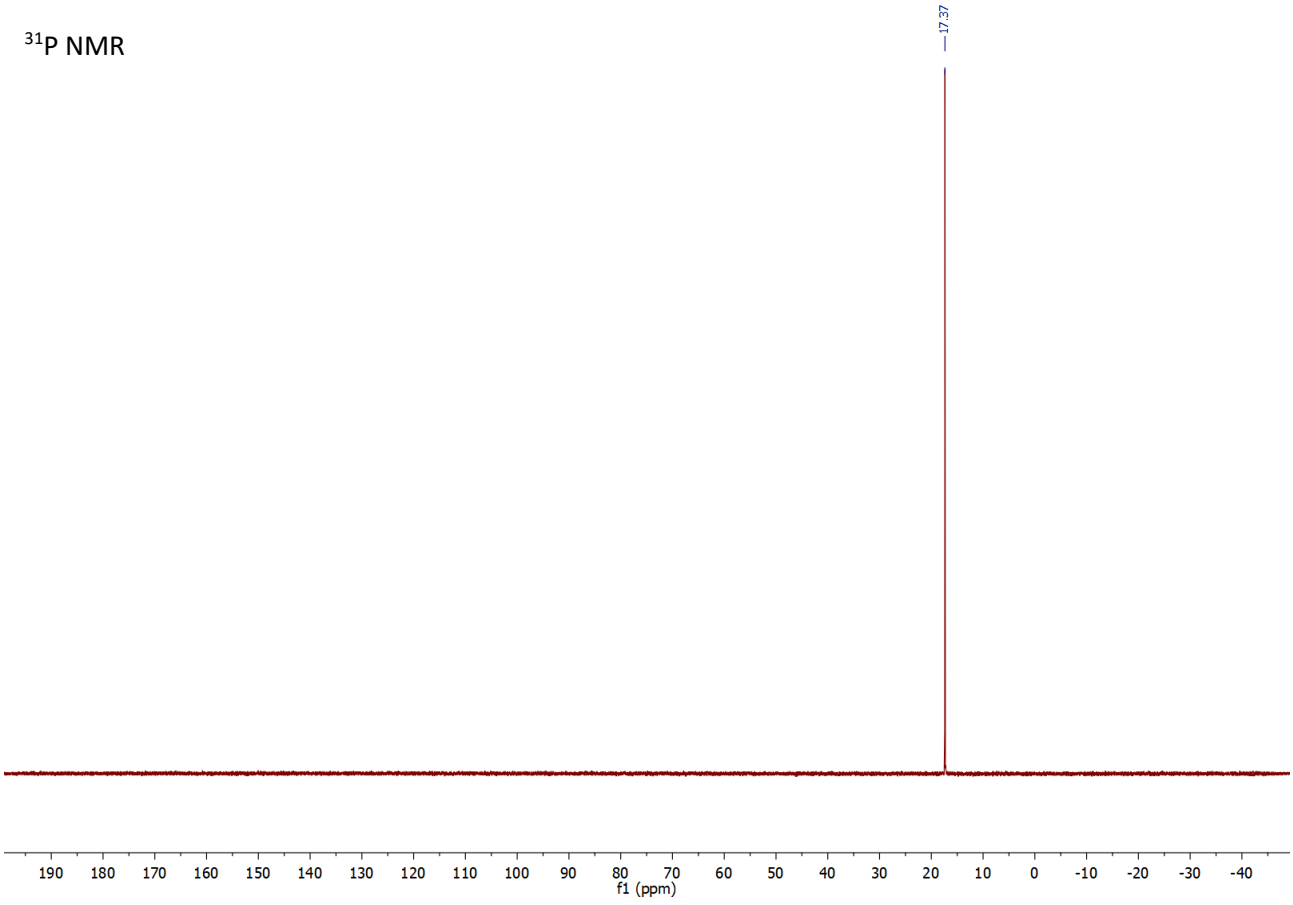

^{1}H NMR

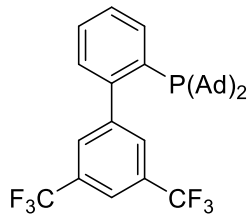

L2

^{13}C NMR

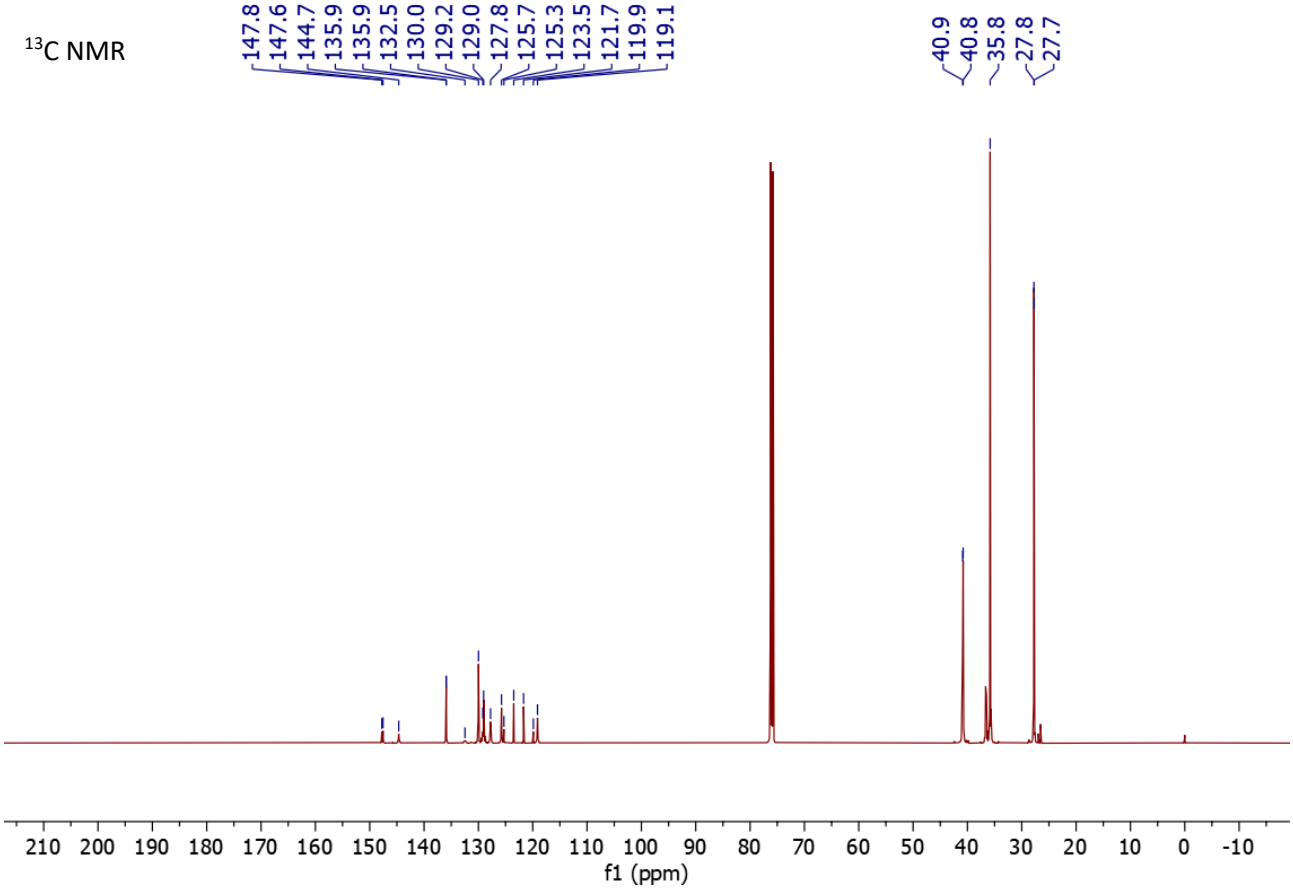

^{19}F NMR

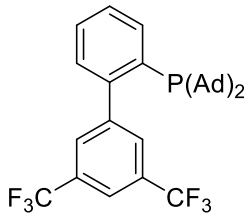

L2

^{31}P NMR

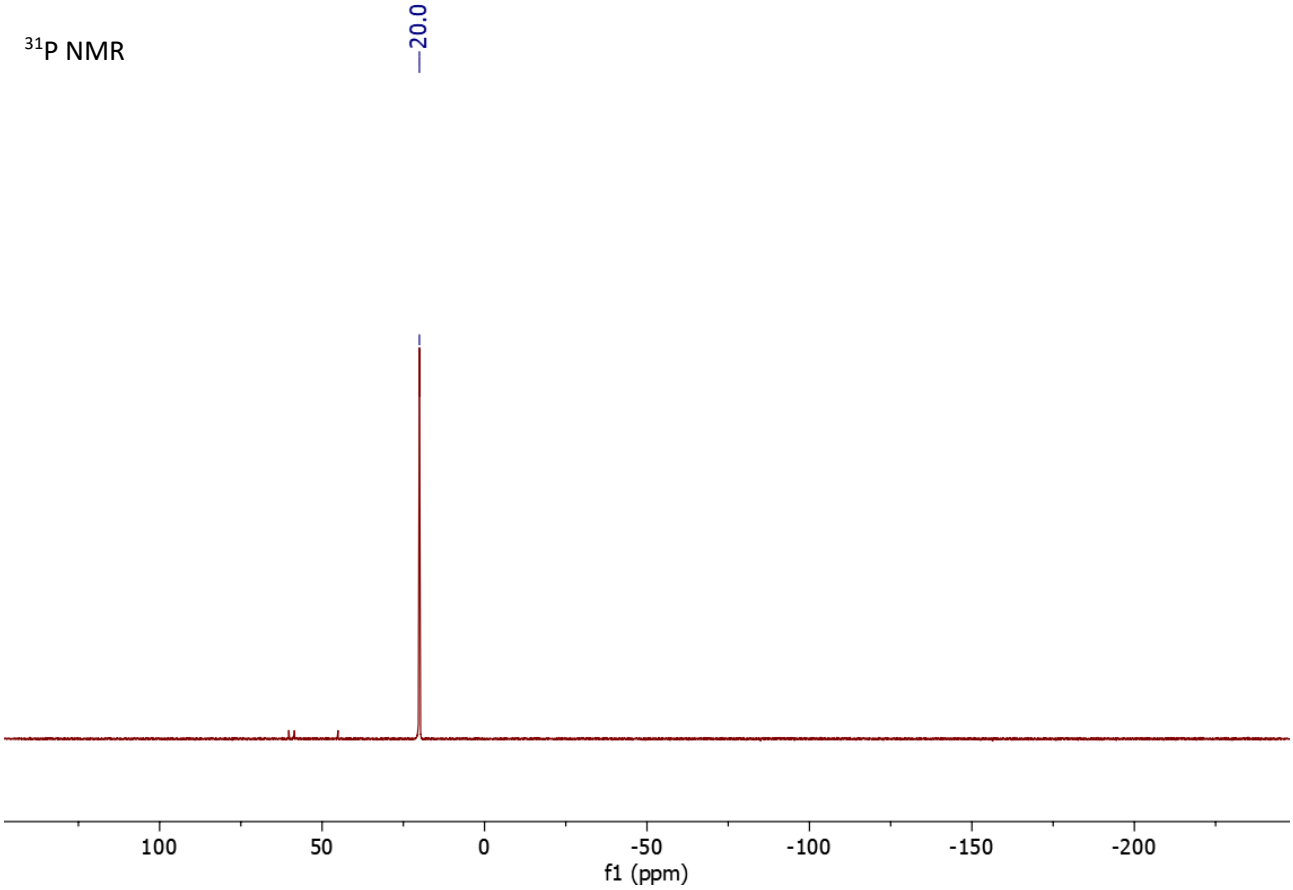

^{1}H NMR

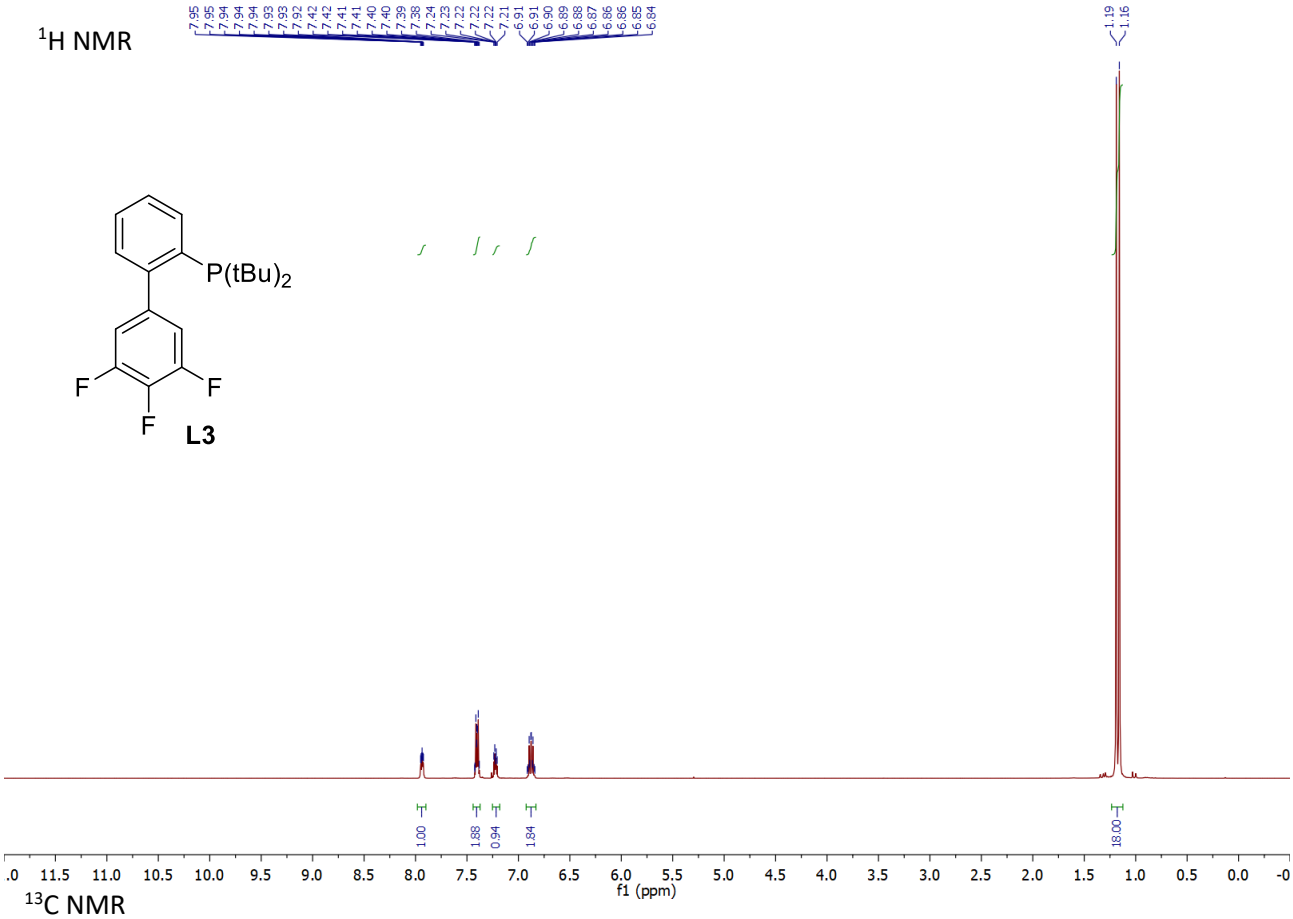

L3

^{13}C NMR

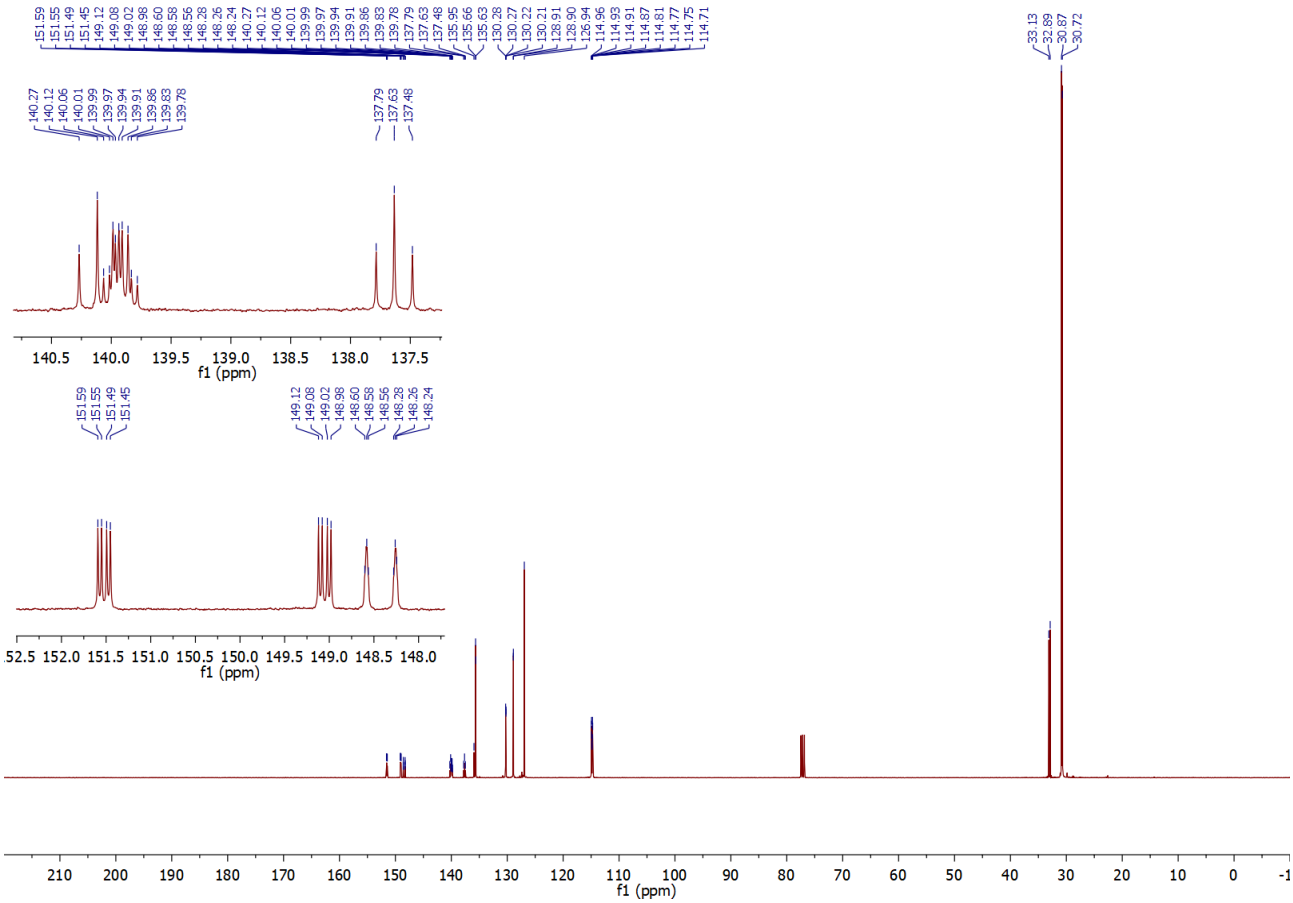

^{19}F NMR

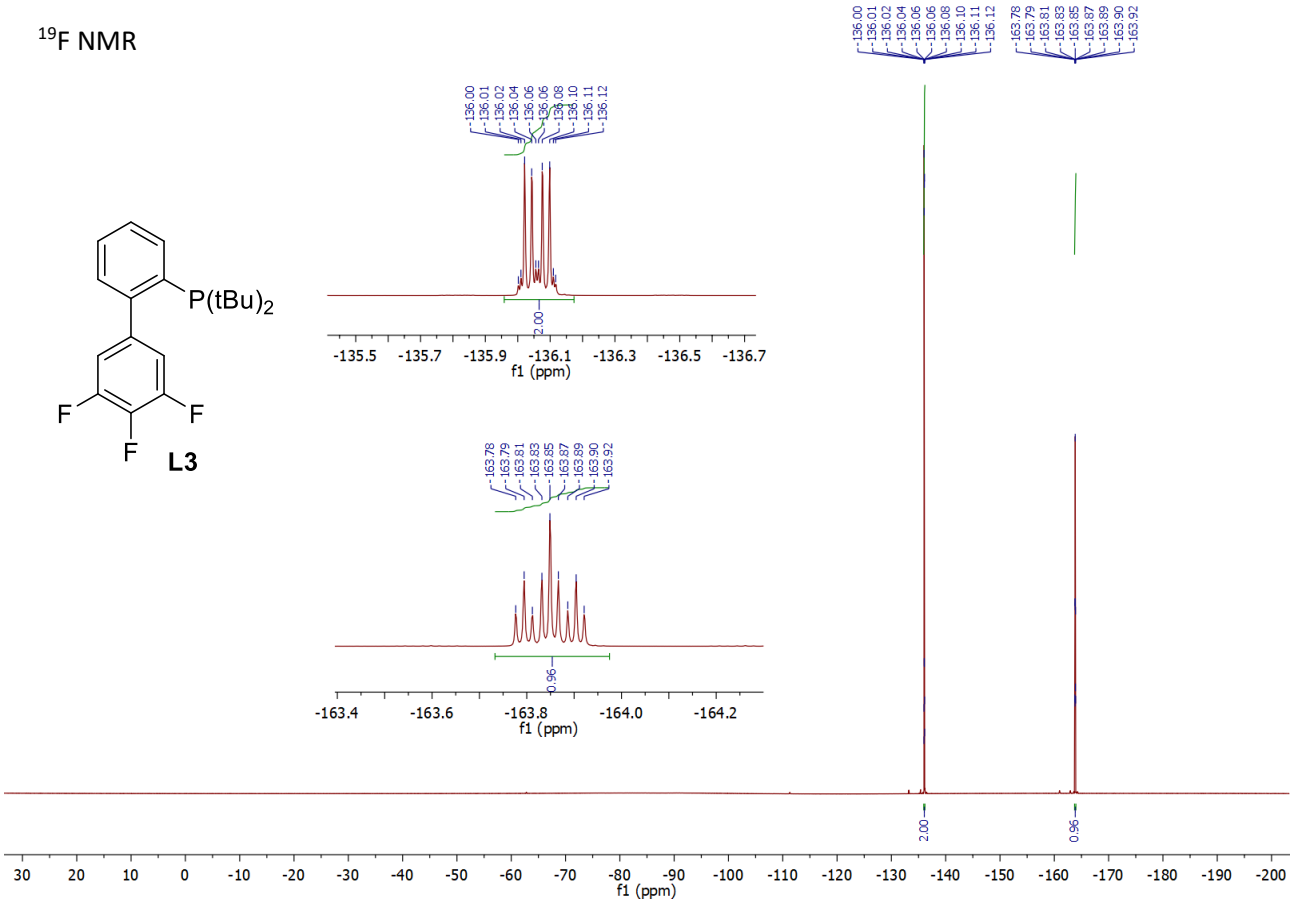

^{31}P NMR

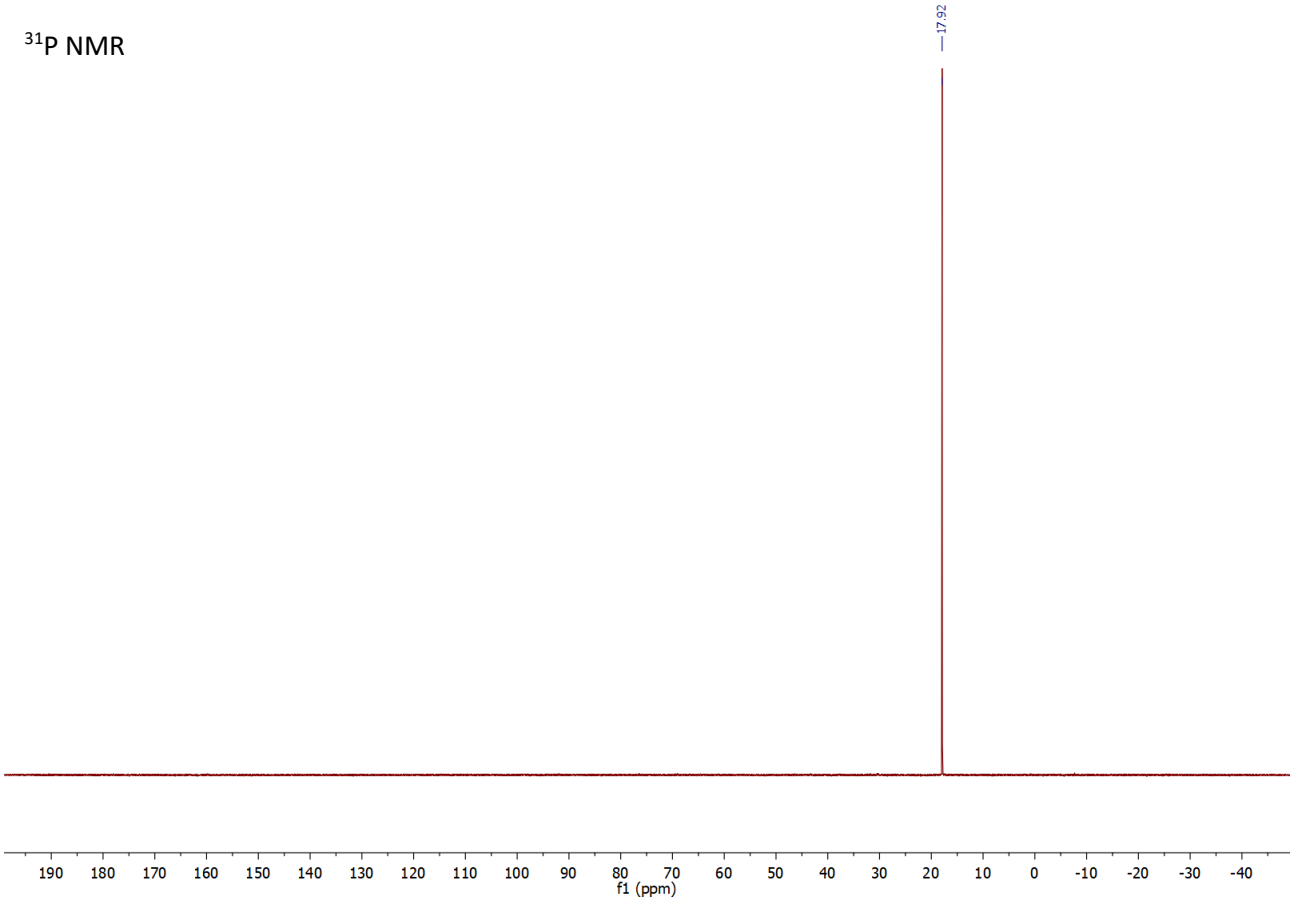

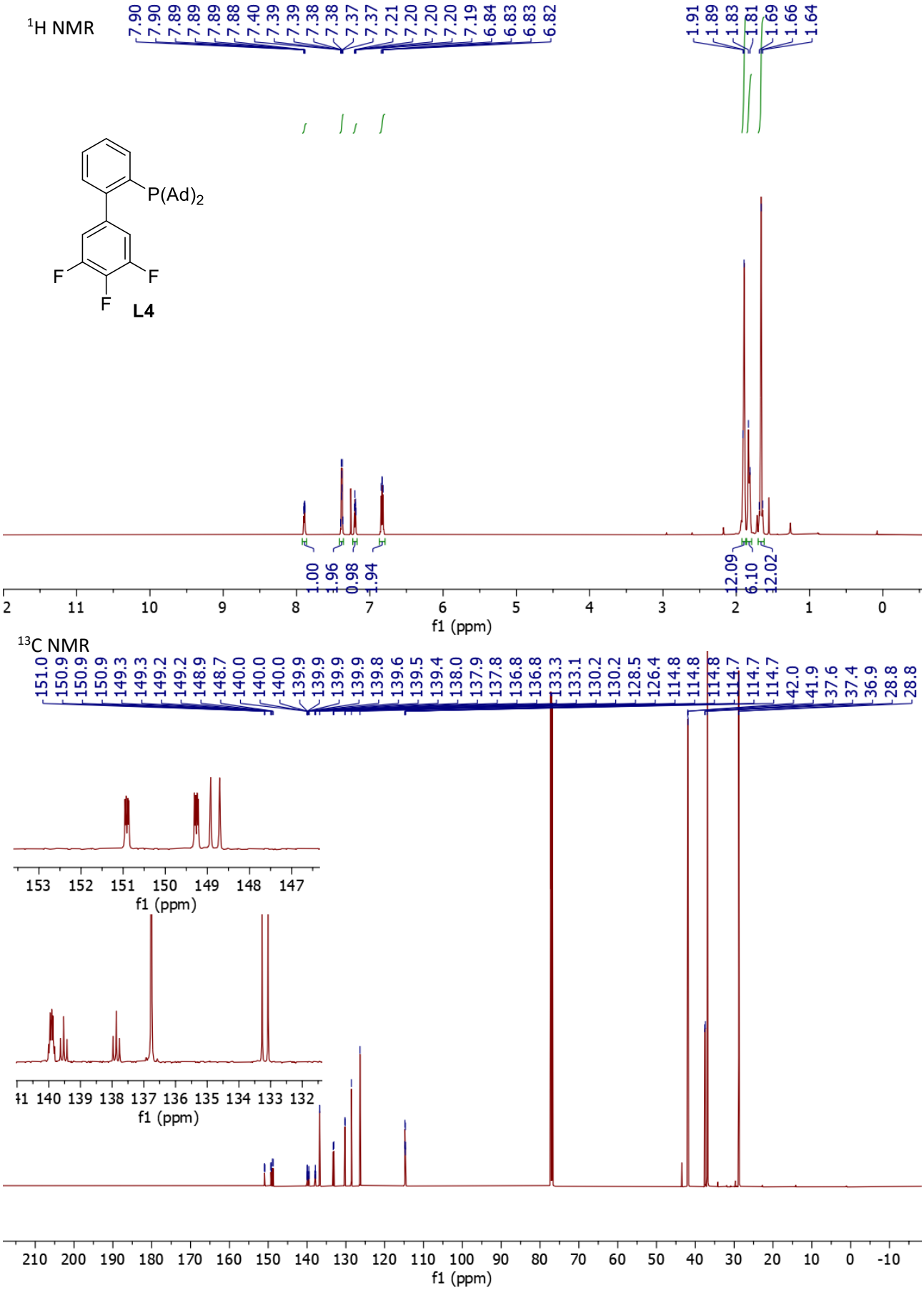
^{1}H NMR
7.90 7.90 7.89 7.89 7.89 7.88 7.40 7.39 7.39 7.38 7.38 7.37 7.37 7.21 7.20 7.20 7.20 7.19 6.84 6.83 6.83 6.82
1.91 1.89 1.83 1.81 1.69 1.66 1.64
P(Ad)2
F
F
F
L4
1.00 1.96 0.98 1.94
12.09 6.10 12.02
f1 (ppm)
^{13}C NMR
151.0 150.9 150.9 150.9 149.3 149.3 149.2 149.2 148.9 148.7 140.0 140.0 140.0 139.9 139.9 139.9 139.9 139.8 139.6 139.5 139.4 138.0 137.9 137.8 136.8 136.8 133.3 133.1 130.2 130.2 128.5 126.4 114.8 114.8 114.8 114.7 114.7 114.7 42.0 41.9 37.6 37.4 36.9 28.8 28.8
f1 (ppm)
f1 (ppm)
f1 (ppm)

^{19}F NMR

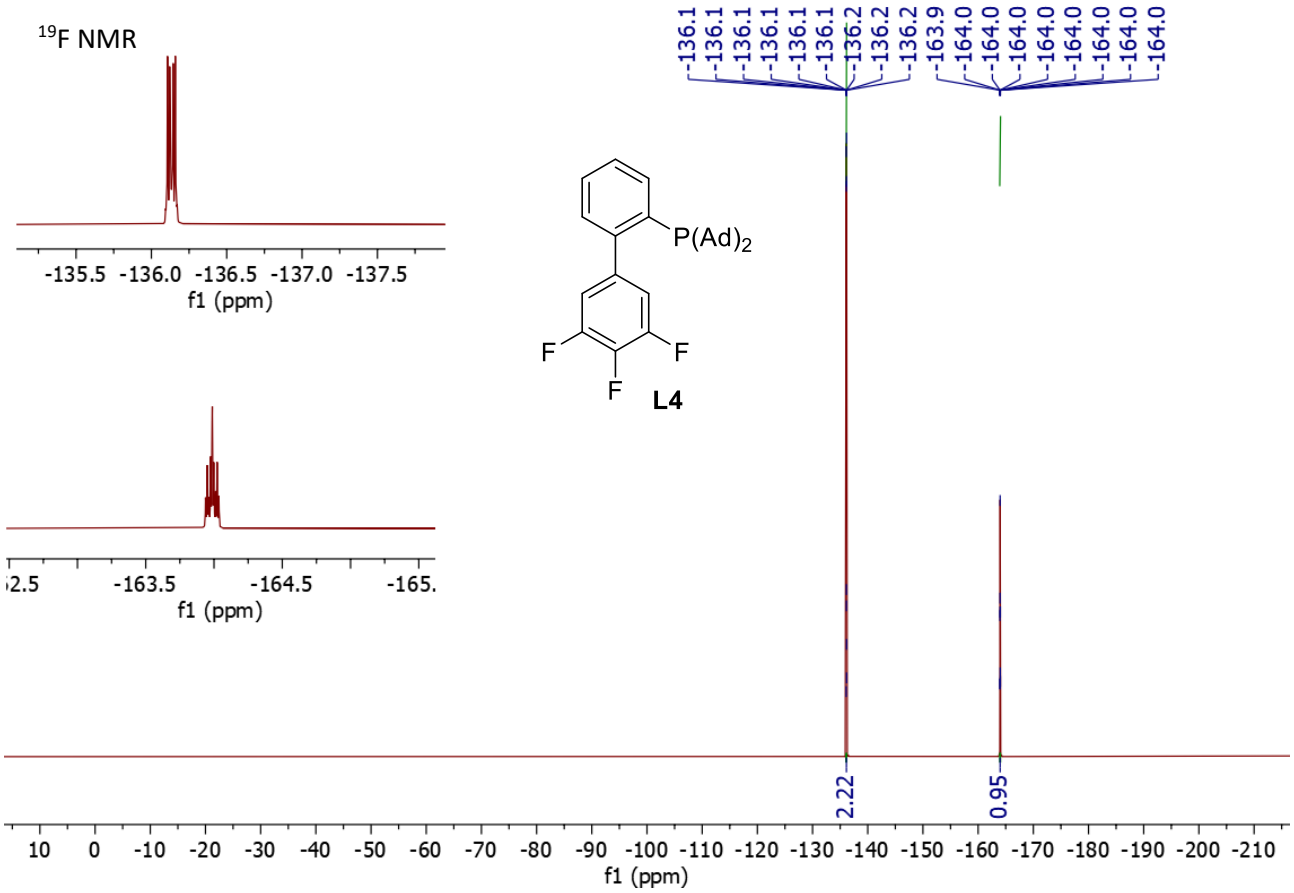

^{31}P NMR

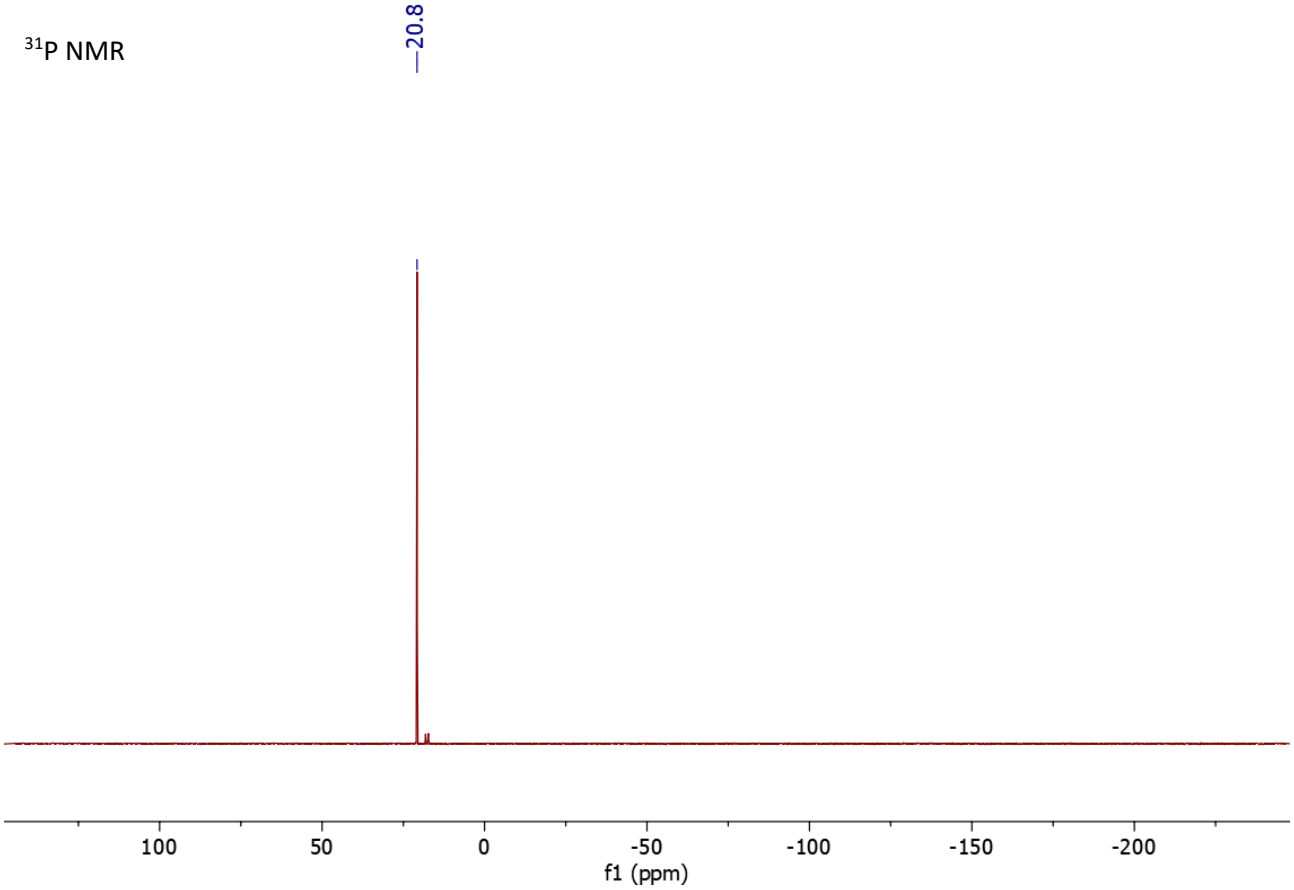

[1]H NMR

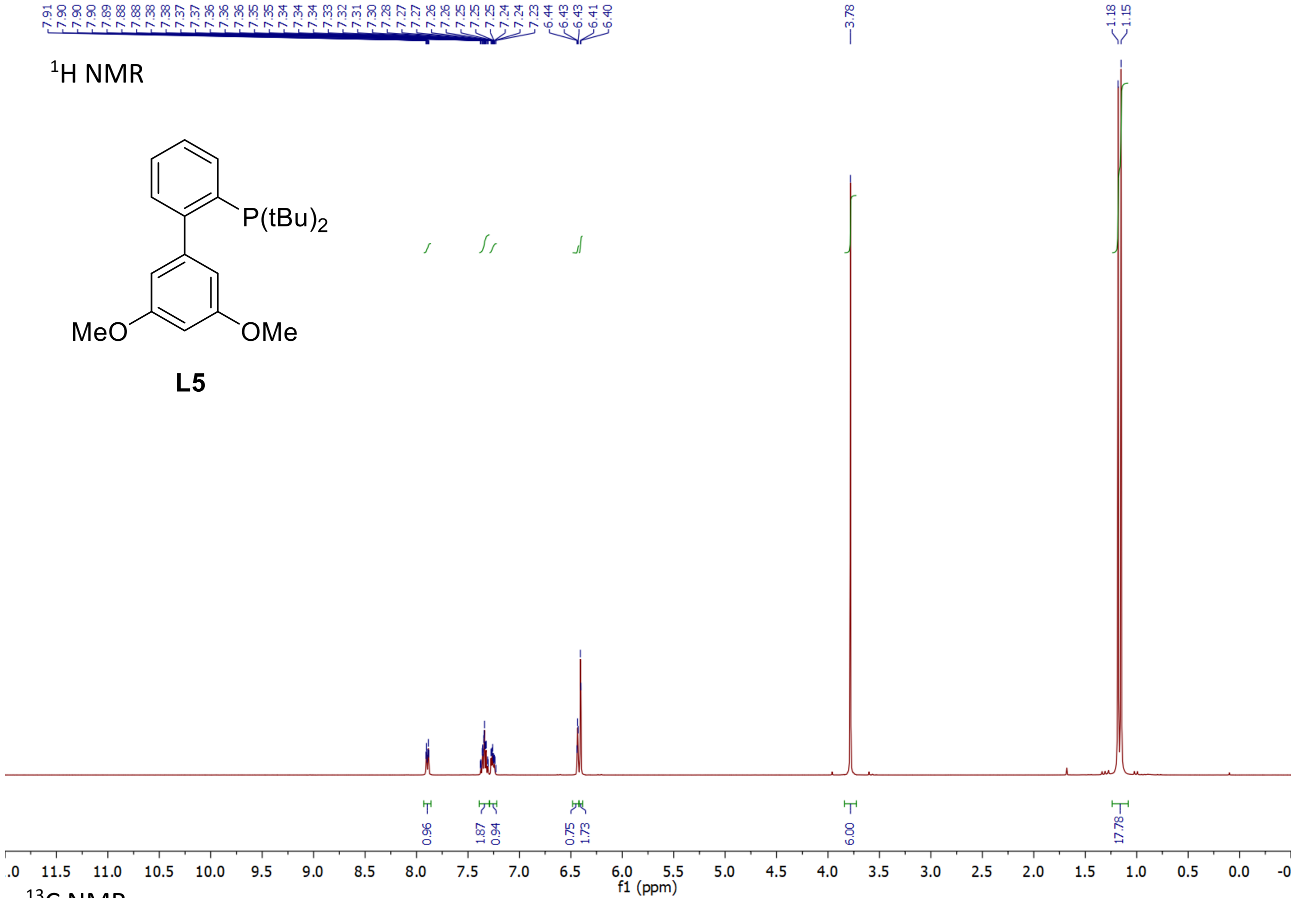

L5

[13]C NMR

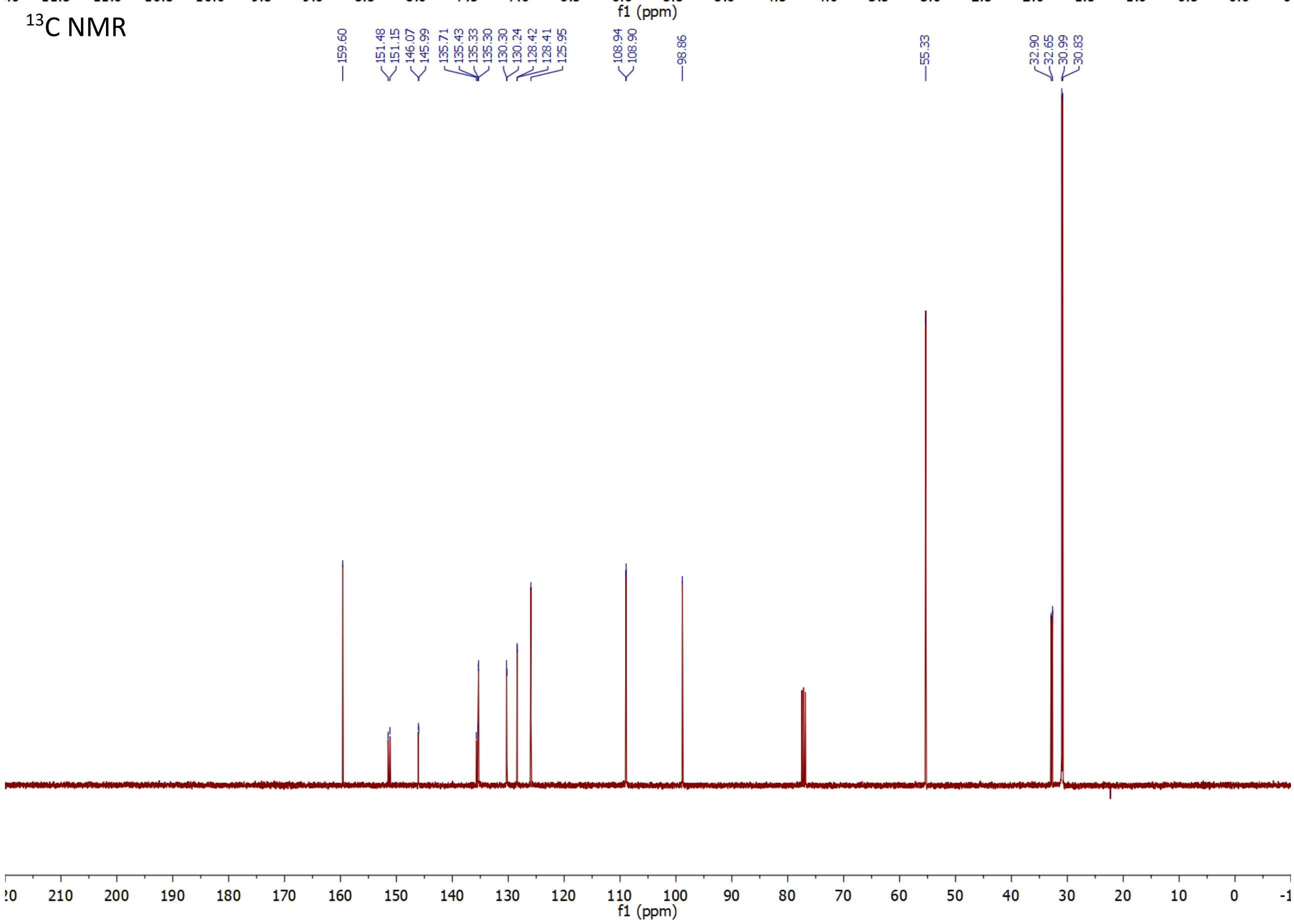

^{31}P NMR

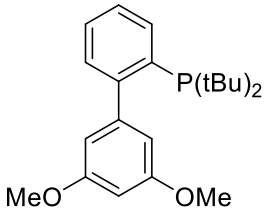
P(tBu)2
MeO
OMe

L5

18.50
190 180 170 160 150 140 130 120 110 100 90 80 70 60 50 40 30 20 10 0 -10 -20 -30 -40
f1 (ppm)

^{1}H NMR

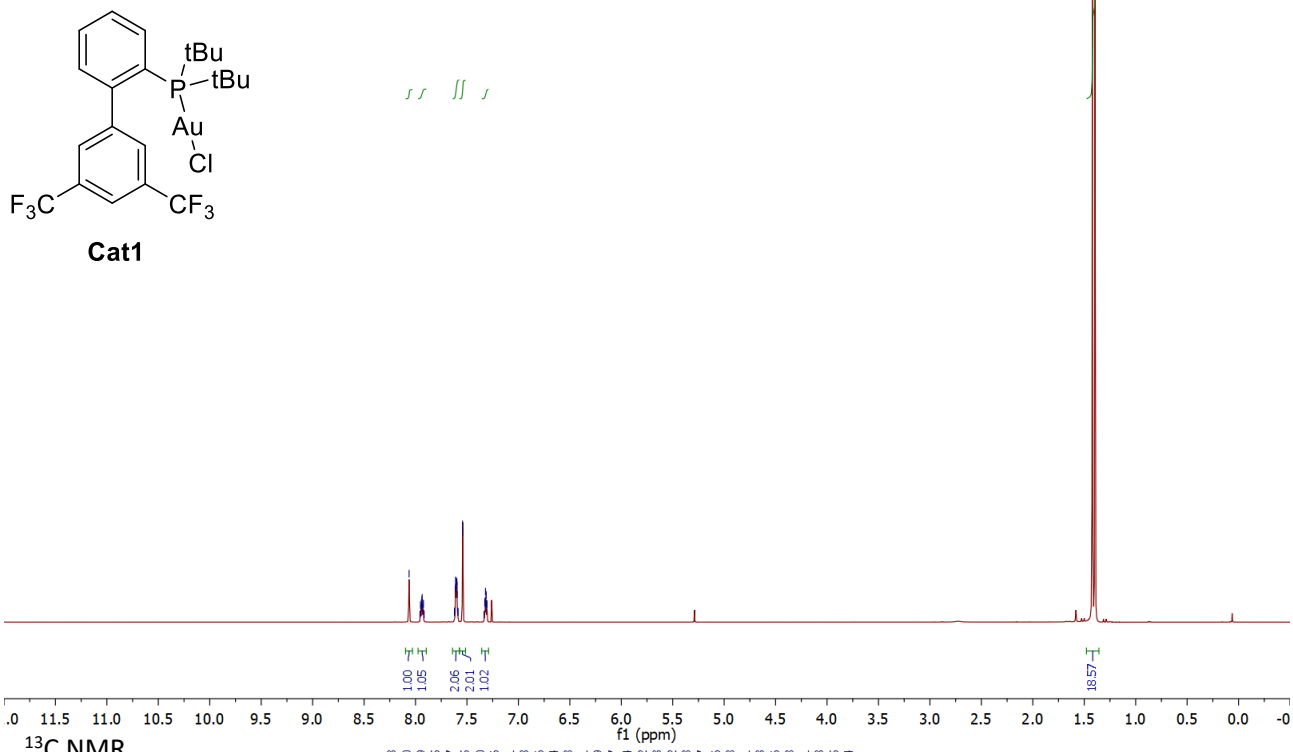

Cat1

^{13}C NMR

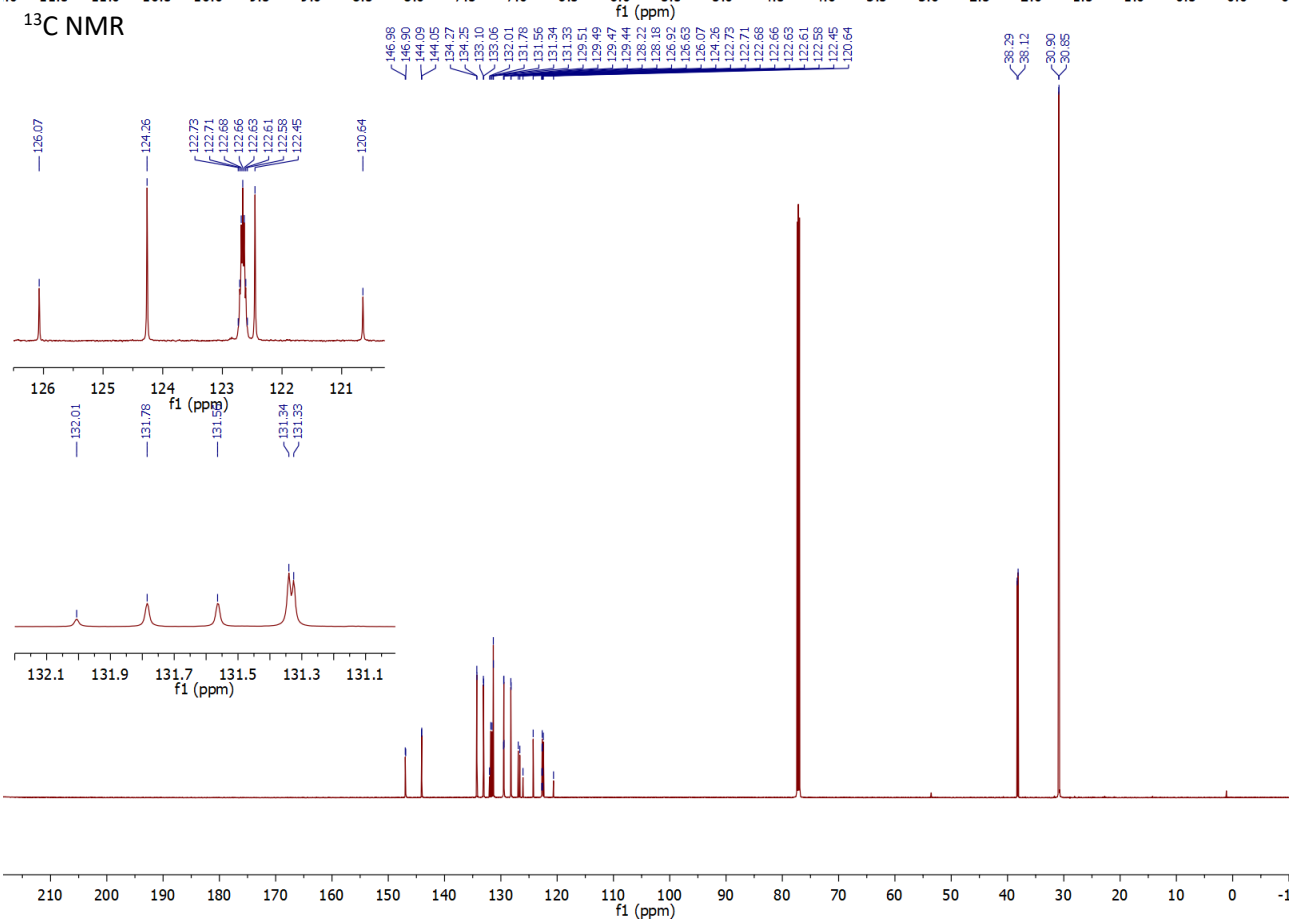

^{19}F NMR

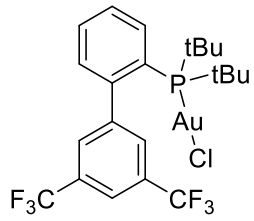

Cat1

^{31}P NMR

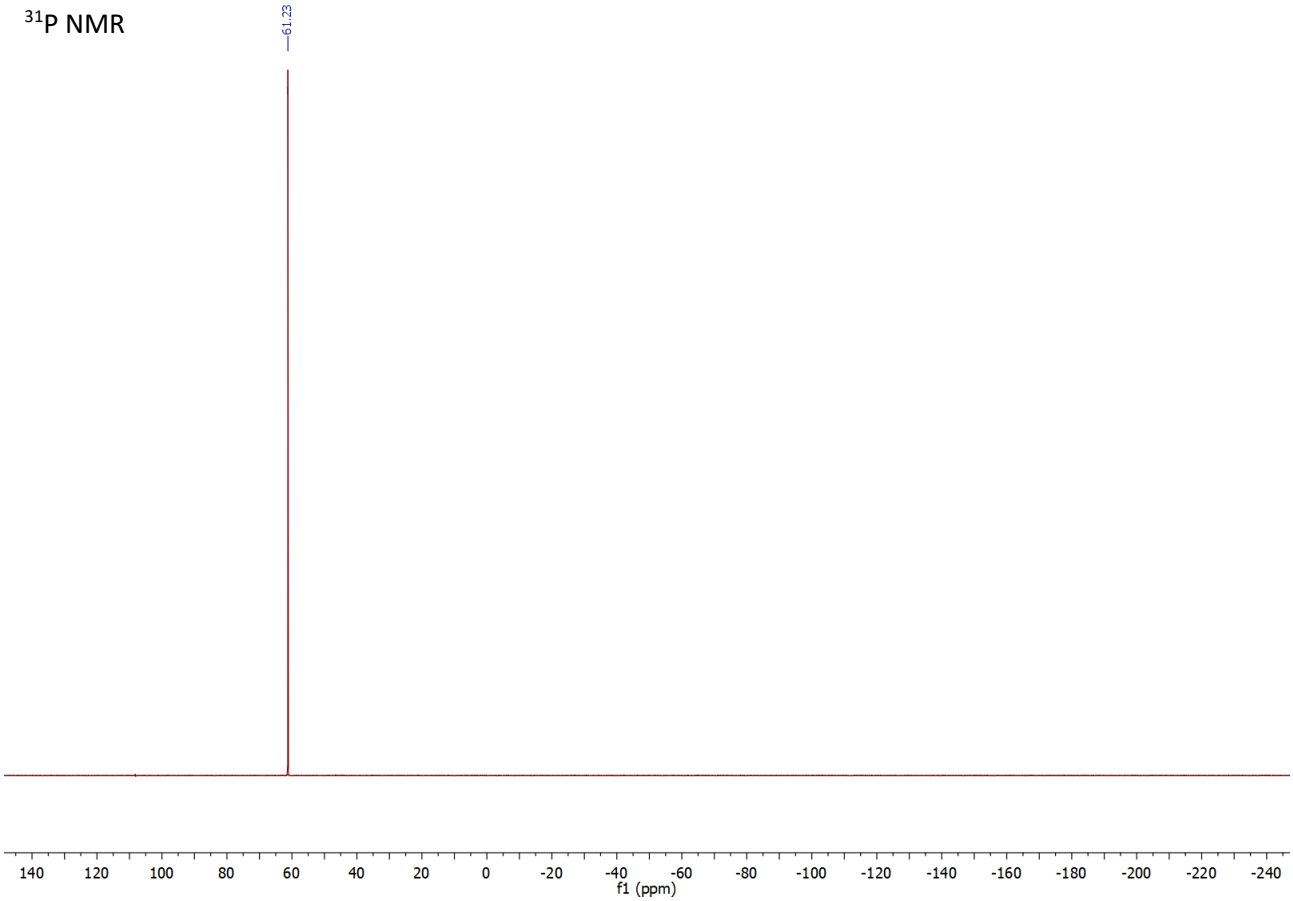

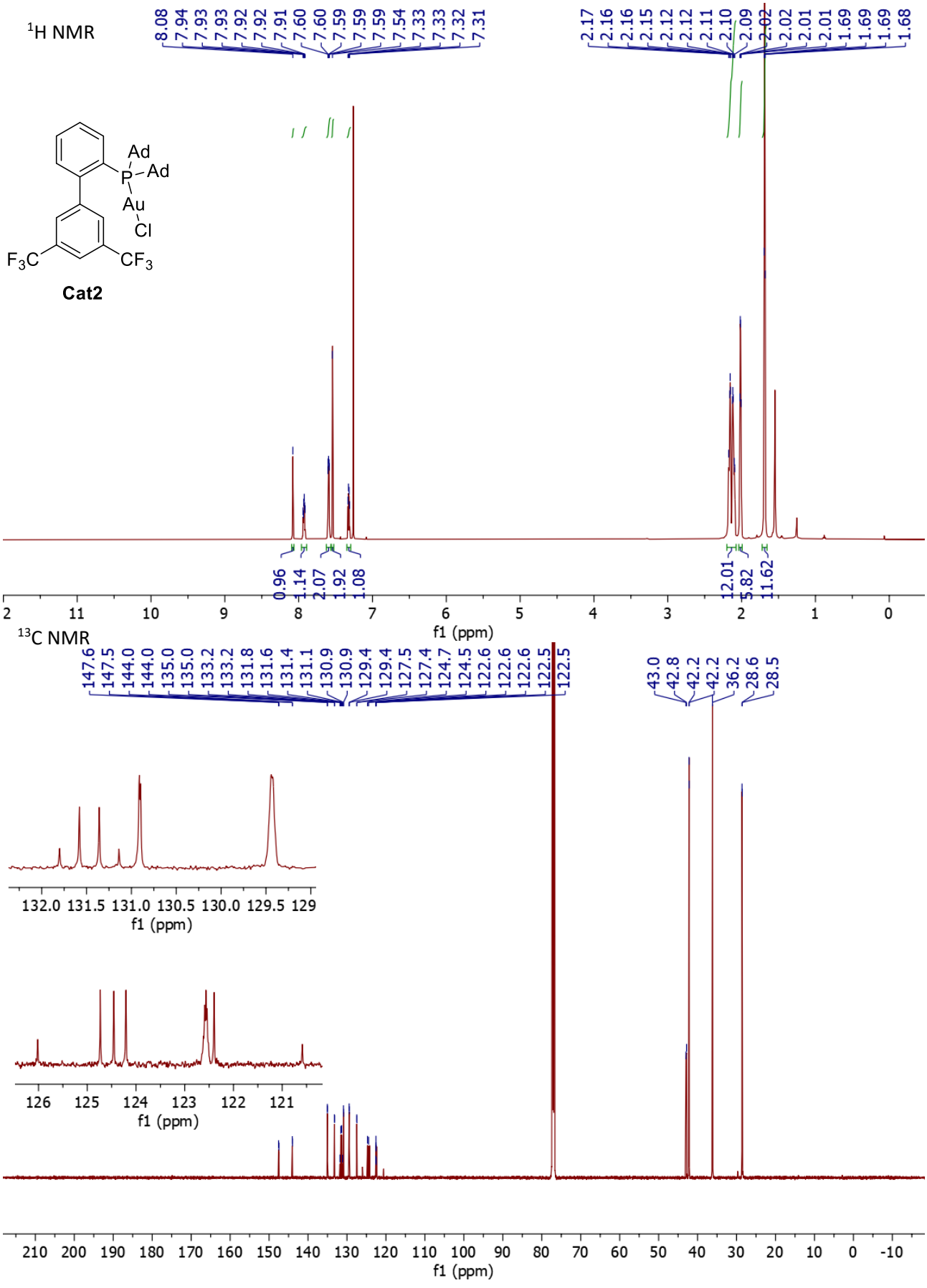
^{1}H NMR
8.08 7.94 7.93 7.93 7.92 7.92 7.91 7.60 7.60 7.59 7.59 7.59 7.54 7.33 7.33 7.32 7.31
2.17 2.16 2.16 2.15 2.12 2.12 2.11 2.10 2.09 2.02 2.02 2.01 2.01 1.69 1.69 1.69 1.68
Ad
P
Ad
Au
Cl
F_3C
CF_3
Cat2
0.96 1.14 2.07 1.92 1.08
12.01 5.82 11.62
f1 (ppm)
^{13}C NMR
147.6 147.5 144.0 144.0 135.0 135.0 133.2 133.2 131.8 131.6 131.4 131.1 130.9 130.9 129.4 129.4 127.5 127.4 124.7 124.5 122.6 122.6 122.6 122.5 122.5
43.0 42.8 42.2 42.2 36.2 28.6 28.5
132.0 131.5 131.0 130.5 130.0 129.5 129
f1 (ppm)
126 125 124 123 122 121
f1 (ppm)
f1 (ppm)

^{19}F NMR

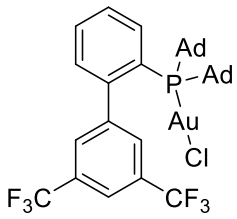

Cat2

^{31}P NMR

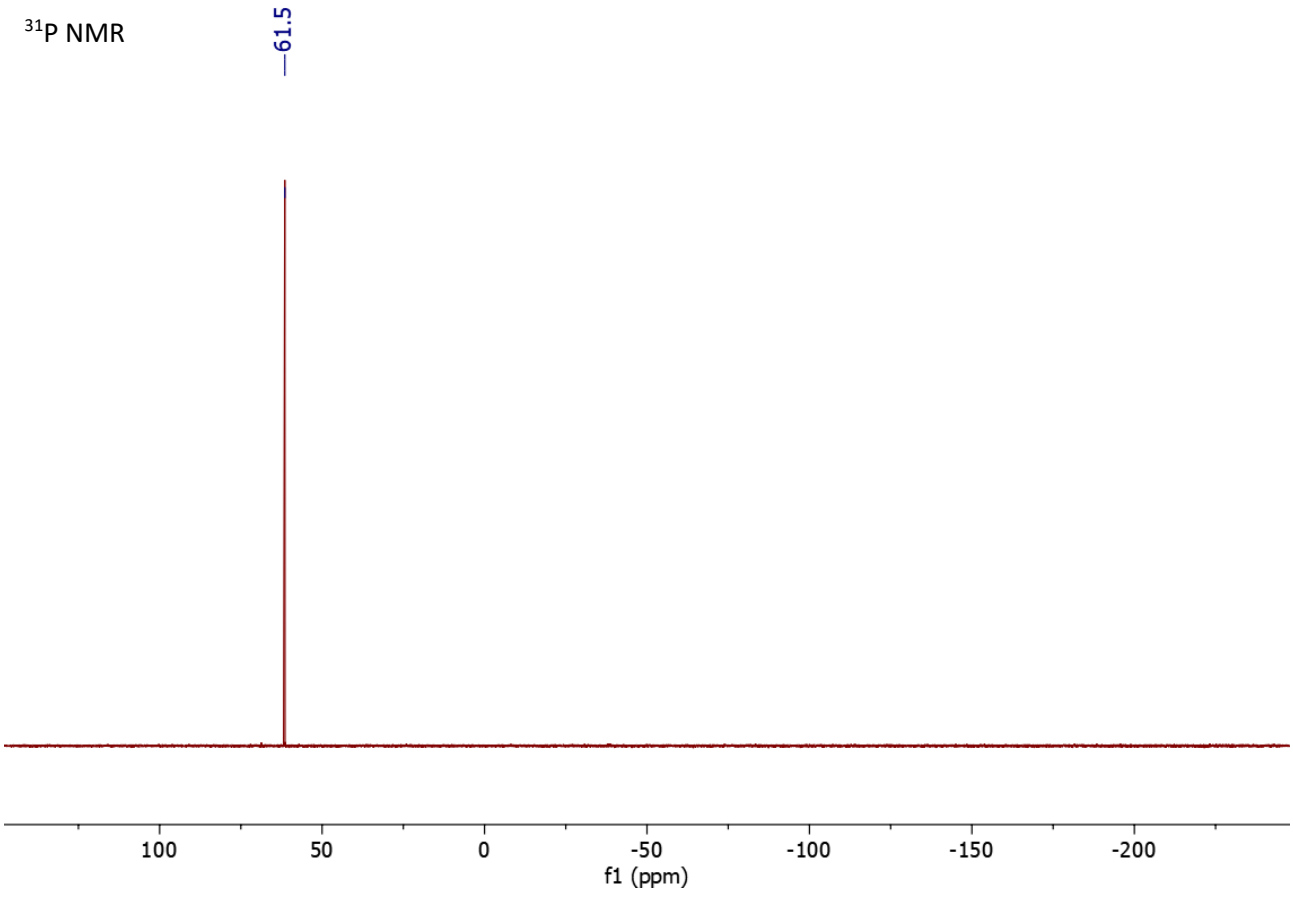

^{1}H NMR

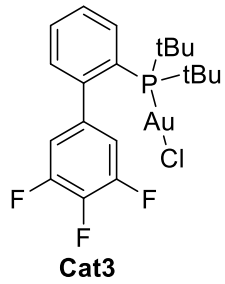

Cat3

^{13}C NMR

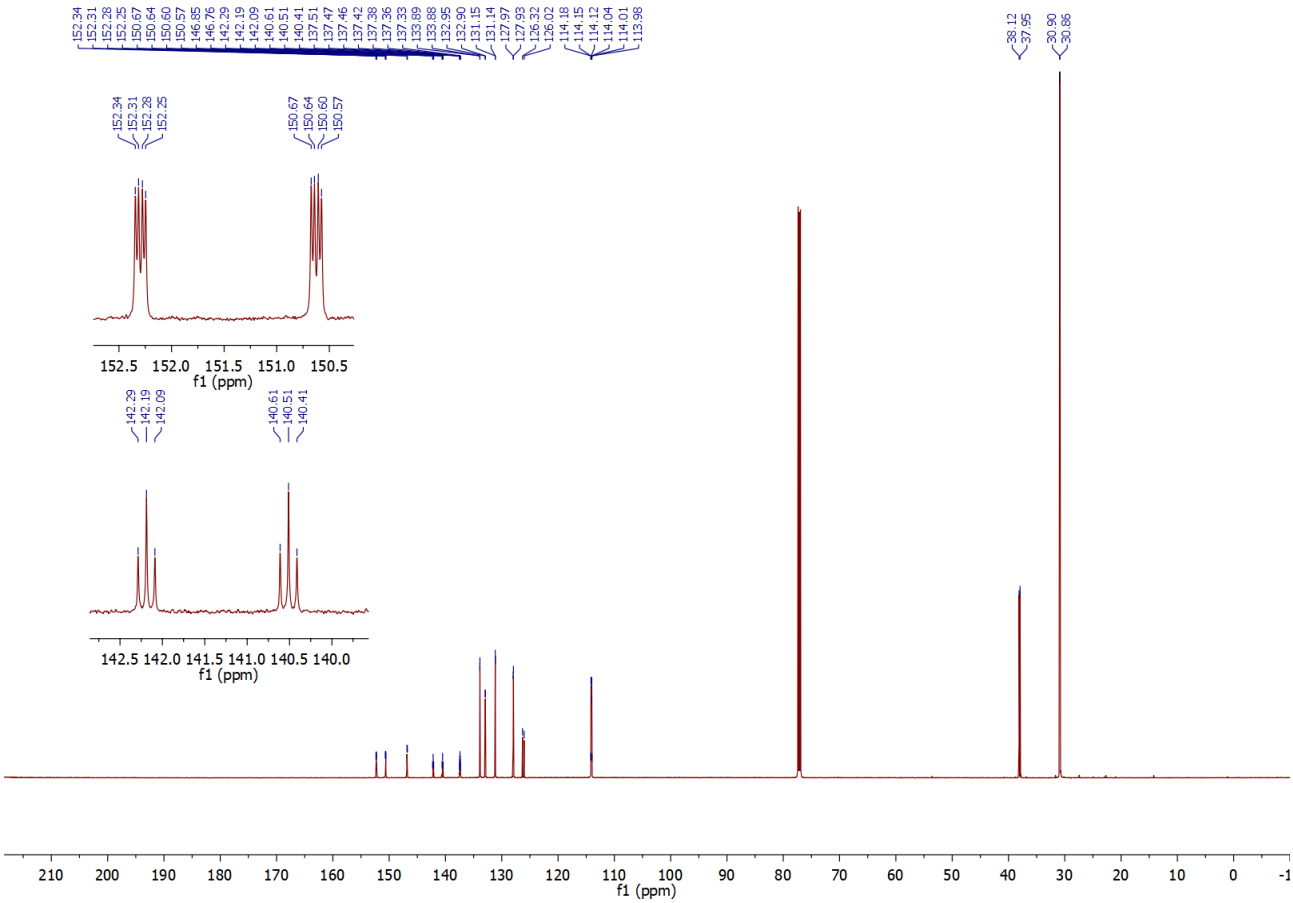

^{19}F NMR

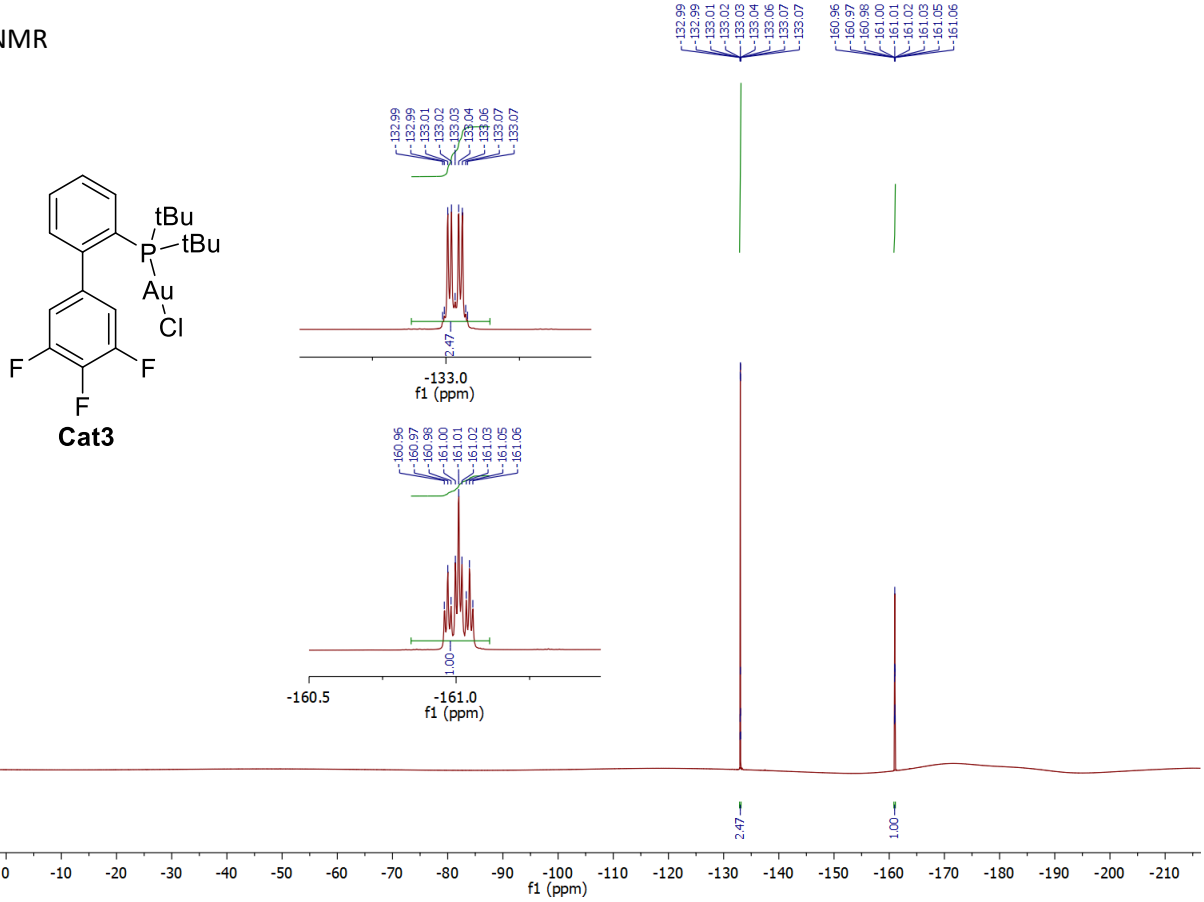

^{31}P NMR

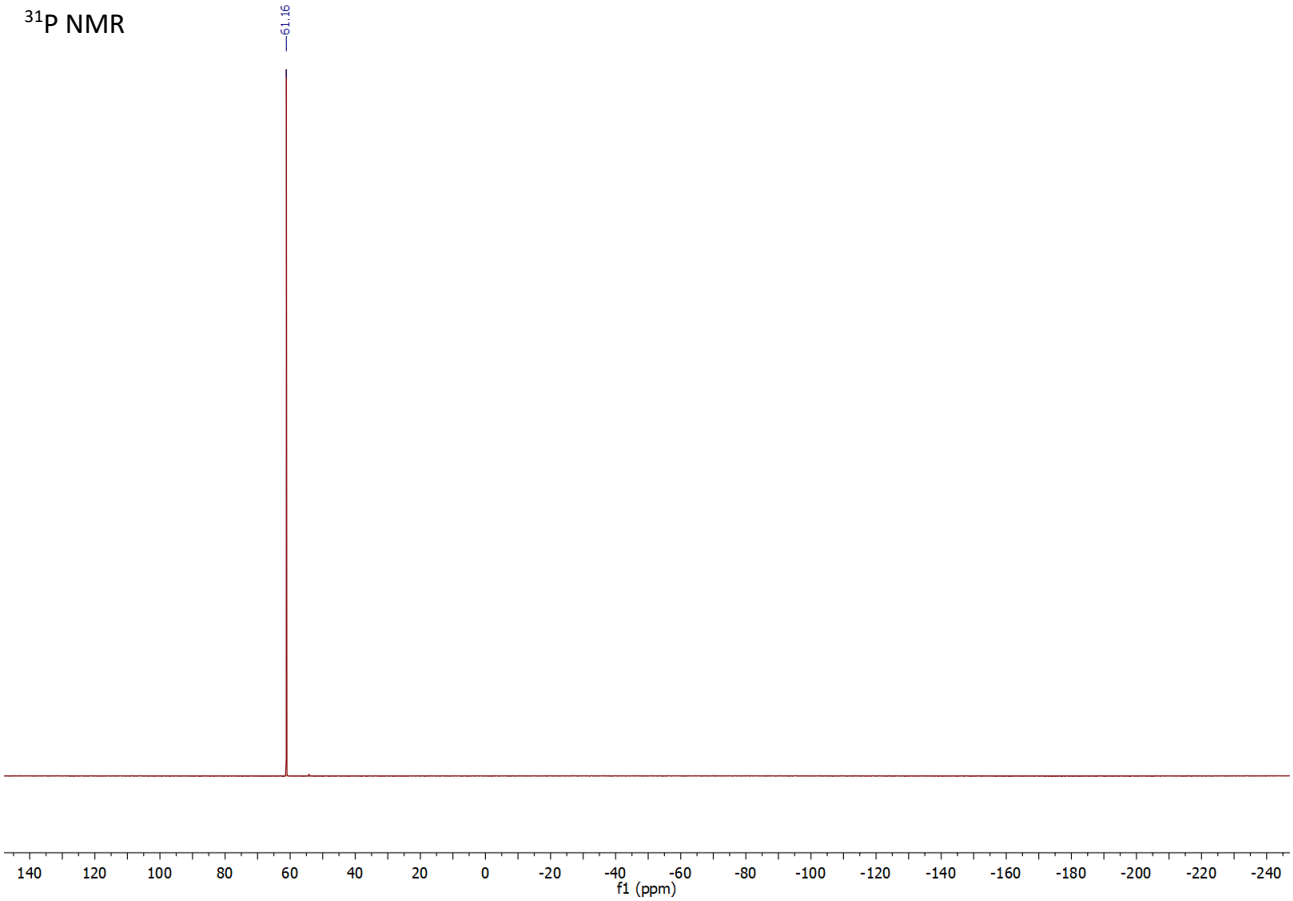

^{1}H NMR

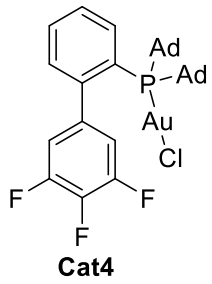

Cat4

^{13}C NMR

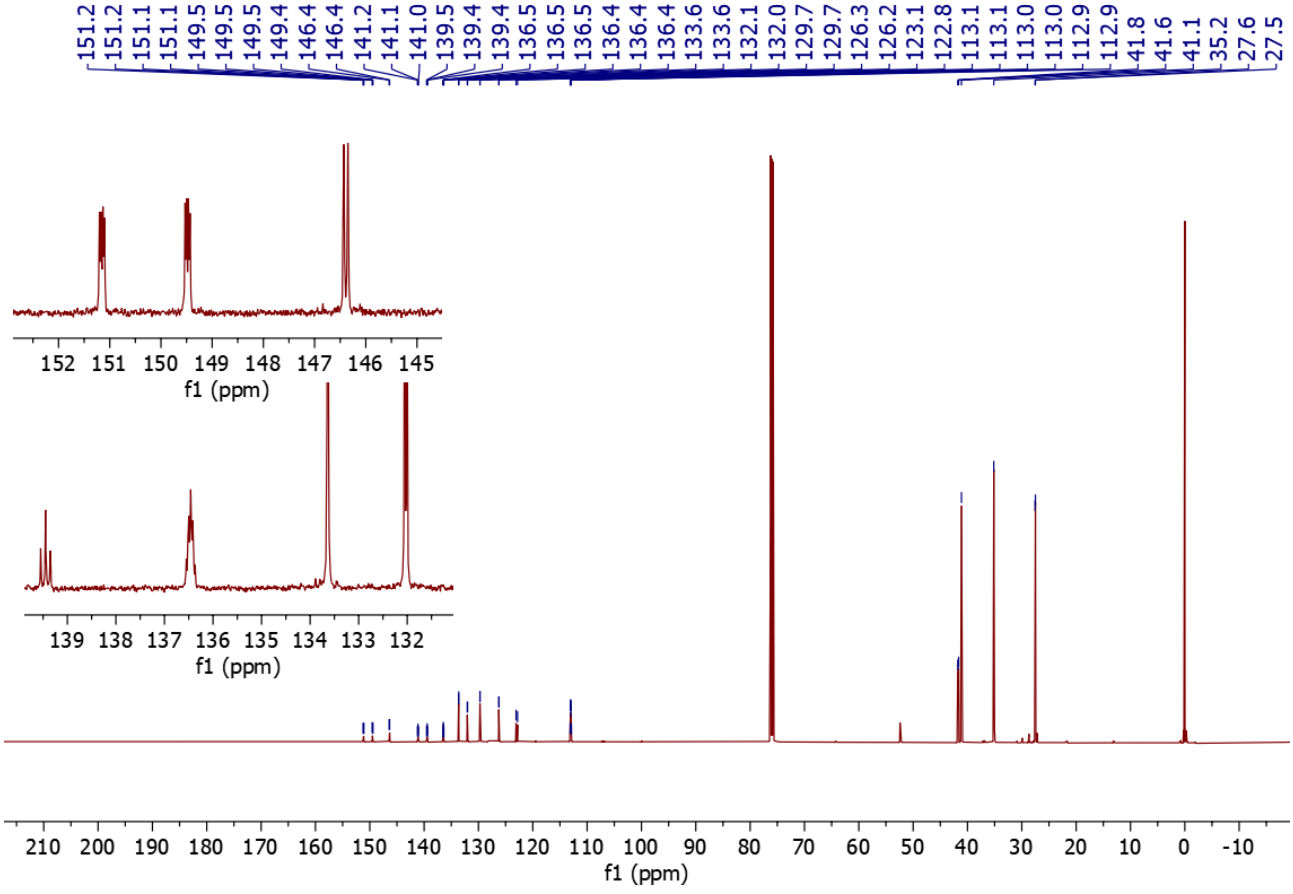

^{19}F NMR

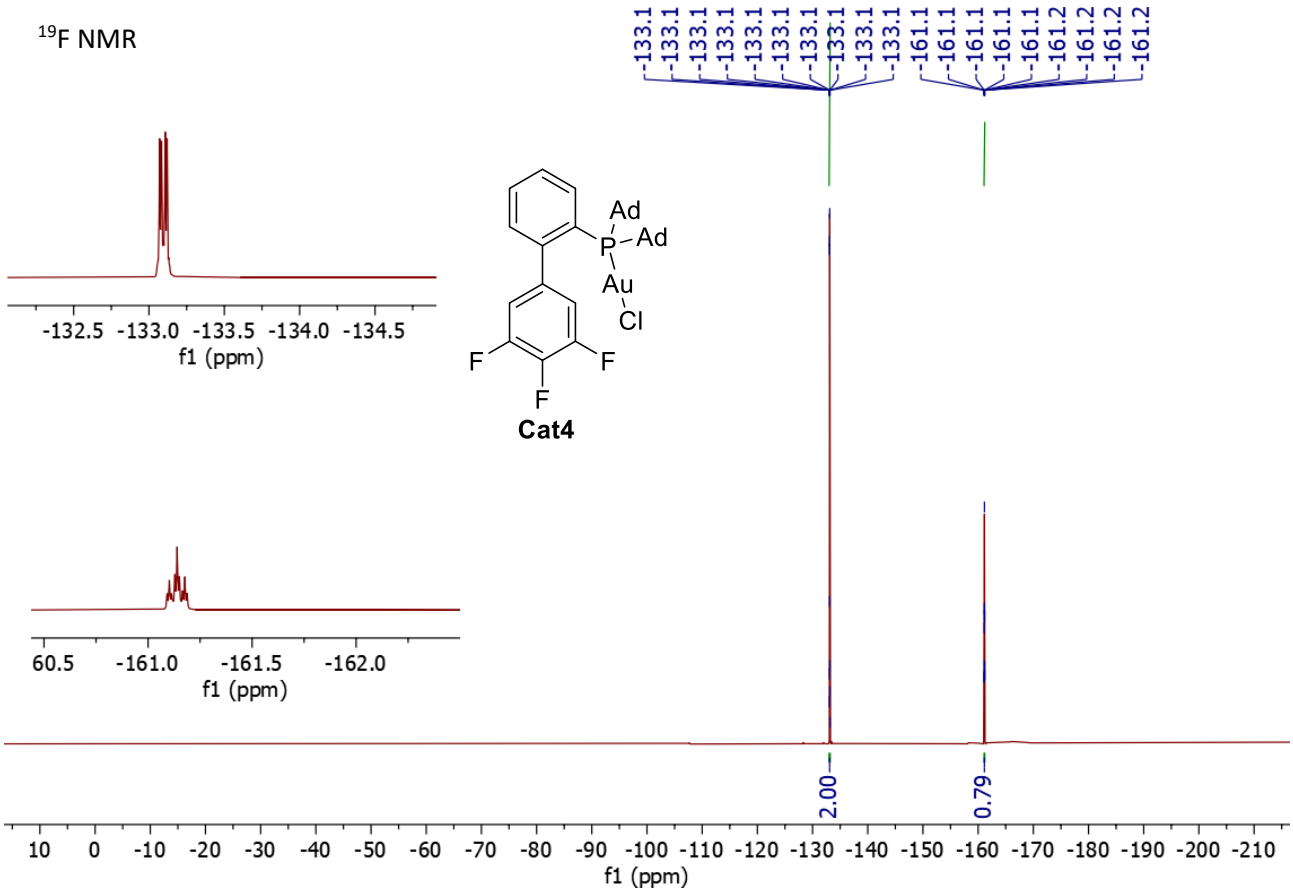

^{31}P NMR

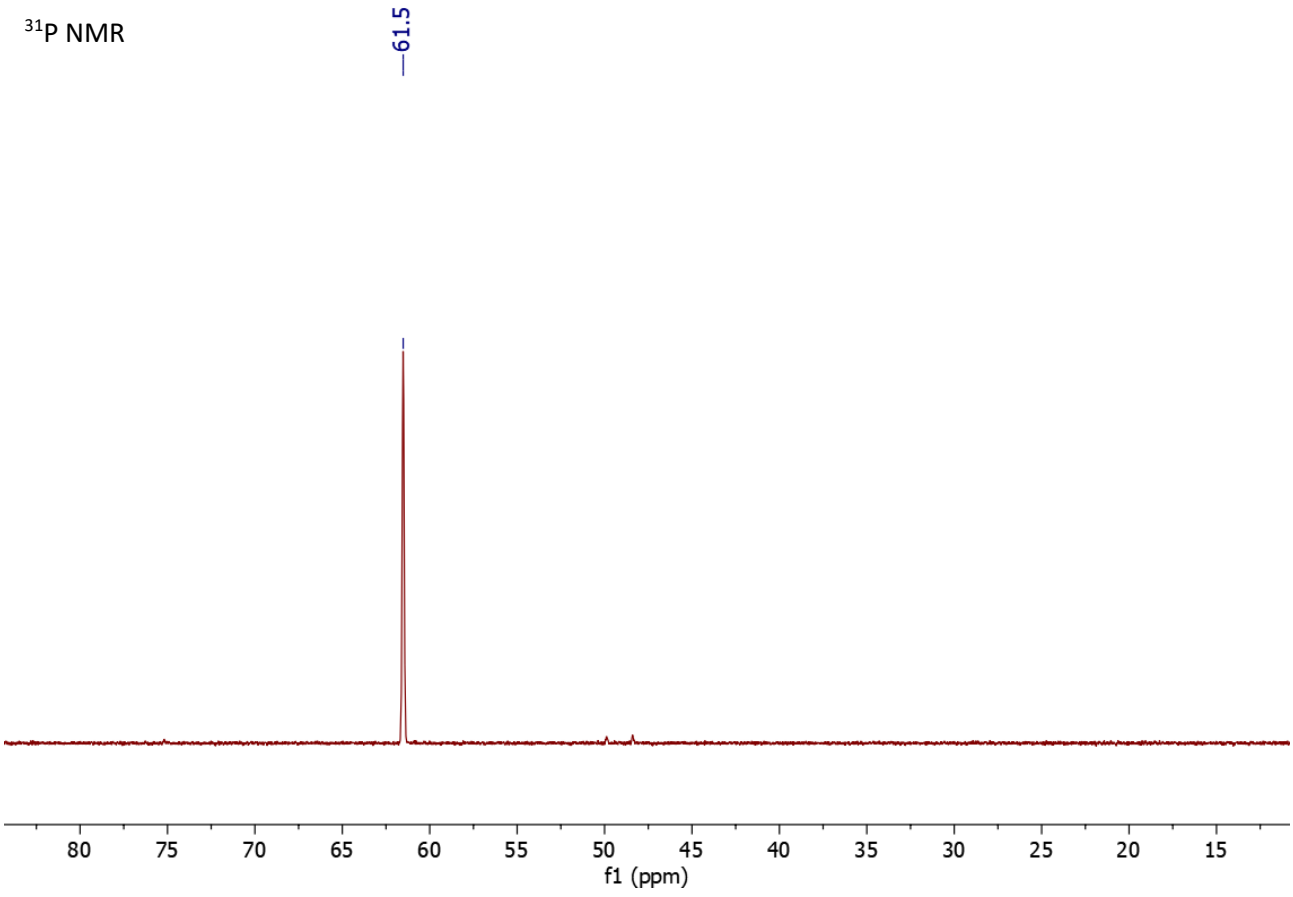

^{1}H NMR

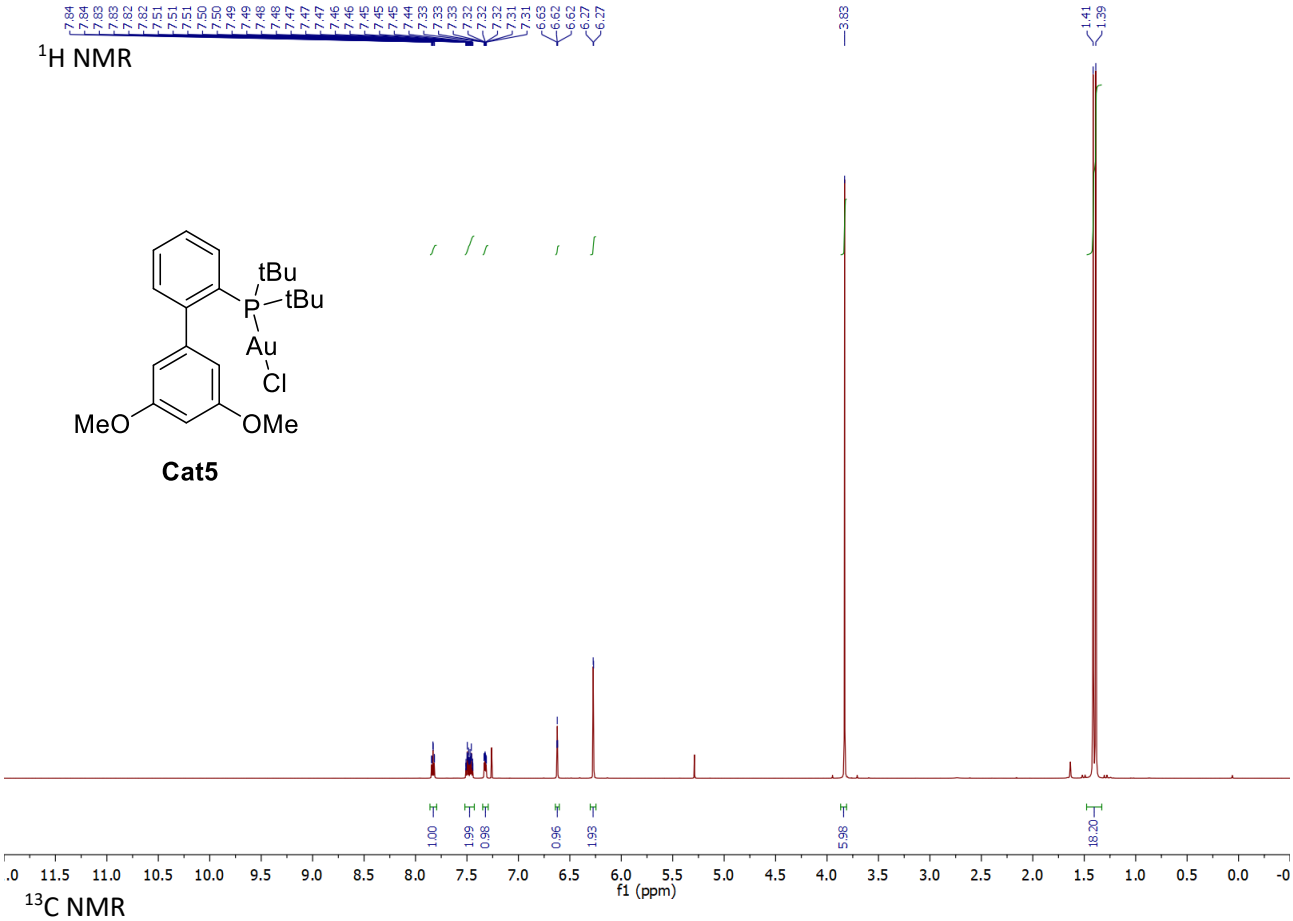

Cat5

^{13}C NMR

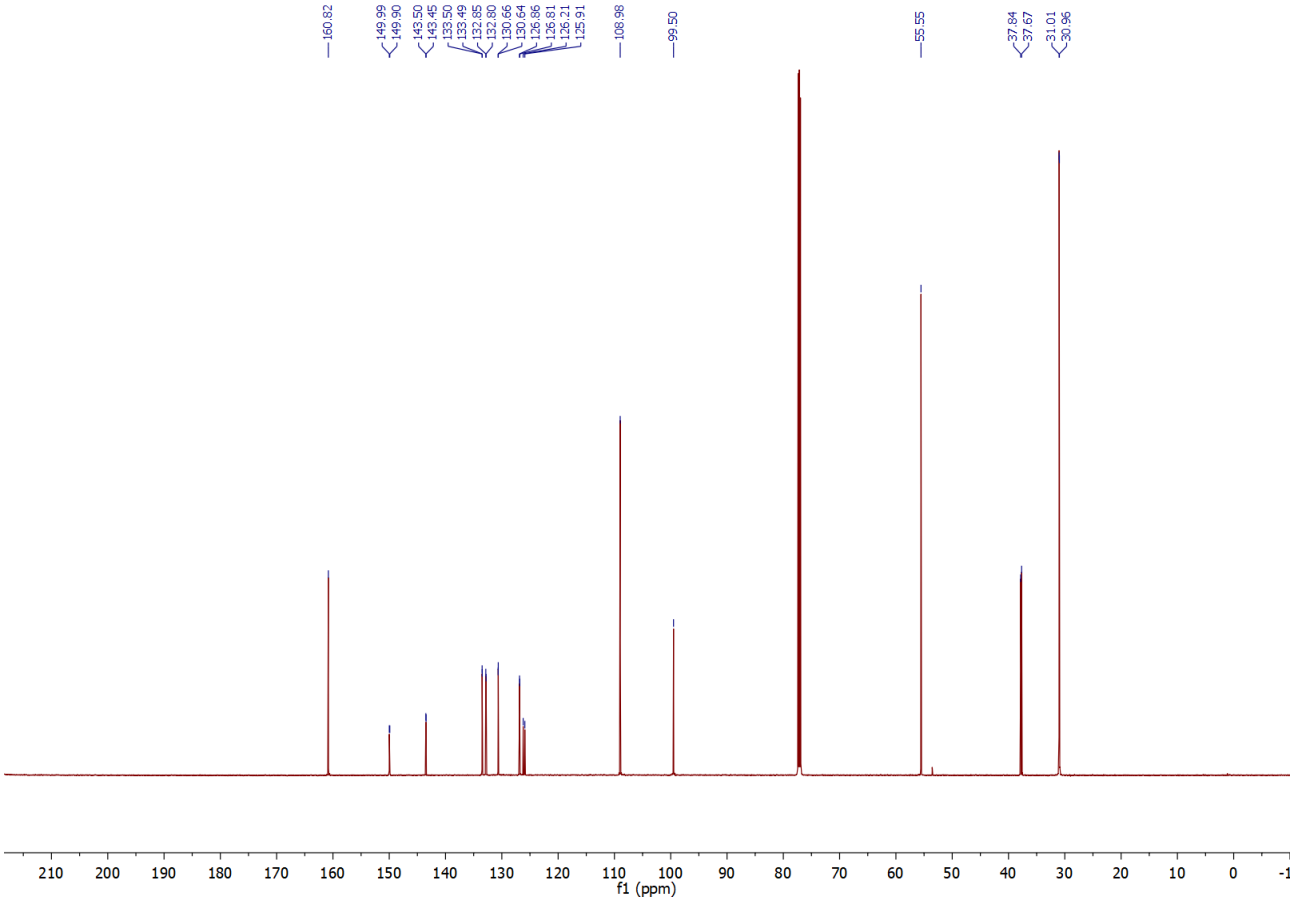

^{31}P NMR

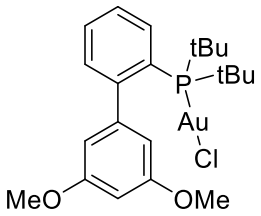
tBu
tBu
P
Au
Cl
MeO
OMe

Cat5

60.94
140
120
100
80
60
40
20
0
-20
-40
-60
-80
-100
-120
-140
-160
-180
-200
-220
-240
f1 (ppm)

^{1}H NMR

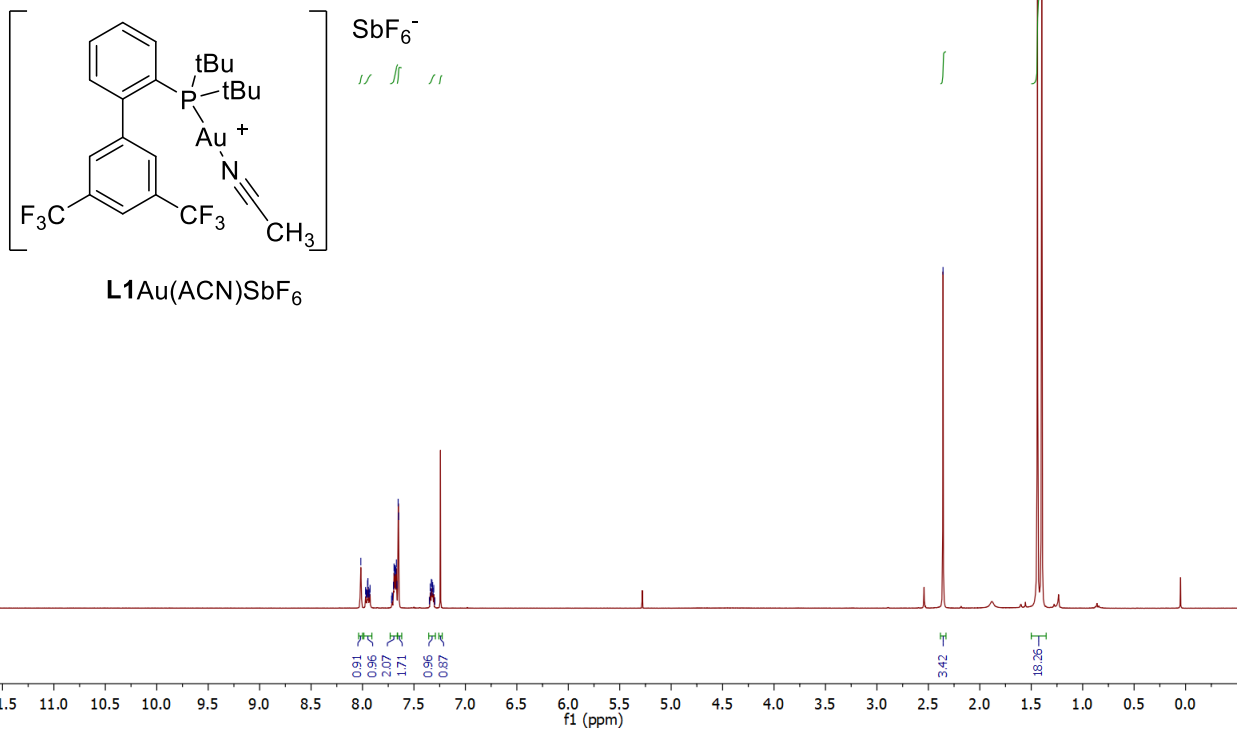

SbF_6^-

L1Au(ACN)SbF_6

^{13}C NMR

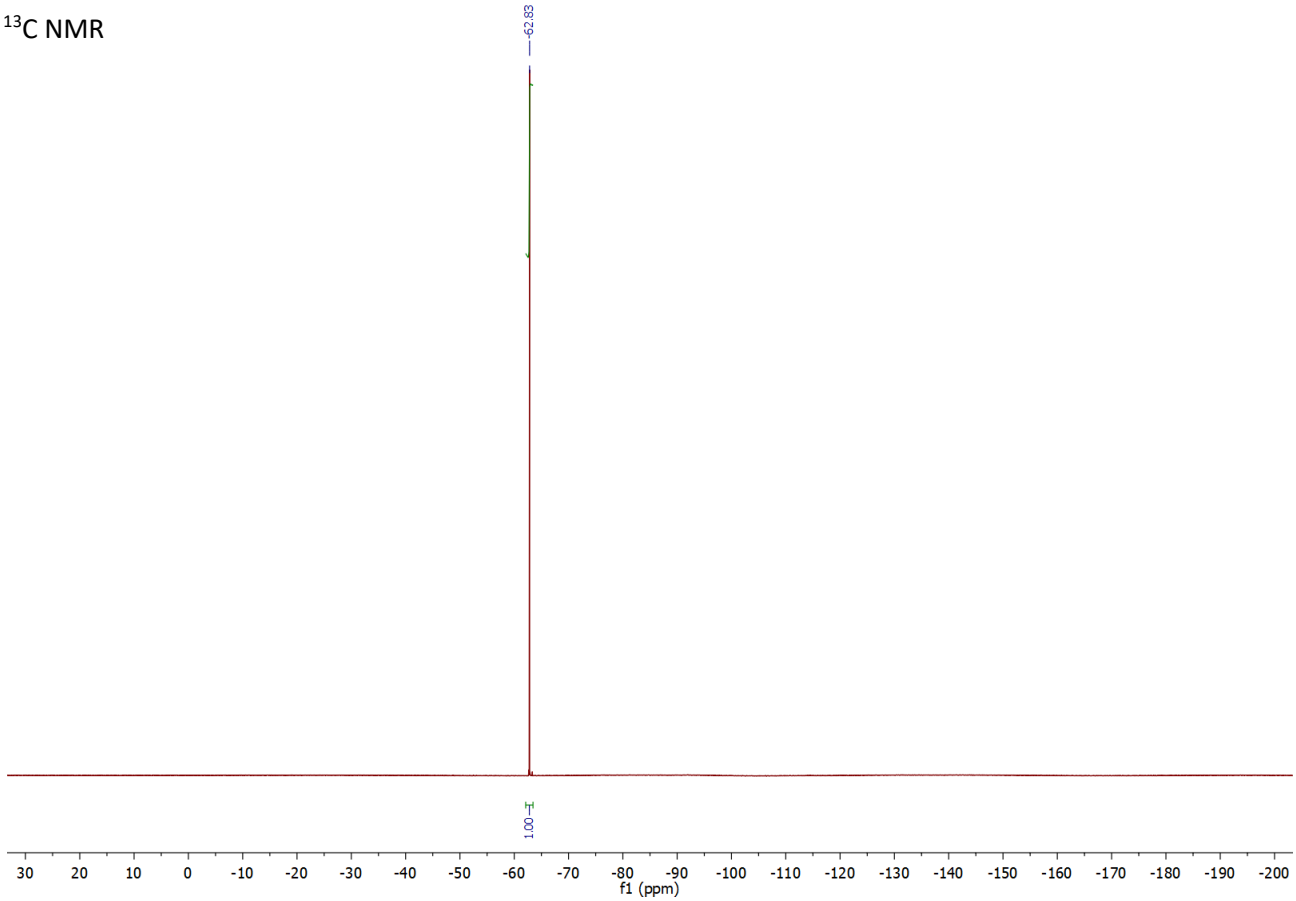

^{31}P NMR

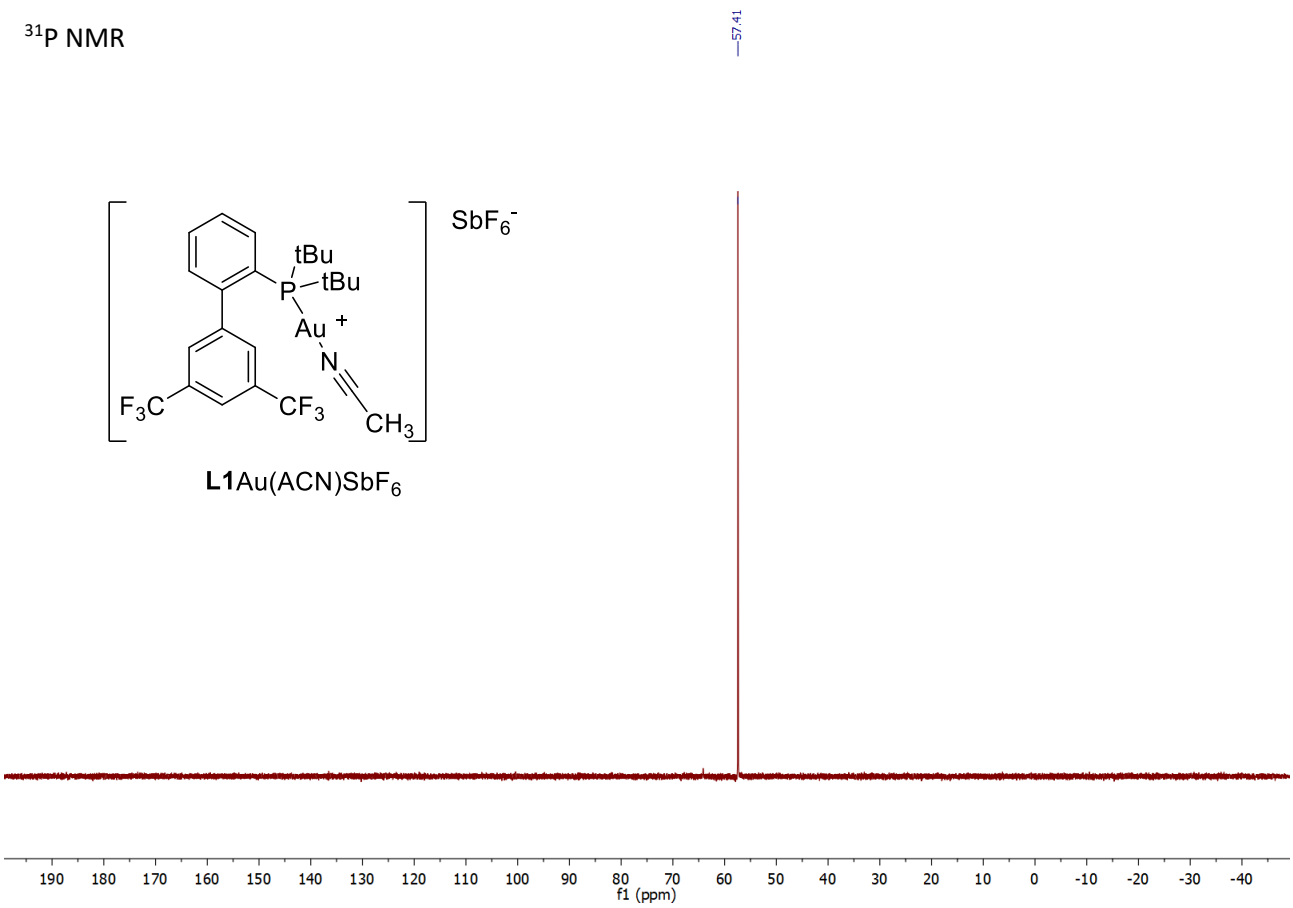

L1Au(ACN)SbF_6

References

[1] Biletskyi, B.; Tenaglia, A.; Clavier, H. Cobalt-catalyzed versus uncatalyzed intramolecular Diels-Alder cycloadditions, *Tetrahedron Lett.,* **2018**, *59*, 103-107.

[2] Zhu, Y.; Colomer, I.; Donohoe, T. J. Hypervalent iodine initiated intramolecular alkene dimerisation: a stereodivergent entry to cyclobutanes, *Chem. Commun.*, **2019**, *55*, 10316-10319.

[3] Matsuoka, J.; Kumagai, H.; Inuki, S.; Oishi, S.; Ohno, H. Construction of the Pyrrolo[2,3-d]carbazole Core of Spiroindoline Alkaloids by Gold-Catalyzed Cascade Cyclization of Ynamide, *J. Org. Chem.*, **2019**, *84*, 9358-9363.

[4] APEX3 Software Package V2019; Bruker AXS Inc.: Madison, WI, **2019**.

[5] Bruker SAINT, v8.40A: Part of the APEX3 Software Package V2019; Bruker AXS Inc.: Madison, WI, **2019**.

[6] Bruker SADABS V2016/2: Part of the APEX3 Software Package V2019; Bruker AXS Inc.: Madison, WI, **2019**.

[7] Sheldrick, G. M. SHELXT − Integrated Space-Group and Crystal-Structure Determination. *Acta Crystallogr., Sect. A: Found. Adv*. **2015**, *71*, 3-8.

[8] Macrae, C. F.; Bruno, I. J.; Chisholm, J. A.; Edgington, P. R.; McCabe, P.; Pidcock, E.; Rodriguez-Monge, L.; Taylor, R.; Streek, J.; van de Wood, P. A. Mercury CSD 2.0 − New Features for the Visualization and Investigation of Crystal Structures. *J. Appl. Crystallogr*. **2008**, *41*, 466-470.

[9] a) Becke, A. D. Density-functional thermochemistry. III. The role of exact exchange, *J.Chem.Phys.,* **1993**, 98, 5648-5652. b) Stephens, P.J.; Devlin, F.J.; Chabalowski, C.F.; Frisch, M.J. Ab Initio Calculation of Vibrational Absorption and Circular Dichroism Spectra Using Density Functional Force Fields, *J.Phys.Chem*, **1994**, 98, 11623-11627.

[10] Andrae, D.; Haußermann, U.; Dolg, M.; Stoll, H.; Preuß, H. Energy-adjusted ab initio pseudopotentials for the second and third row transition elements, *Theoret. Chim. Acta,* **1990**, 77, 123-141.

[11] a) Faza, O.N.; Rodríguez, R.Á.; López, C.S. *Theor. Chem. Acc.* **2011**, *128*, 647-661 b) Faza, O.N., López, C.S. (**2014**). Computational Approaches to Homogeneous Gold Catalysis. In: Slaughter, L. (eds) Homogeneous Gold Catalysis. *Topics in Curr. Chem.*, vol 357. Springer, Cham.

[12] Mennucci, B.; Tomasi, J.; Cammi, R.; Cheeseman, J. R.; Frisch, M. J.; Devlin, F. J.; Gabriel, S.; Stephens, P. J. Polarizable Continuum Model (PCM) Calculations of Solvent Effects on Optical Rotations of Chiral Molecules, *J. Phys. Chem. A,* **2002**, *106*, 6102-6113.

[13] Lu, T.; Chen, F.; Multiwfn: A multifunctional wavefunction analyzer, *J. Comput. Chem.*, **2012**,*33*, 580–592.